Principles and Applications of Magnetic Sensors

Dept. of Photonics and Sensors
Hannam University
Prof. Derac Son

INTRODUCTION OF SENSORS

What is sensor?

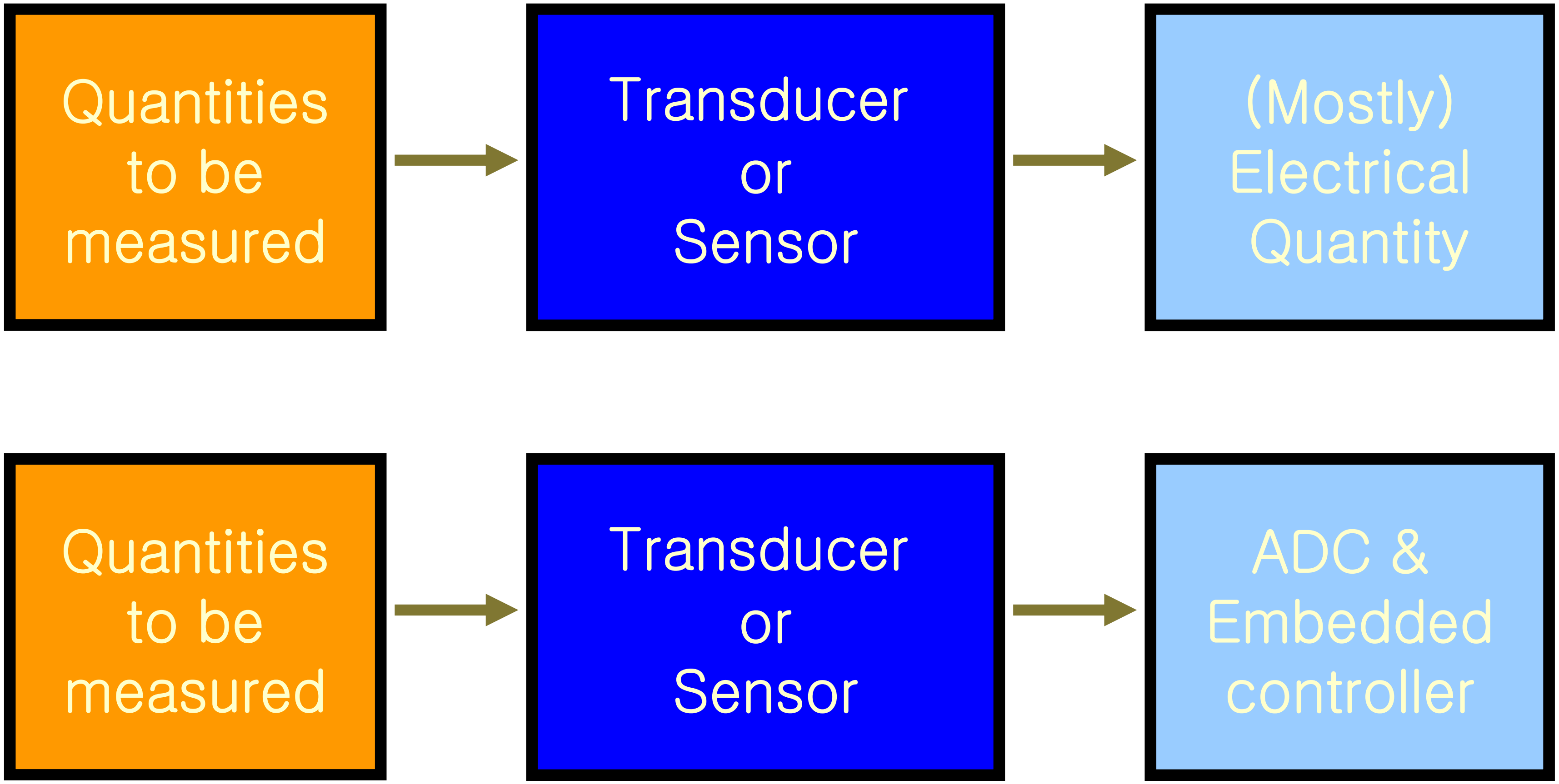

Why are sensors important?

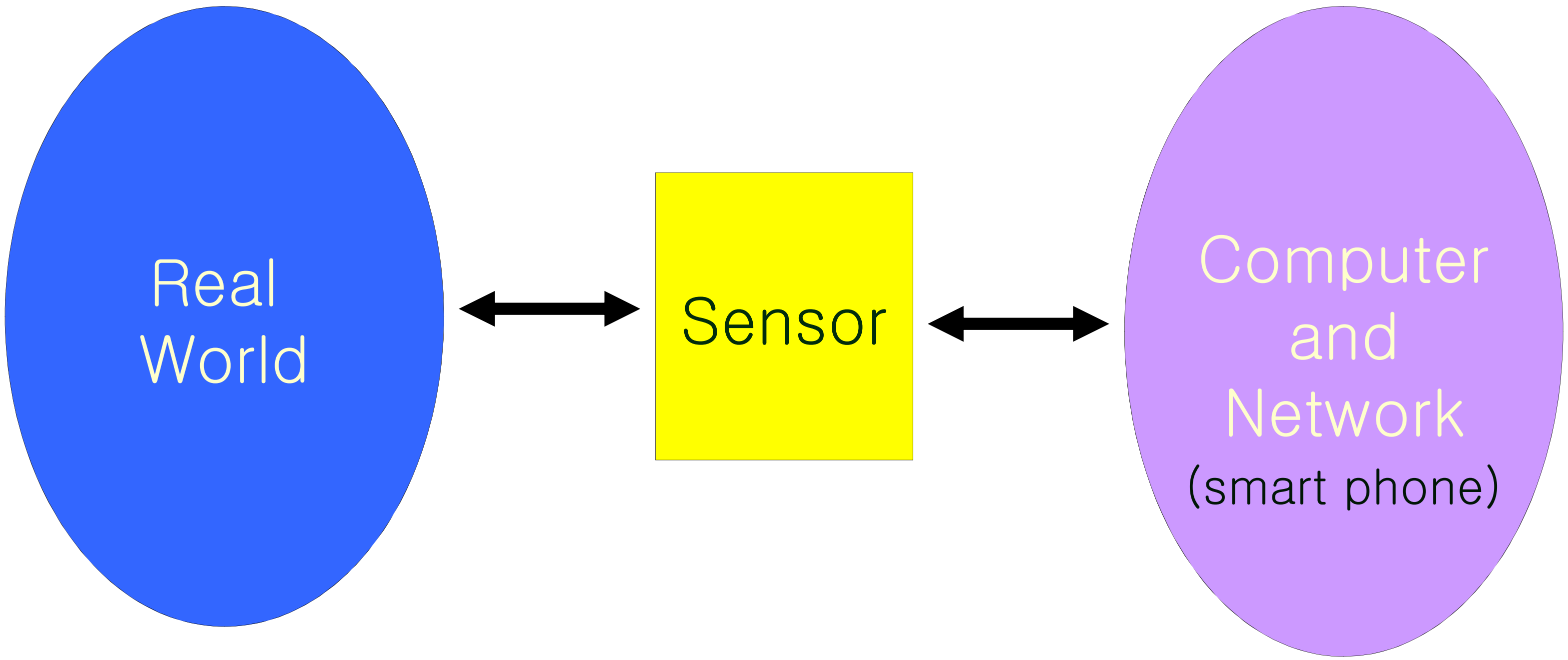

* Traditionally, sensors are used for research and production

World market of sensors

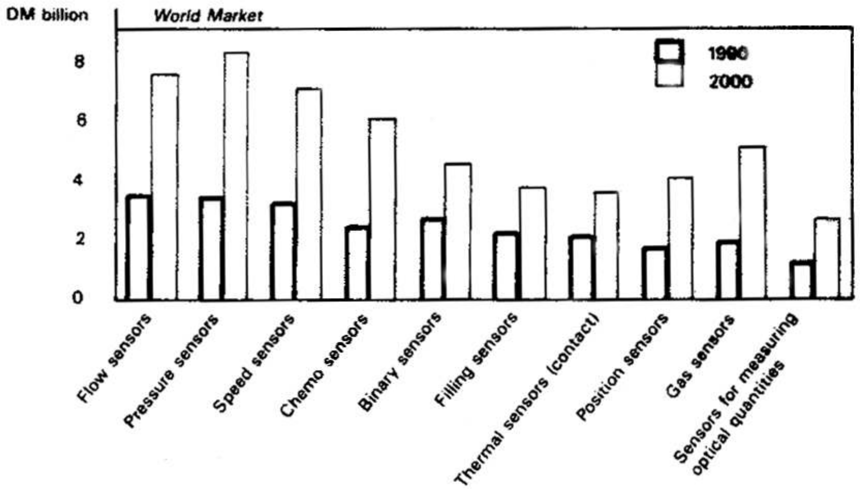

West European market of sensors

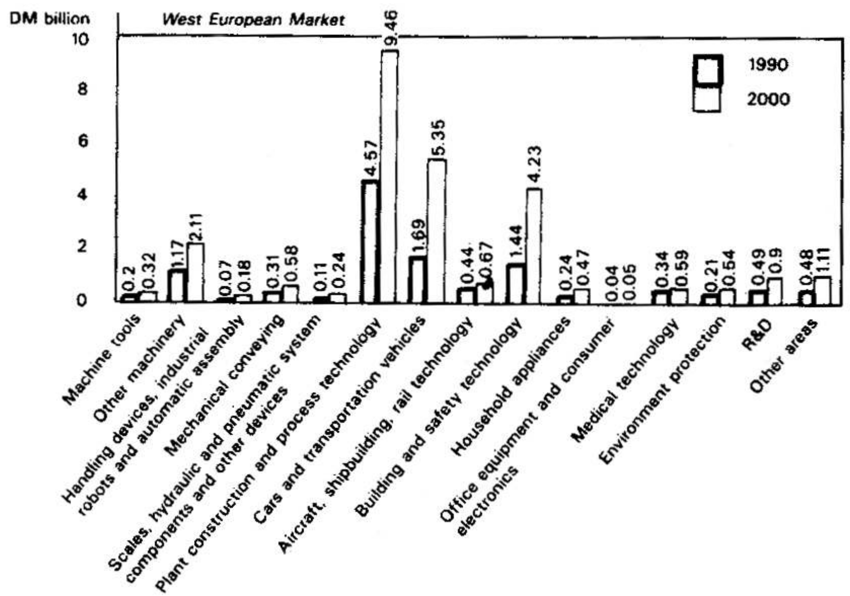

Sensor Variables

Primary Signal \ Secondary Signal	Mechanical	Thermal	Electrical	Magnetic	Radiant	Chemical
Mechanical	(Fluid) Mechanical and Acoustic Effects : eg, Diaphragm, Gravity Balance, Echo Sounder	Friction Effects (eg, Friction Calorimeter) Coolings Effects (eg, Thermal Flow Meters)	Piezoeletricity Peizoresistivity Resistive, Capacitive, and Inductive Effects	Magnetomechanical Effects : eg, Piezomagnetic Effect	Photoelastic Systems (Stress-induced Birefringence) Interferometers Sagnac Effect Doppler Effect	
Thermal	Thermal Expansion (Bimetalic Strip, Liquid-in-Glass and Gas Thermometers, Resonant Frequency) Radiometer Effect (Light Mill)		Seebeck Effect Thermoresistance Pyroelectricity Thermal (Johnsen) Noise		Thermooptical Effects (eg, in Liquid Crystals) Radiant Emission	Reaction Activation eg, Thermal Dissociation
Electrical	Electrokinetic and Electromechanical Effects : eg, Piezoelectricity Electrometer Ampere's Law	Joule (Resistive) Heating Peltier Effect	Charge Collectors Langmuir Probe	Biot-Savart's Law	Electrooptical Effects : eg, Kerr Effect Pockels Effect Electroluminescence	Electrolysis Electromigration
Magnetic	Magnetomechanical Effects : eg, Magnetostriction Magnetometer	Thermomagnetic Effects : eg, Righi-Leduc Effect Galvanomagnetic Effect eg, Ettingshausen Effect	Thermomagnetic Effects : eg, Ettingshausen-Nernst Effect Galvanomagnetic Effects : eg, Hall Effects, Magnetoresistance		Magnetooptical Effects : Faraday Effect Cotton-Mouton Effect	
Radiant	Radiation Pressure	Bolometer Thermopile	Photoelectric Effects : eg, Photovoltaic Effect Photoconductive Effect		Phtorefractive Effects Optical Bistability	Photosynthesis, -dissociation
Chemical	Hygrometer Electrodeposition Cell Photoacoustic Effect	Calorimeter Thermal Conductivity Cell	Potentiometry, Conductimetry Amperometry Flame Ionization Volta Effect Gas Sensitive Field Effect	Nuclear Magnetic Resonance	(Emission and Absorp-tion) Spectroscopy Chemiluminescence	

Important Sensor Variables

Quantities to be measured	Transfer characteristics	Measured quantity
Temp. Force Torque PH Light intensity Current Voltage Magnetic Field Electric Field	Linearity Resolution Noise Measuring range Frequency range (dynamic response)	Charge Voltage Current Frequency Phase

Response Curves of the Sensors

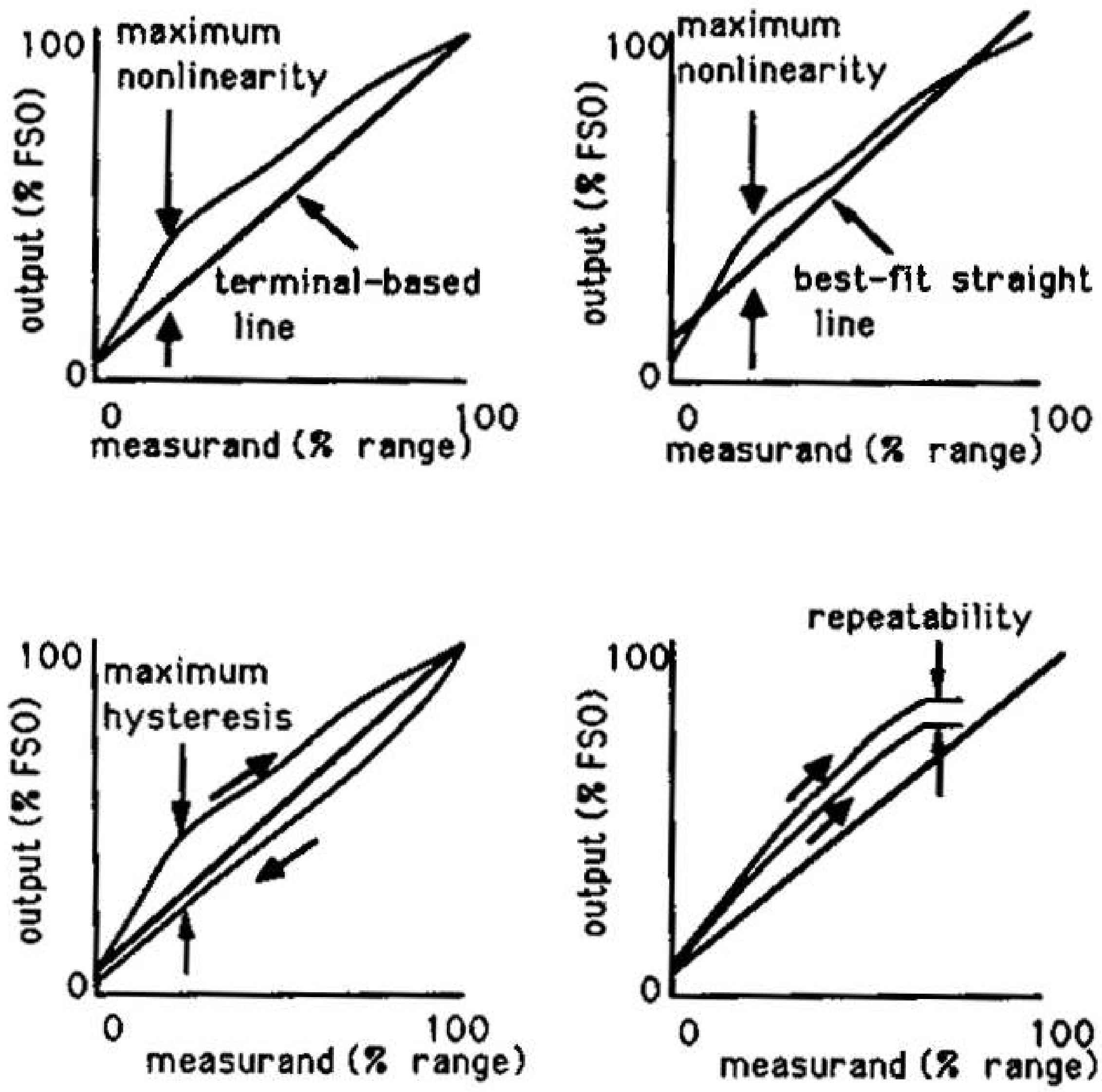

Trends in Sensor Development

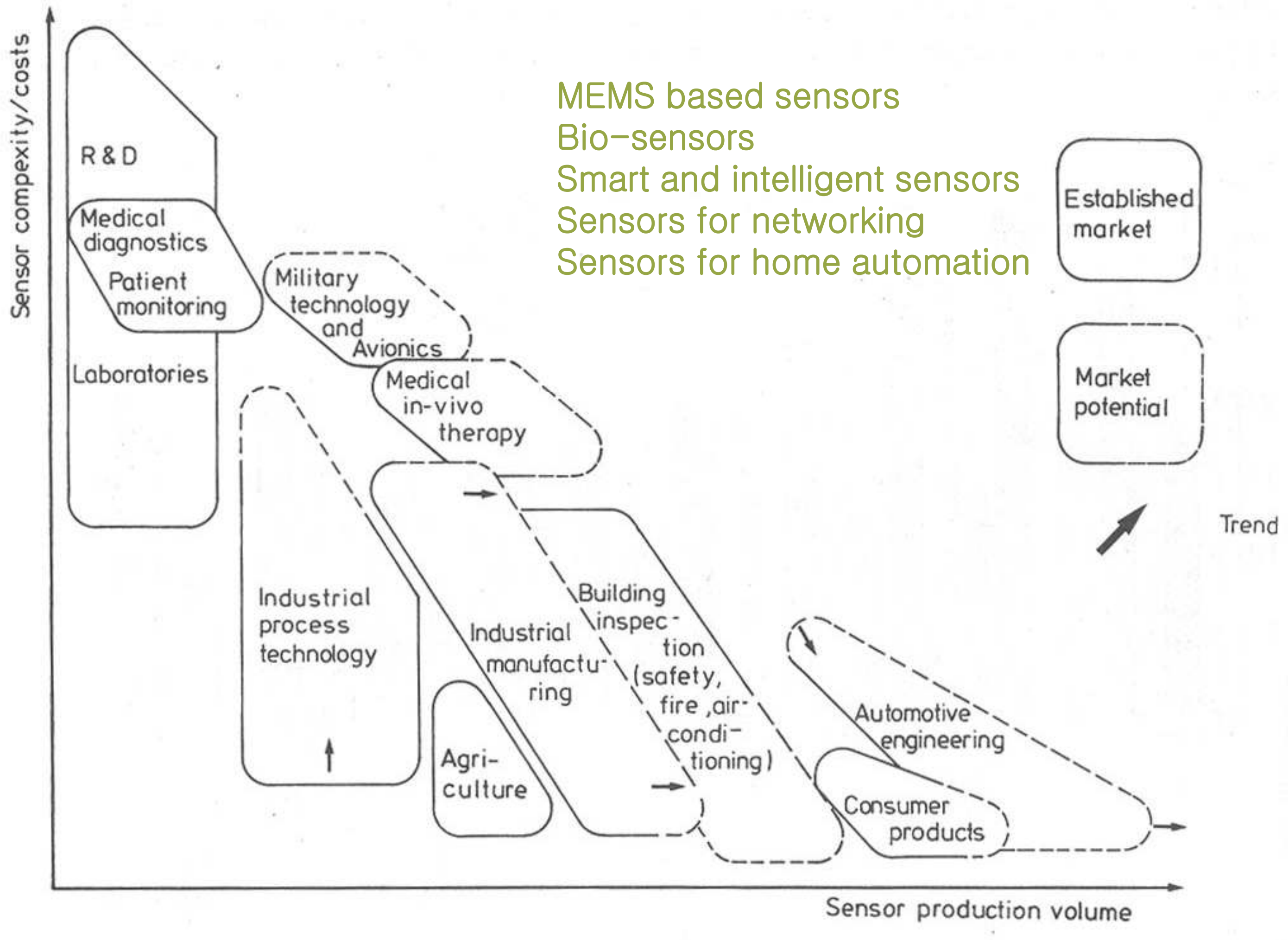

MEMS based sensors
Bio-sensors
Smart and intelligent sensors
Sensors for networking
Sensors for home automation

Sensor in Automobiles

Engine
1. Air mass flow
2. Non-contact throttle angle
3. Non-contact torque
4. In-cylinder combustion monitoring
5. Barometric absolute pressure
6. Crankshaft position on two-stroke engines

Steering
1. Non-contact position and velocity
2. Non-contact torque

Battery state of charge

Liquid level
1. Fuel level
2. Oil level
3. Coolant brake fluid
4. washer bottel level

Brakes
1. Brake temperature and wear
2. Commercial vehicle pneumatic brake circuit pressure sensor
3. Adaptive braking

Internal environment
1. Noise cancellation
2. Commercial vehicle payload condition monitoring

Navigation and vehicle dynamics
1. True speed over ground
2. Navigation
3. Yaw rate
4. Accelerometers
5. Road surface texture

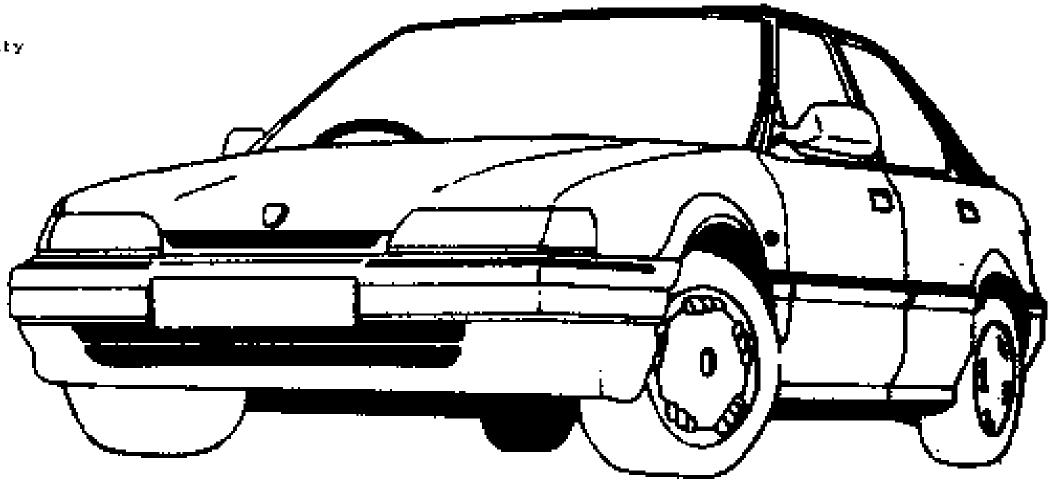

Wheels
1. Tyre pressure
2. Wheel speed

Suspension
1. Non-contact ride height
2. Vertical acceleration of wheel
3. Vertical acceleration of body
4. Load monitoring for commercial vehicles

Safety
1. Object detector
2. Active cruise control
3. Air-bag activation
4. Window and sunroof anti-trapping devices
5. Sleep sensors
6. Automatic breathalyser
7. Magnetic bomb detection
8. Intruder detection
9. Black ice detection
10. Automatic handbrake actuation - "hill hold"

Definition of Magnetic Sensor

Sensors which are associated with the laws and effects of magnetic and electromagnetic fields

Why are Magnetic Sensors Important?

1) High reliability : Military : Flux-gate, Search coil
   Automobile : ABS, non-contact angle
   Air and space : Magnetic torquer, Flux-gate
2) High Temperature: LVDT, Flux-gate
3) High radiation : Eddy current probe and LVDT used in nuclear power plant

Magnetic Effects for Sensors

Year	Effect	Explanation	Technical Use
1842	Joule effect	Change in shape of a ferromagnetic body with magnetization (magnetostriction)	In combination with piezoelectric elements for magnetometers and potentiometers
1846	ΔE effect	Chang in Young's modulus with magnetization	Acoustic delay line components for magnetic field measurement
1847	Matteucci effect	Torsion of a ferromagnetic rod in a longitudinal field changes magnetization	Magnetoelastic sensor
1856	Magnetoresistance (AMR)	Change in resistance with magnetic field	Magnetoresistive sensors
1858	Wiedemann effect	A torsion is produced in a current carrying ferromagnetic rod when subjected to a longitudinal field	Torque and force measurement
1865	Villari effect	Effect on magnetization by tensile or compressive strength	Magnetoelastic sensors
1879	Hall effect	A current carrying crystal produces a transverse voltage when subjected to a magnetic field vertical to its surface	Magnetogalvanic sensors
1903	Skin effect	Displacement of current from the interior of material to surface layer due to eddy currents	Distance sensors, proximity sensors
1931	Sixtus Tonks effect	Pulse magnetization by large Barkhausen jumps	Wiegand and pulse-wire sensors
1962	Josephson effect	Tunnel effect between two superconducting materials with an extremely thin separating layer; quantum effect	SQUID magnetometers
1987	GMR effect	Quantum mechanical magnetoresistance effect observed in thin-film structures composed of alternating ferromagnetic and non-magnetic conductive layers	Magnetic field sensor Sprintonics
1994	GMI effect	Large variations that the electrical impedance of some materials exhibits as a function of an external magnetic field	Magnetic field sensor

Faraday 전자기유도법칙

Principle of search coil type magnetometer

Faraday's Induction Law

$$\oint E \cdot \mathrm{d}s = -\frac{\mathrm{d}}{\mathrm{d}t}\iint_A B \cdot \mathrm{d}A$$

Voltage output from magnetometer

$$U_0 = \omega \cdot n \cdot \Phi_{max} = \omega \cdot n \cdot A \cdot \mu \cdot H$$

Sensitivity and Noise of Air Cored Induction Coil

$$U_0 = \omega \cdot n \cdot \Phi_{max} = \omega \cdot n \cdot A \cdot \mu_0 \cdot H = \frac{\pi^2}{2} \cdot n \cdot D^2 \cdot \mu_0 \cdot f \cdot H$$

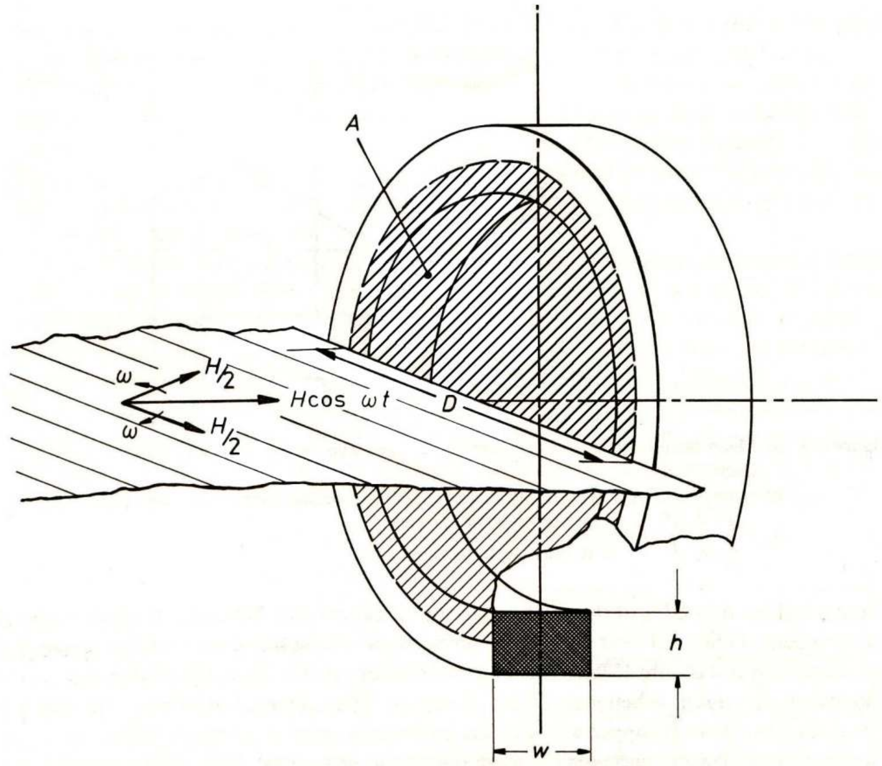

$$S_0 = \frac{U_0}{f \cdot H} = \frac{\pi^2 n \cdot D^2 \cdot \mu_0}{2}$$

$$U_0 = \frac{\pi^2}{2} n \cdot D^2 \cdot 10^{-9} \left[\frac{\mathrm{V}}{\mathrm{nT} \cdot \mathrm{Hz}} \right]$$

$$\mu_0 = 4\pi \cdot 10^{-7} \left[\frac{\mathrm{V} \cdot \mathrm{S}}{\mathrm{A} \cdot \mathrm{m}} \right] = 10^{-9} \left[\frac{\mathrm{V}}{\mathrm{nT} \cdot \mathrm{Hz} \cdot \mathrm{m}^2} \right]$$

Air-cored induction coil in a time-varying magnetic field.

$$U_0 = \frac{\pi^2}{2} n \cdot D^2 \cdot 10^{-9} \left[\frac{\text{V}}{\text{nT} \cdot \text{Hz}} \right]$$

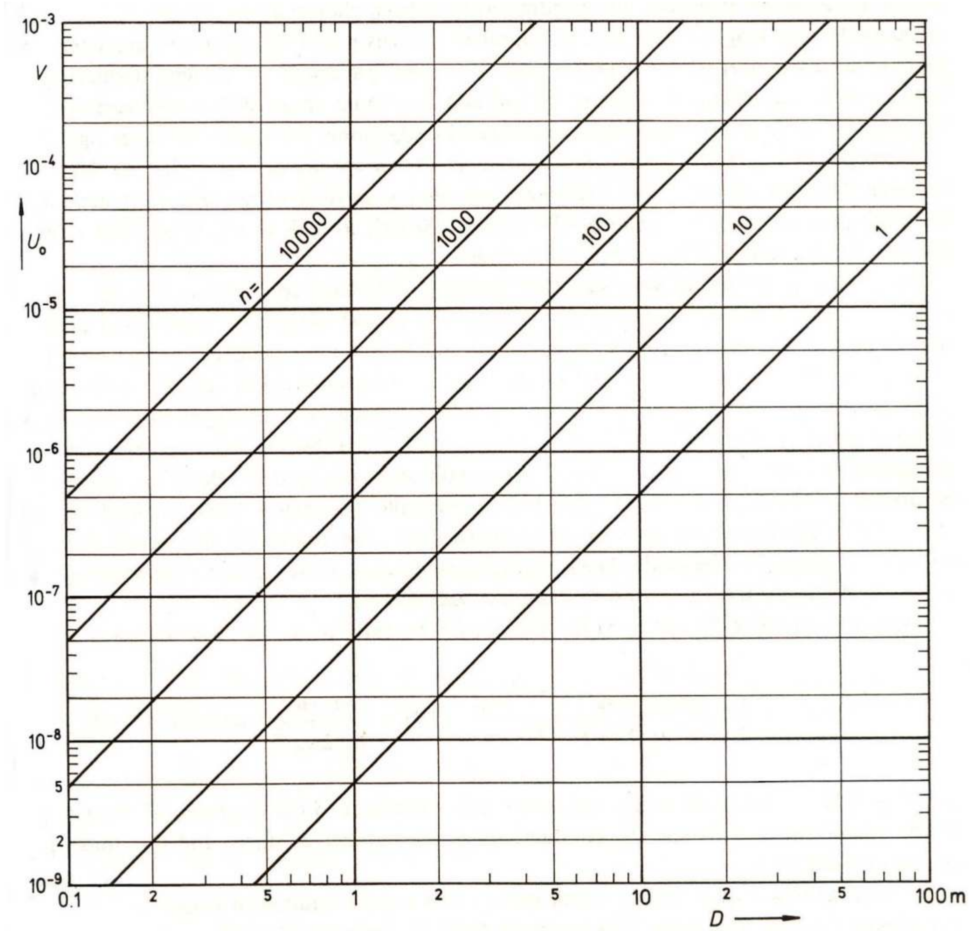

Air-cored coil output voltage U_0 at a magnetic field x frequency product 1 nT · Hz versus diameter *D* with number of turns *n* as parameter

$$R_{DC} = \frac{4\rho n D}{d^2}$$ Coil resistance

$$U_N = \sqrt{4\kappa_B T R_{DC} \Delta f}$$ Thermal voltage noise

$$W_W = \frac{\pi^2 \cdot \gamma \cdot n \cdot D \cdot d^2}{4}$$ Weight of coil

$$U_N = \sqrt{4\kappa_B T \Delta f} \cdot \frac{\sqrt{\gamma\rho} \cdot \pi \cdot n \cdot D}{\sqrt{W_{\mathrm{W}}}}$$ Noise voltage

$$S / N = \frac{U_0}{\sqrt{2} U_N} = \frac{\pi \cdot \mu_0}{4\sqrt{2k_B T}} \cdot \sqrt{\frac{W_{\mathrm{w}}}{\gamma\rho}} \cdot DfH = \frac{\pi^2 \cdot \mu_0}{8\sqrt{2k_B T}} \cdot d(\sigma n D^3)^{1/2} \cdot fH$$

Equivalent circuit diagram of an air-cored induction coil.

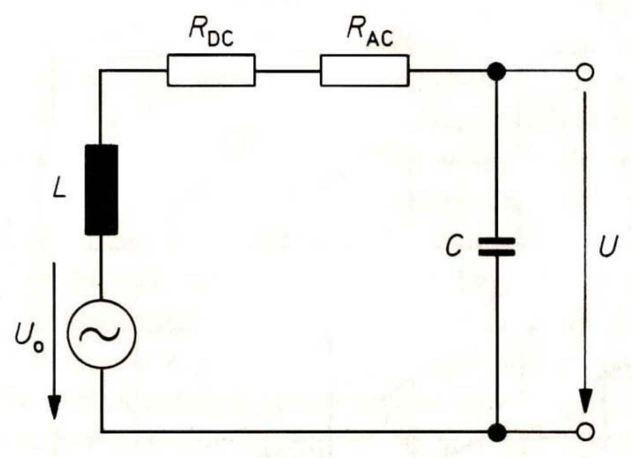

For single turn loop D>>d

$$L = 6.28D\left(\ln\frac{8D}{d} - 2 + \alpha\right)\cdot 10^{-9}$$

Long single layer solenoid

$$L \approx \frac{\pi^2 \cdot D^2 \cdot n^2}{w}\cdot 10^{-9}\ \ [\mathrm{H}] = \frac{\pi^2 \cdot D^2 \cdot n}{d_w}\cdot 10^{-9}\ \ [\mathrm{H}]$$

$$L \approx \frac{D^2 \cdot n^2}{46\ D + 101\ w}\cdot 10^{-6}$$ Short single layer solenoid w>1.6D

$$L \approx \frac{78.7\ D^2 \cdot n^2}{3\,D + 9\,w + 10\,h}\cdot 10^{-9}$$ Multi-layer solenoid D>>w,h

Capacitance C of a coil

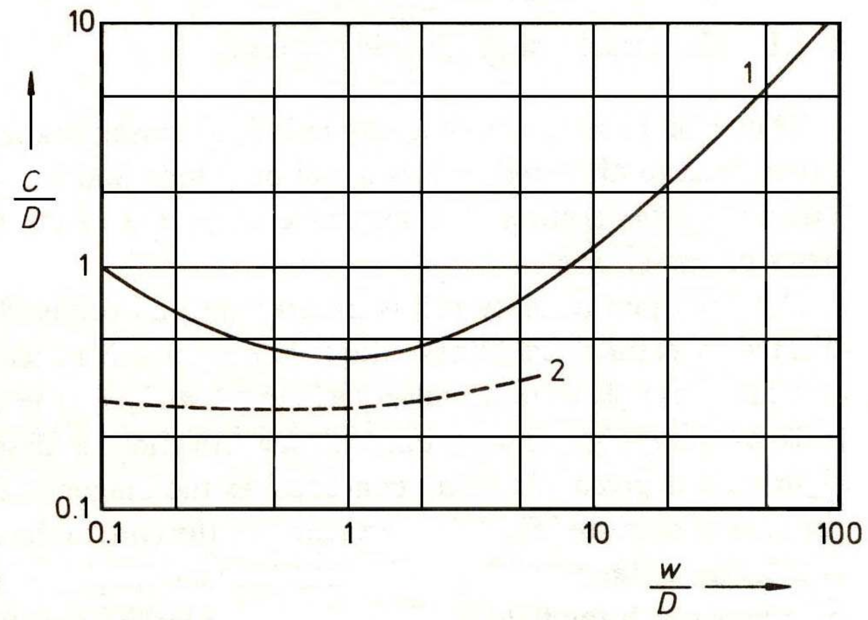

$$C = \frac{0.37 \cdot \varepsilon_r \cdot w \cdot D}{(c-d) \cdot n_1}$$

$$C_{\text{tot}} = \frac{C}{k^2} + \frac{C_{\text{i}}}{k-1}$$

Capacitance C of a single-layer coil normalized to its diameter D versus length-to-diameter ratio w/D of the coil (capacitance C in pF and geometrical dimensions w and D in cm)

High permeability core induction coil

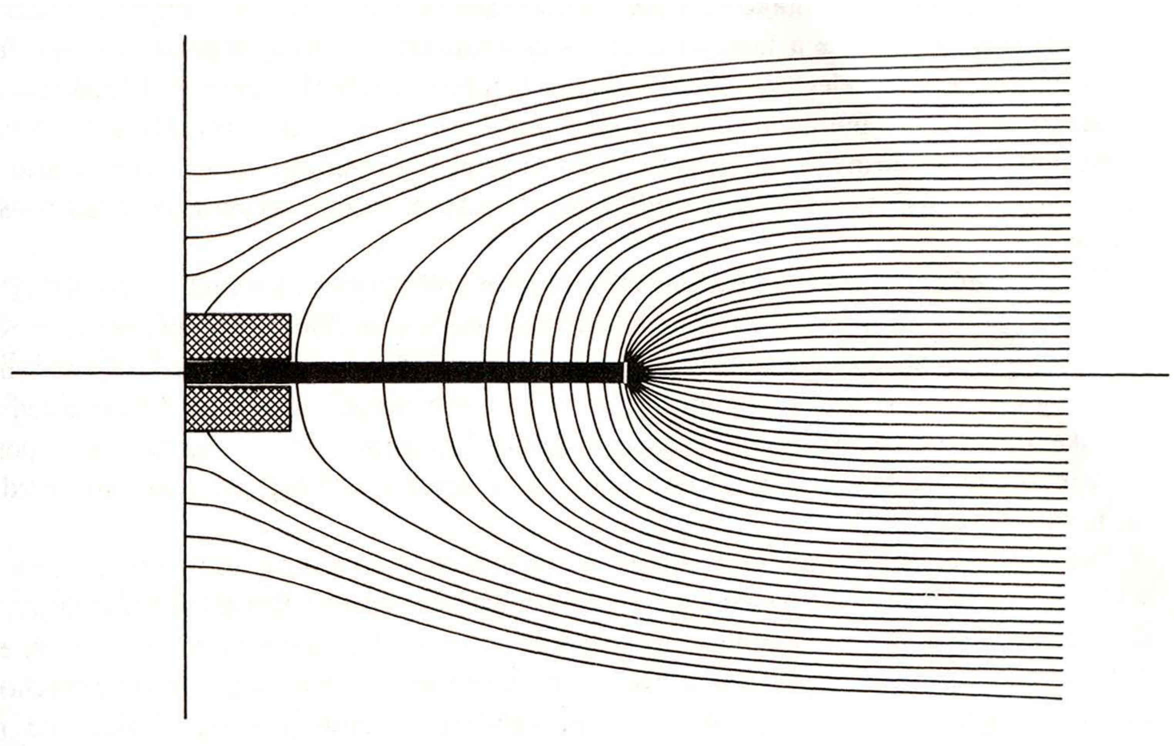

Magnetic field pattern around high permeability core when it is inserted into a homogeneous field. It is valid for low frequencies and if the coil, indicated at the middle of the core, is without current.

Magnetization of a high permeability core

$$u_{\mathrm{i}} = -n \cdot \frac{d\Phi_{\mathrm{i_c}}}{dt} \qquad \Phi_{\mathrm{i_c}} = \Phi_{\mathrm{c_{max}}} \cdot \cos(\omega t)$$

$$U_0 = \omega \cdot n \cdot \Phi_{\mathrm{c_{max}}} = \omega \cdot n \cdot \mu_{\mathrm{r}} \mu_0 \cdot H_{\mathrm{i}} \cdot A_{\mathrm{c}}$$

$$H_i = H + H_{dm} = H - N(\mu_r - 1) H_i$$

$$H_{\mathrm{i}} = \frac{1}{1 + N(\mu_{\mathrm{r}} - 1)} \cdot H$$

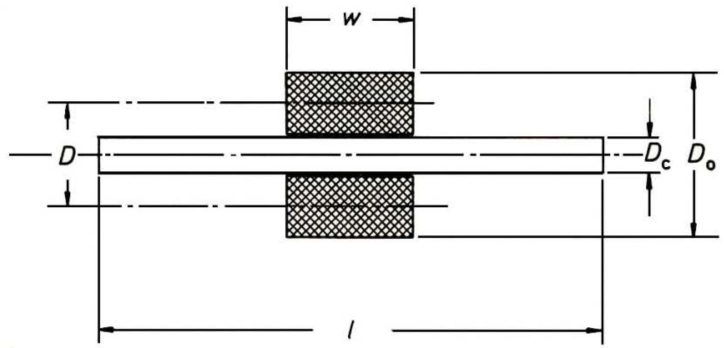

$$U_0 = 2\pi \cdot n \cdot A_{\mathrm{c}} \cdot \mu_{\mathrm{c}} \cdot \mu_0 \cdot f \cdot H$$

$$\mu_{\mathrm{c}} = \frac{\mu_{\mathrm{r}}}{1 + N(\mu_{\mathrm{r}} - 1)}$$

$$N_{\mathrm{ell}_\infty} = \frac{1}{m^2 - 1}\left[\frac{m}{\sqrt{m^2 - 1}}\ln(m + \sqrt{m^2 + 1}) - 1\right]$$

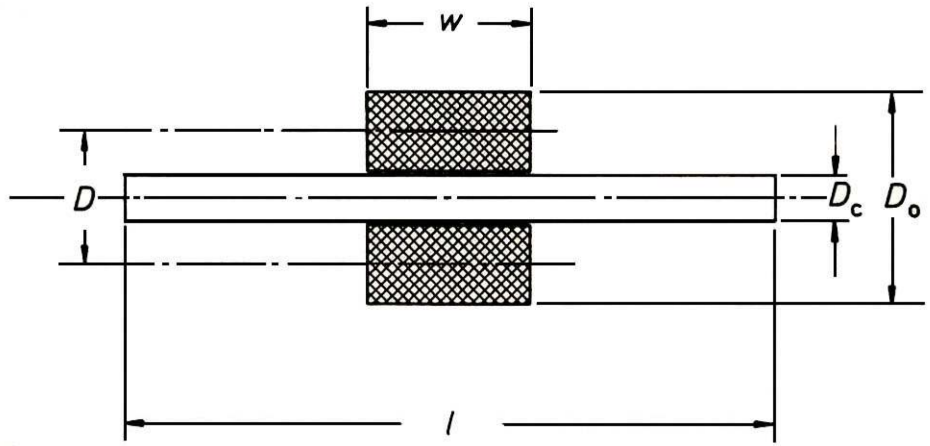

$$\frac{N_{\mathrm{cyl}_\infty}}{N_{\mathrm{ell}_\infty}} = \frac{2.26\ \ln(1 + \ 0.156) + 1}{2.15\ \ln(1 + \ 0.326) + 1}$$

Induction coil on a cylindrical high permeability core.

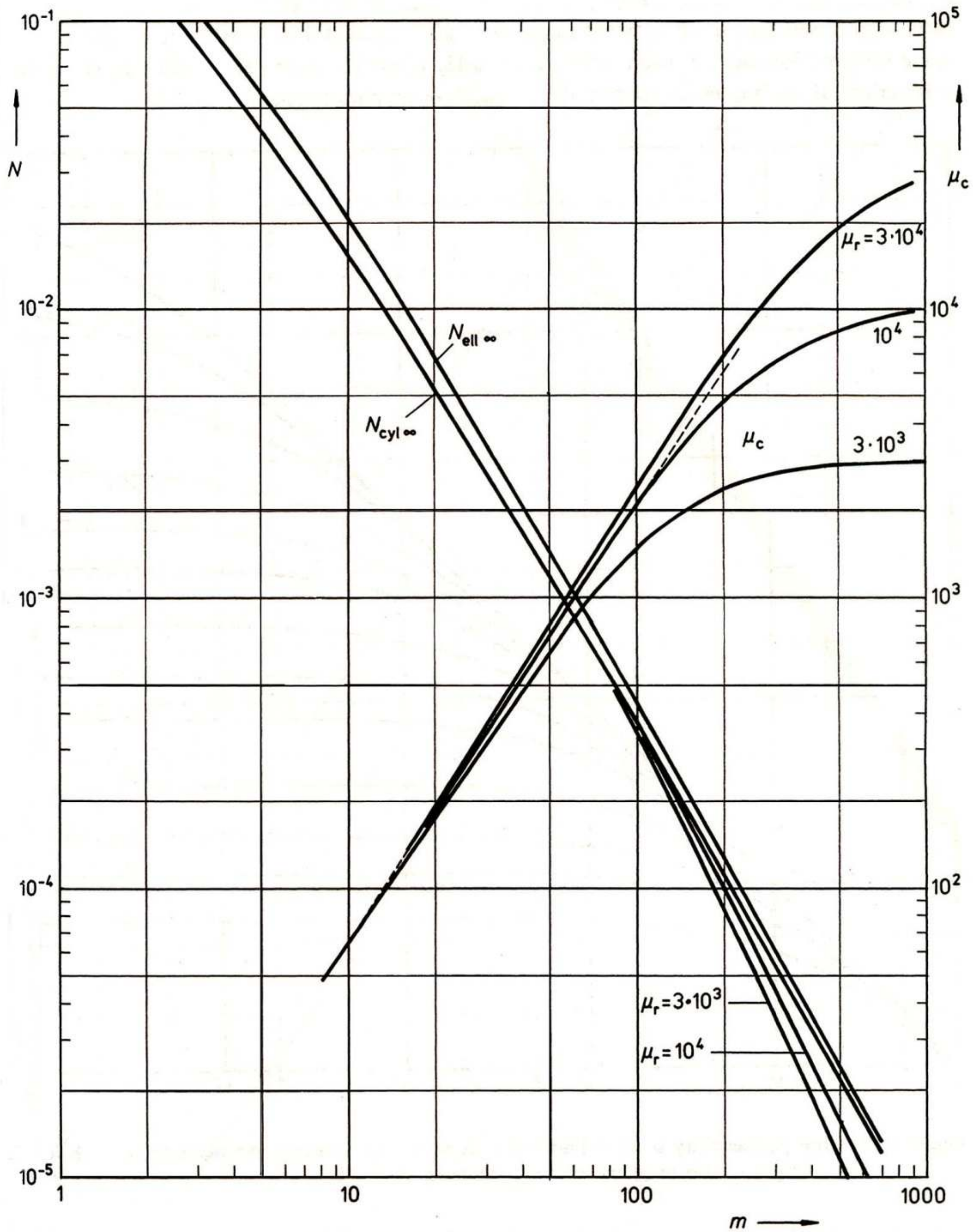

Demagnetization factor N of prolate ellipsoids and cylindrical rods (descending curves) and core permeability μ_c (ascending curves) of cylindrical rods versus the length-to-diameter ratio m of the rod with material permeability μ_r as parameter.

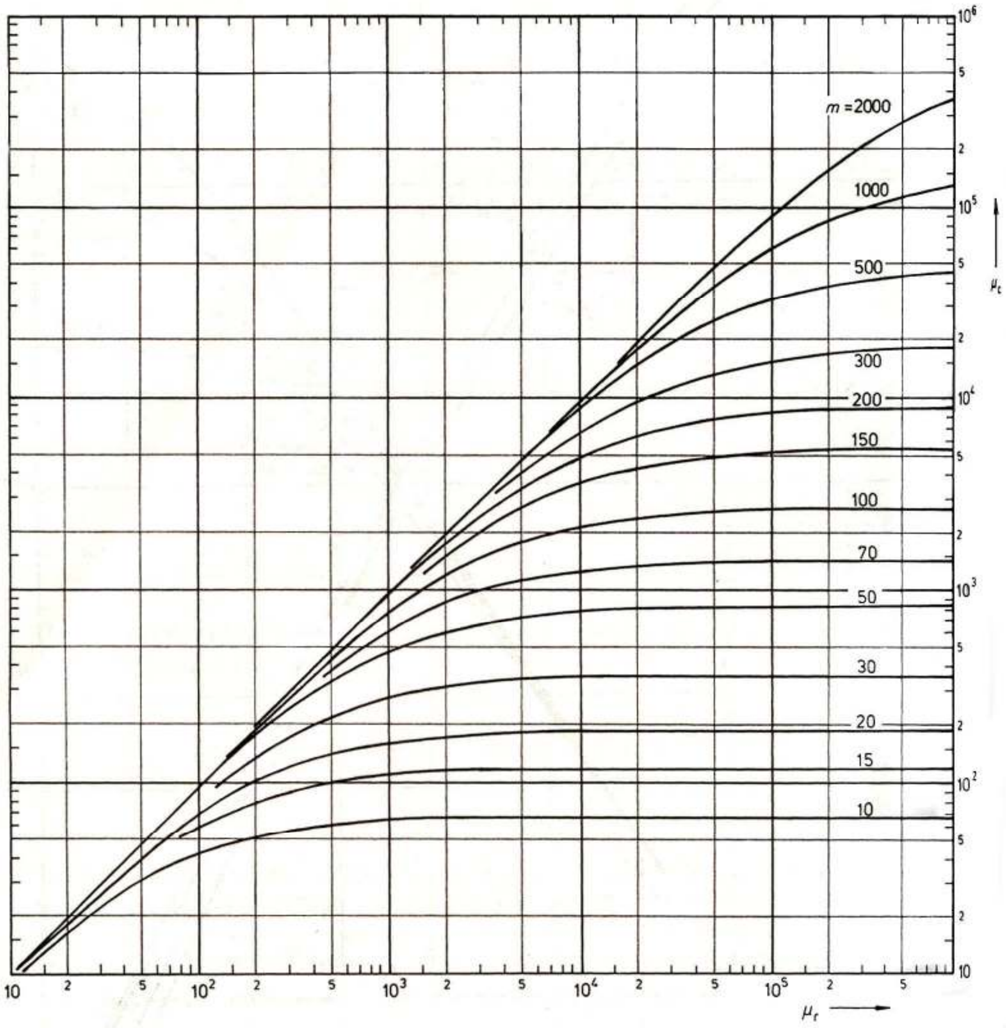

Core permeability μ_c of cylindrical rods versus the material permeability μ_r with length-to-diameter ratio *m* of the rod as parameter, after

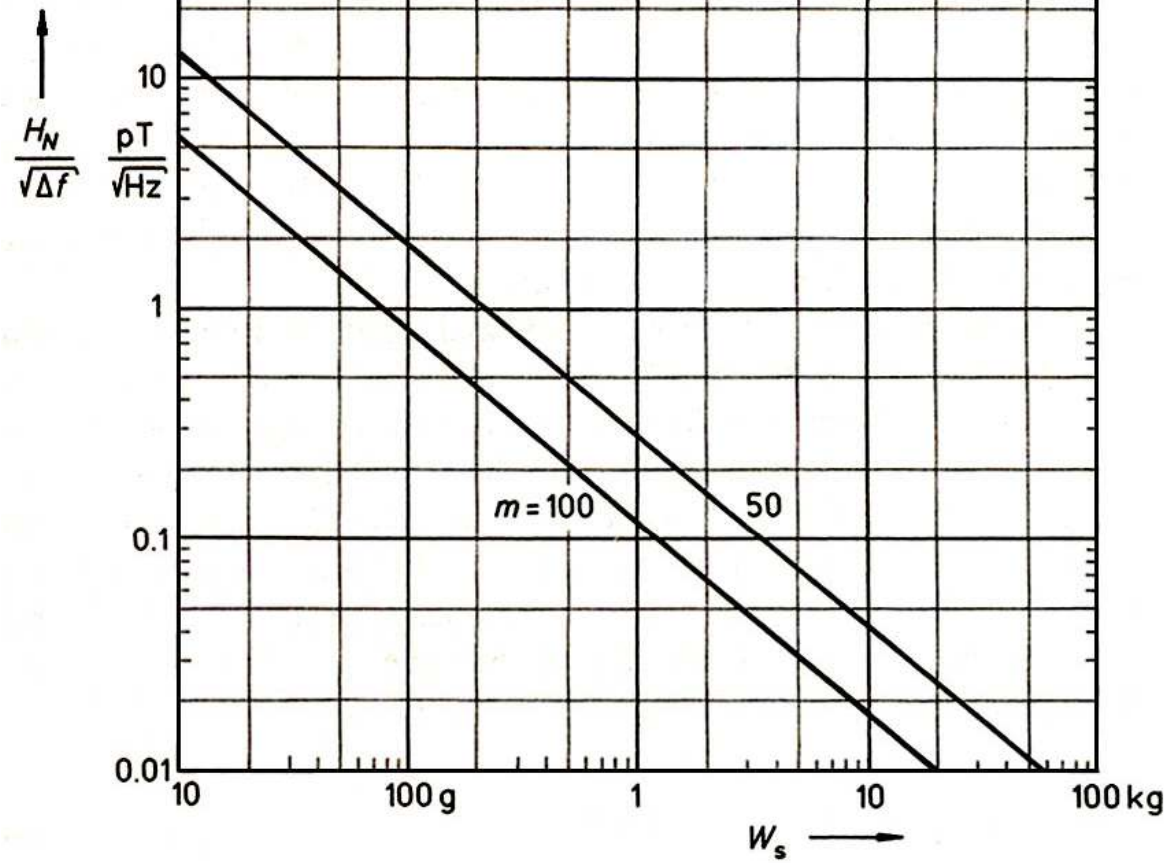

Minimum noise equivalent magnetic field spectral density of an induction coil sensor with high permeability core versus sensor weight *Ws* (at length-to-diameter ratios *m* = 50 and 100, permeability μ_r = 10000 of the core material, and *f* = 1 Hz).

Induction coil sensors with electronic amplifier

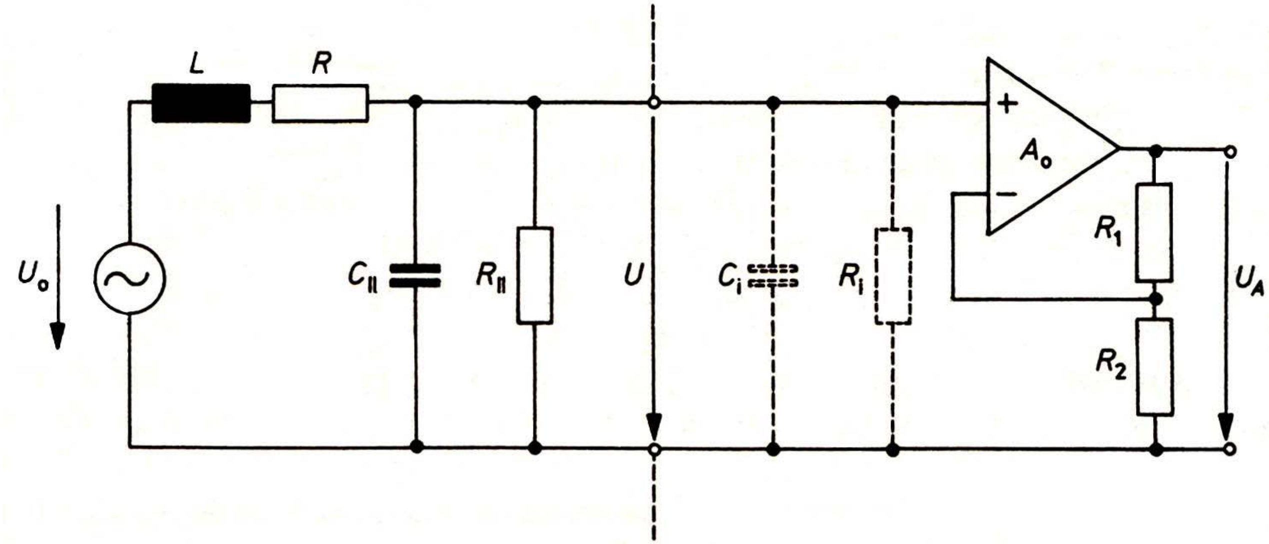

$$\omega_r = \frac{1}{\sqrt{KLC_{II}}} \qquad K = \frac{R_{II}}{R + R_{II}}$$

$$F(\omega) = \frac{K}{1 - \left(\frac{\omega}{\omega_r}\right) + \mathrm{i}\ 2D\frac{\omega}{\omega_r}} \qquad D = \frac{\sqrt{K}}{2}\left[\frac{\sqrt{\frac{L}{C_{II}}}}{R_{II}} + \frac{R}{\sqrt{\frac{L}{C_{II}}}}\right]$$

Frequency responses of the search coil

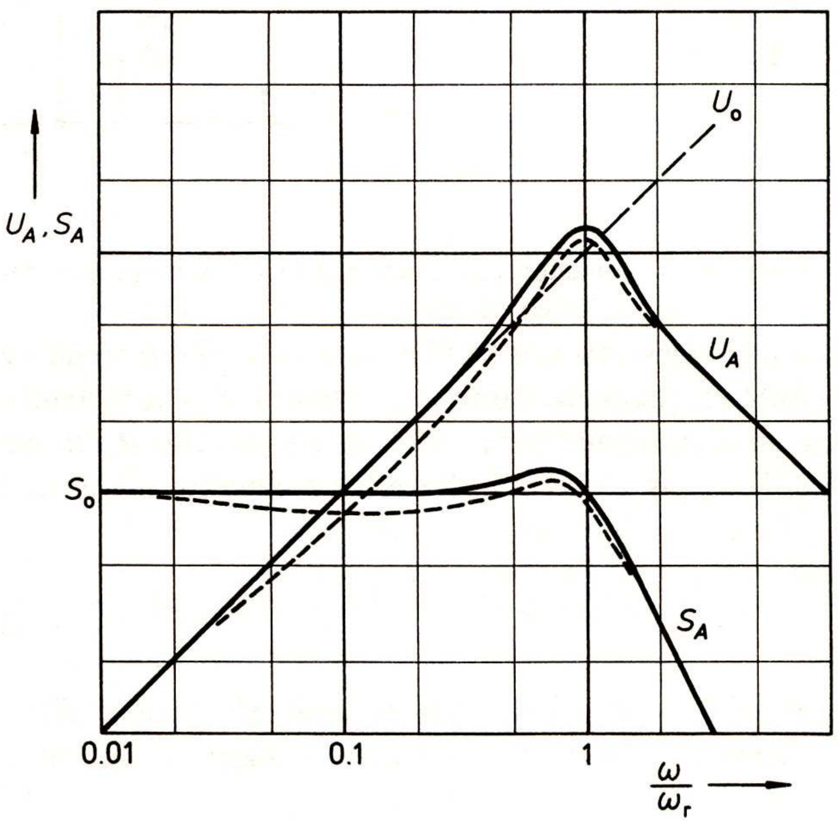

Frequency responses of the sensitivity S_A and the output voltage U_A of an induction coil sensor with a voltage amplifier at a constant magnetic field amplitude.

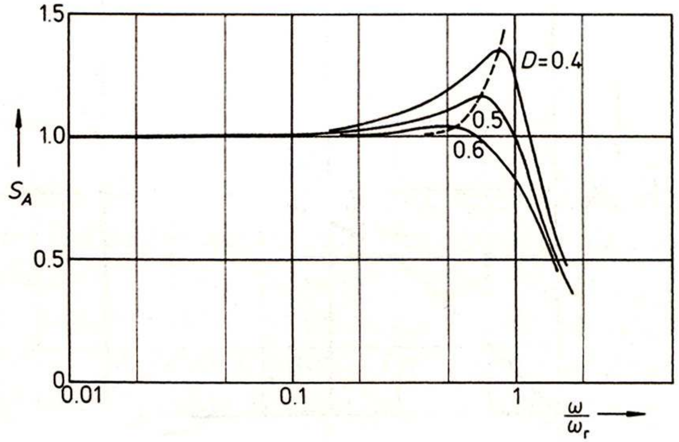

Resonance step-up of the sensitivity S_A at different values of the damping D.

Sensor with transformer coupled negative feedback to the coil.

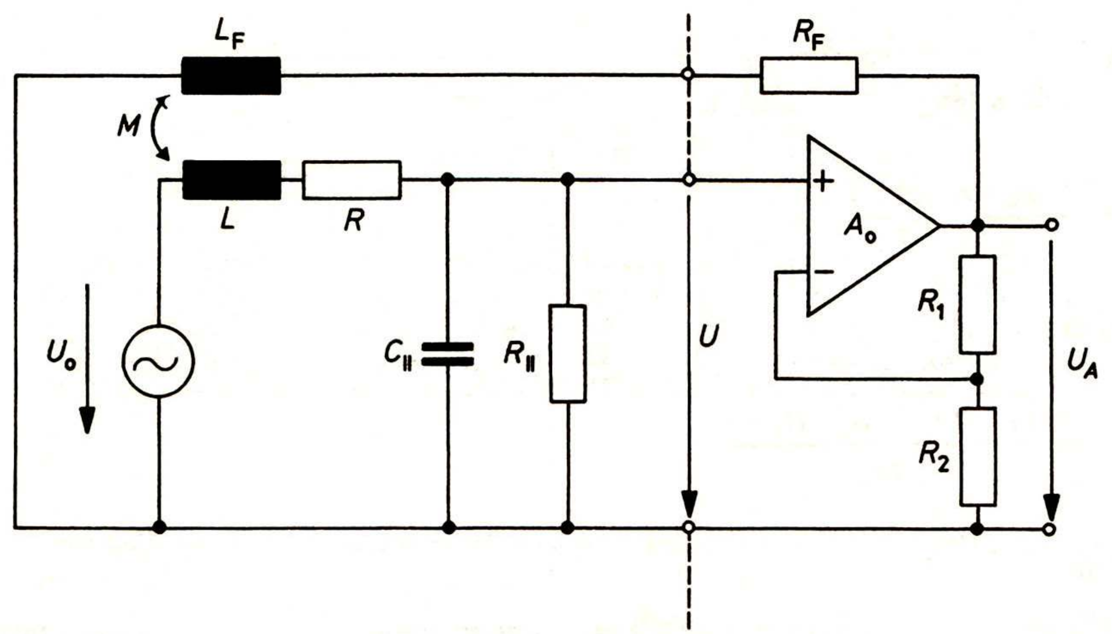

$$U_A(\omega) = A\left(U_0(\omega) - \mathrm{i}\omega M \frac{U_A}{R_F}\right) \cdot F(\omega)$$

$$U_A = U_0 \frac{A \cdot F(\omega)}{1 + \mathrm{i}\omega A \dfrac{M}{R_F} \cdot F(\omega)}$$

$$U_A = \frac{U_0(\omega)\, R_K}{\omega M} \cdot \frac{\mathrm{i}\omega / \omega_1}{1 + \mathrm{i}\omega / \omega_1} \cdot \frac{1}{1 + \mathrm{i}\omega / \omega_2}$$

$$\Delta f = \frac{A \cdot M}{2\pi \cdot L \cdot R_F \cdot C_{II}}$$

Induction coil connected to a voltage amplifier with transformer coupled negative feedback to the coil.

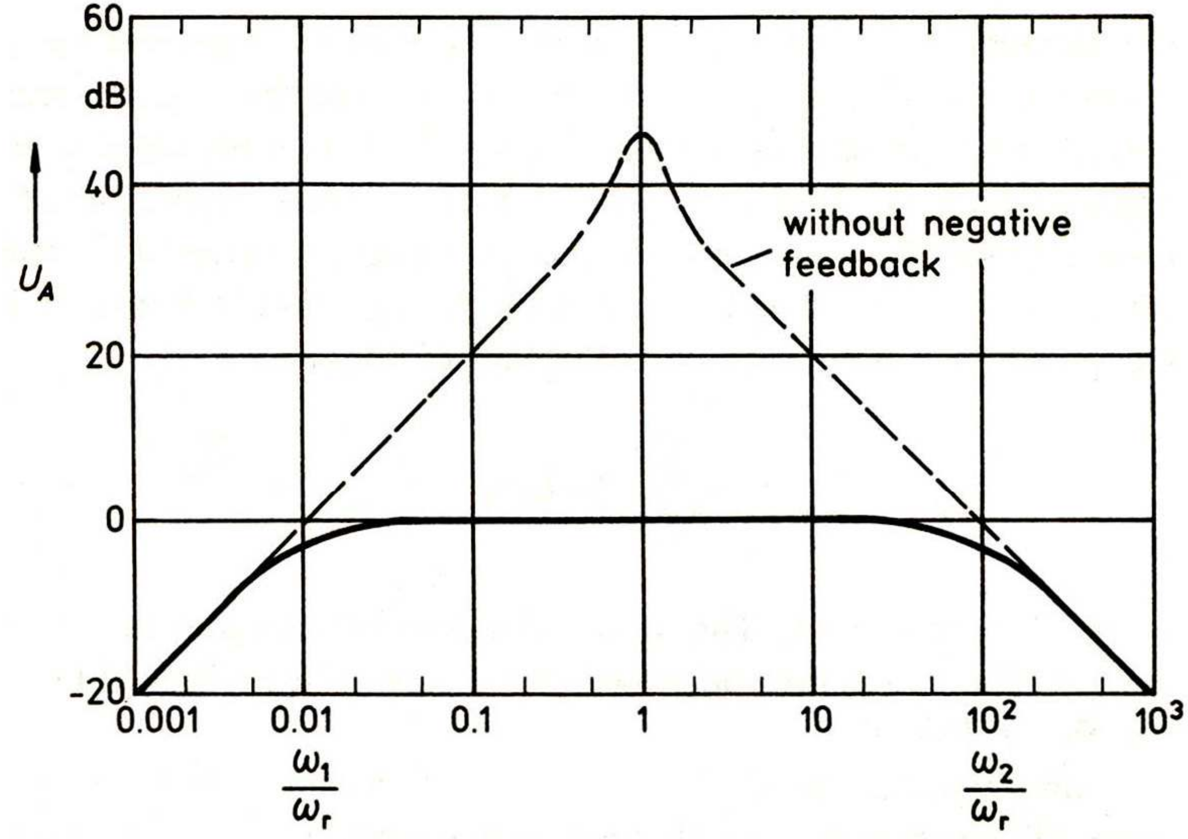

Frequency response of the output voltage U_A of an induction coil sensor with negative feedback transformer coupled to the coil

Schlumberger

BF-4 Magnetic Field Induction Sensor

PERFORMANCE

- Frequency range: 0.0001 to 700 Hz
- 3-dB frequency corners: 0.3 Hz, 500 Hz
- Sensitivity (flat region): 0.3 V/nT (standard)
- Power consumption: 12 mA at ±12 V

MECHANICAL SPECIFICATIONS

- Housing: Black Amalgon® straight tube
- Length: 142 cm (56 in)
- Diameter: 6 cm (2.4 in)
- Weight: 7.9 kg (17.4 lbm)
- Connector: 8-pin Tajimi

FREQUENCY RANGE

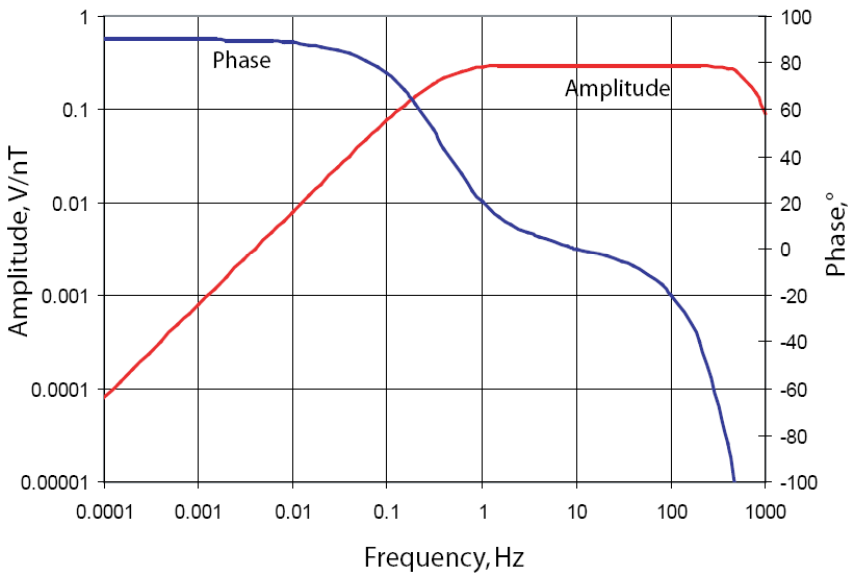

NOISE PERFORMANCE

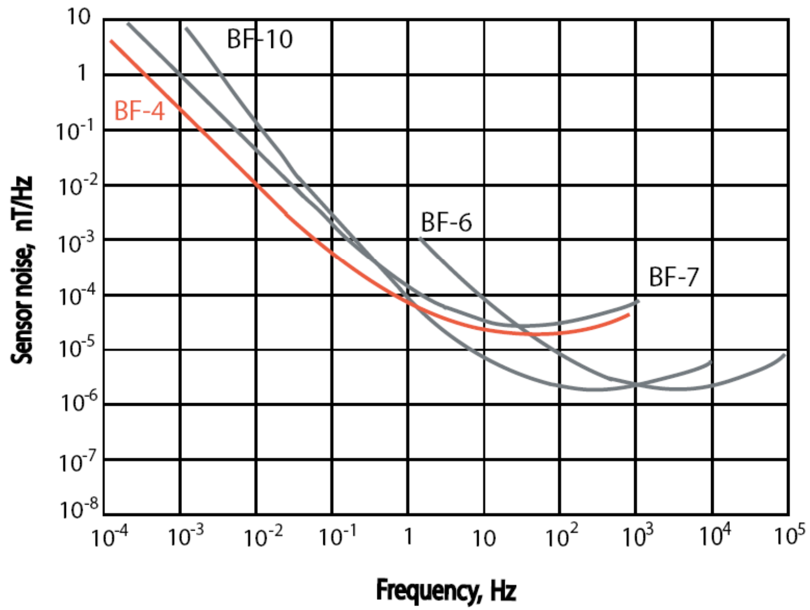

Applications of search coil magnetometer

Application	Observation station or Manufac-turer/Type	Number of meas-uring com-ponents	Coil (turns/wire)	Core material	Core length × diameter [cm]	Frequency range	Coil sensitivity	Remarks	Infor-mation source
Micropulsations	Siple, Antarctica	3	$5 \cdot 10^5$/AWG 36	annealed Permalloy	180 × 2.5	0.001...10Hz		0.4 pT · Hz ≙ 1 quant. step	[45]
	L'Aquila, Italy	3	$2 \cdot 10^5$	Vacoperm 100	200 × 1.5	0.001...10 Hz	0.7 mV/(nT·Hz)	flux feedback	[46]
Magnetotellurics	–		$5.6 \cdot 10^5$	Mumetal	150 × 3.5 ϕ	0.001... 2 Hz	2.6 mV/(nT·Hz)		[47]
	–	3	$3 \cdot 10^4$/AWG 22	laminated Moly-permalloy	183 × 2.5 ϕ	0.0006...10 Hz			[48]
	Metronix 878	1	40000	laminated Mumetal	120 ×2.3 ϕ	0.00025...300 Hz	73 μV/(nT·Hz)	flux feedback	[49]
Audio-Magnetotellurics	University of California	1	45000/AWG 31	laminated Mumental	60 × 1.6 ϕ	0.2 Hz... ≈ 10 kHz		current amplification	[50]
	US Geological Survey	2	2372/AWG 14	ferrite frame (2 components)	36 × 36 × 3.8/1.8		23 μV/(nT·Hz)	80 : 1 iron core transformer output; f_{res} = 1.3 kHz	[50]
	Metronix 879	1	10000	ferrite	90 × 2.2 ϕ	1 Hz...20 kHz	8.6 μV/(nT·Hz)	flux feedback	[49]

Spacecraft (Experiment)	Number of measuring components	Coil (turns/wire)	Core		Frequency range	Coil sensitivity	Remarks	Information source
			material	length × diameter [mm]				
HELIOS A and B (AC Magnetometer)	3	60000/50 μm	bundle of 0.2 ⌀ Mumetal wires	350(320) ×6 ⌀	5 Hz...2.2 kHz	6 μV/(nT·Hz)		[51]
ISEE 1 (2) (Plasma Wave Investigation)	3 (1)	10000	Mumetal	410	...10 kHz	3.5 μV/(nT·Hz)		[52]
ISEE 3 (as above)	1	80000/AWG47	nickle-iron	394 × 4.8 ⌀	...500 Hz	13 μV/(nT·Hz)		[53]
Dynamic Explorer A	1	5000/AWG40	laminated high-μ material	400	1 Hz...1 kHz			[54]
(Plasma Wave Instrument)	1	1/aluminium-tube	air-core	frame 800 × 1250	0,1...400 kHz		matching transformer	
AMPTE	1		laminated Mumetal	260 × 11 ⌀	20 Hz...60 kHz		flux feedback	[55]
(Plasma Wave Instrument)	1		ferrite	260 × 11	10kHz...2MHz			
Sakigake/MST 5 (Plasma Wave Probe)	1	10^5	ferrite	5 ⌀	70 Hz...2.8 kHz	threshold 5 pT		[56]
GALILEO Jupiter Orbiter	1	50000/70 μm		266	10 Hz...3.5 kHz			[57]
(Plasma Wave Investigation)	1	2000/140 μm		275	1...50 kHz			
GALILEO Jupiter Atmospheric Probe (Lightning and Radio Emission Detector)	1	1500/60 μm	ferrite	300 × 5 ⌀	0,1...100 kHz	0.18 μV/(nT·Hz)		[57]
ULYSSES (Radio and Plasma Wave Experiment)	2		laminated high-μ material		10...500 Hz		flux feedback	[58]

Developed search coil magnetometer using amorphous ribbon

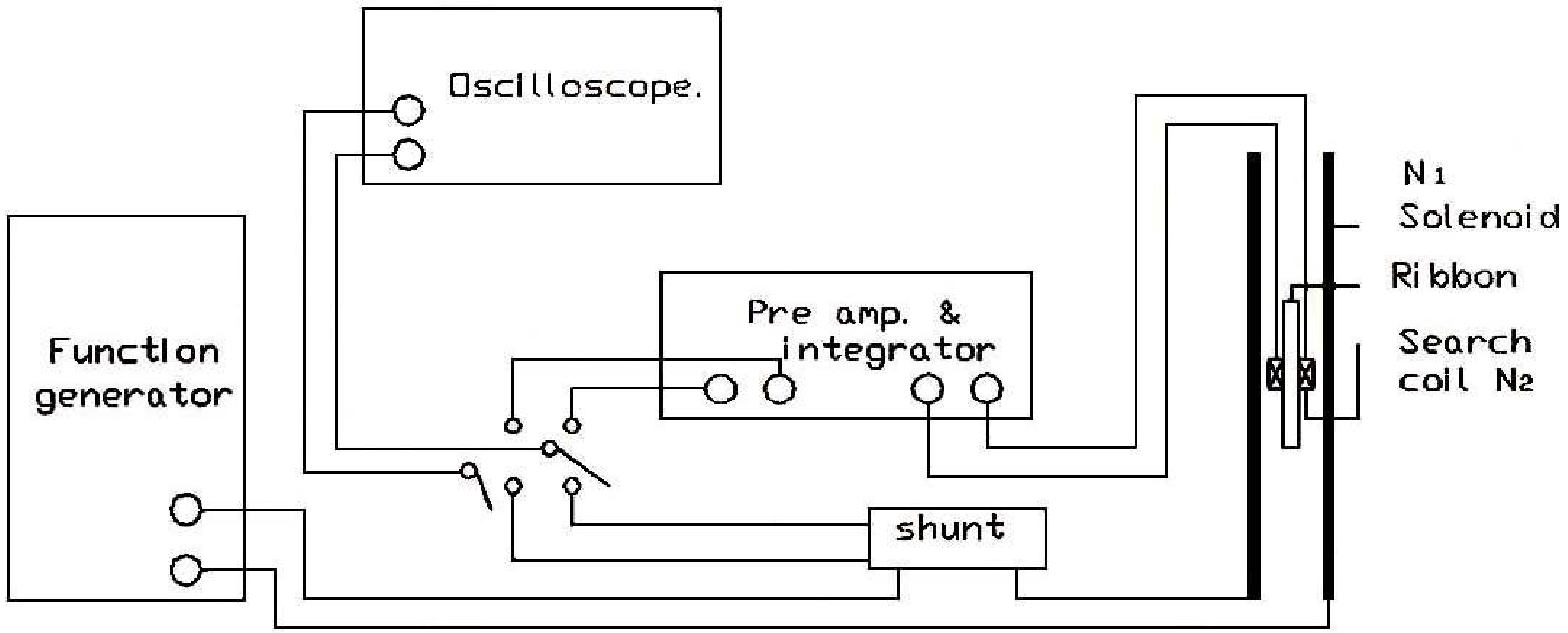

Experimental setup for the effective permeability measurement

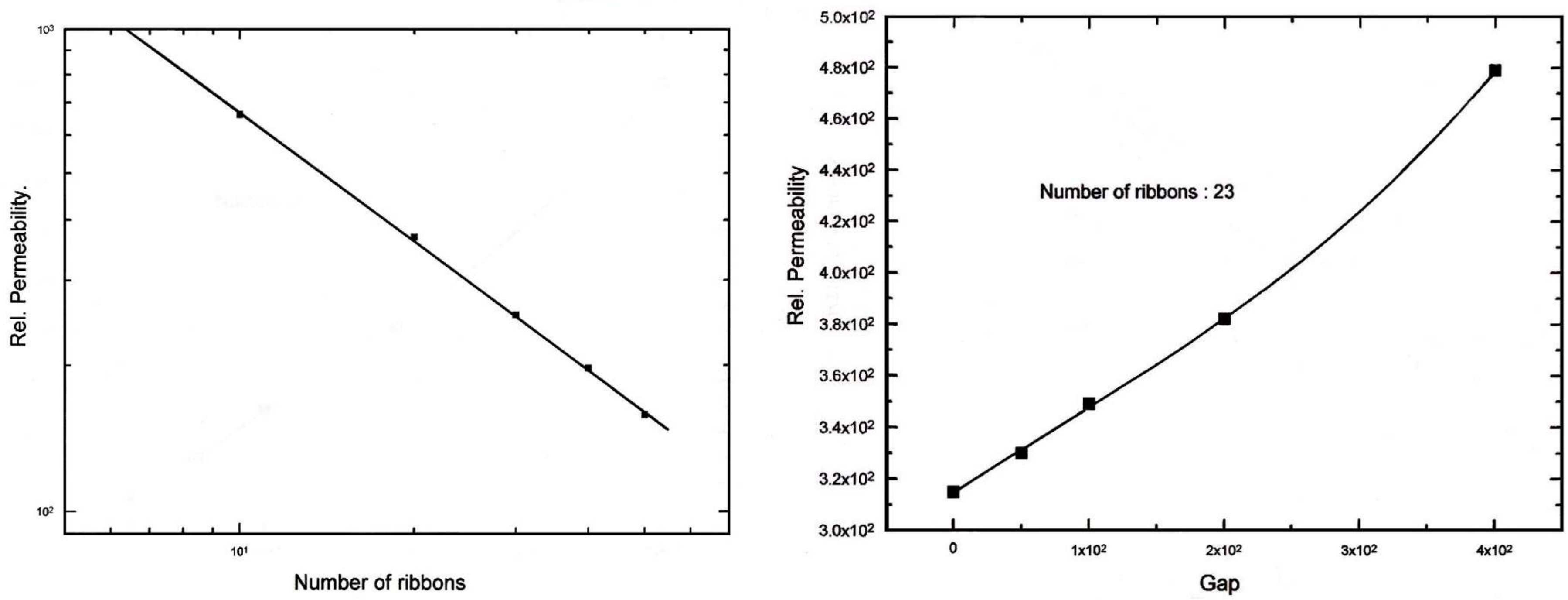

Relative permeability depending on the numbers of ribbon(a)
and the air gap between ribbons.

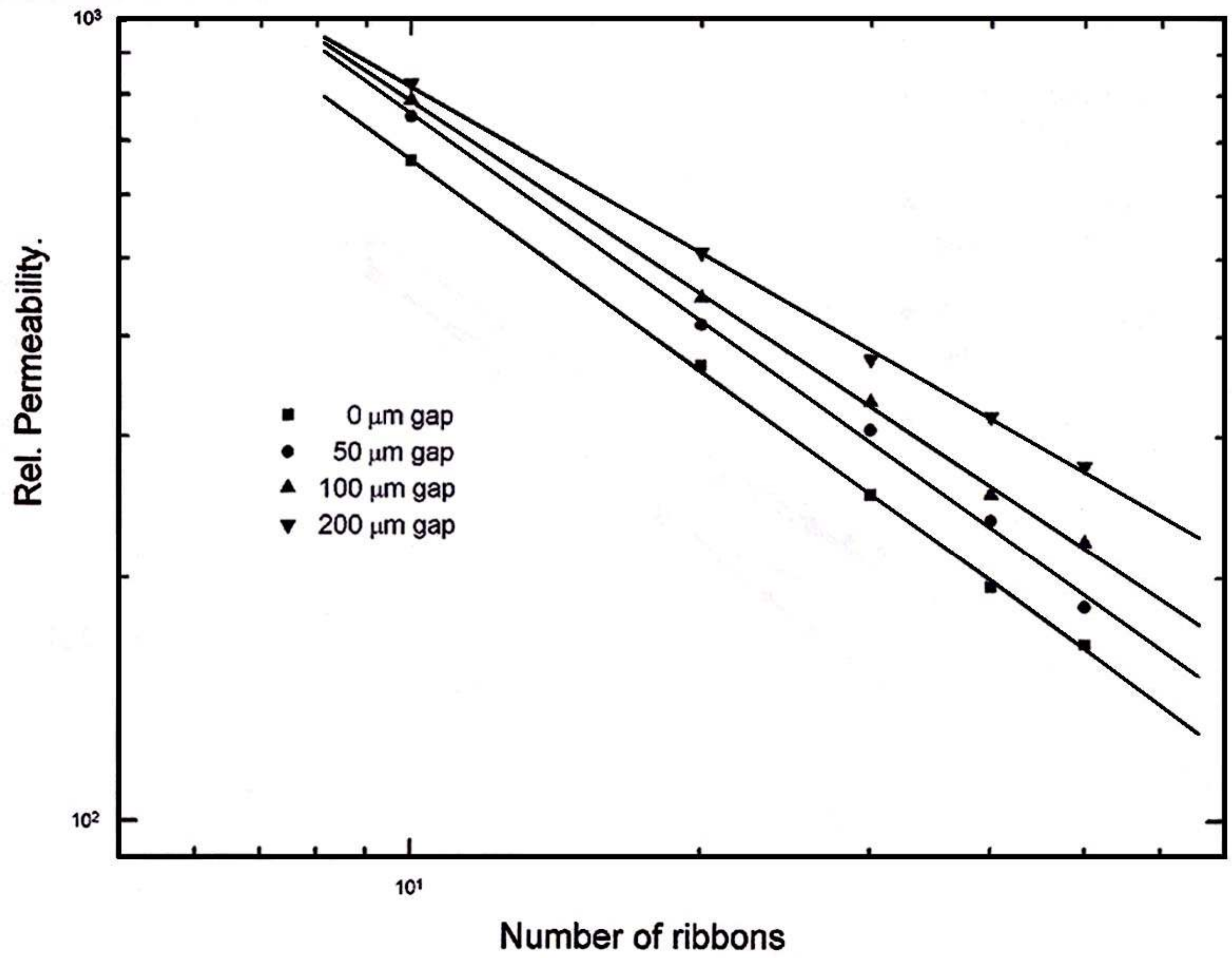

Relative permeability depending on the number of ribbons
for the different air gap between ribbons.

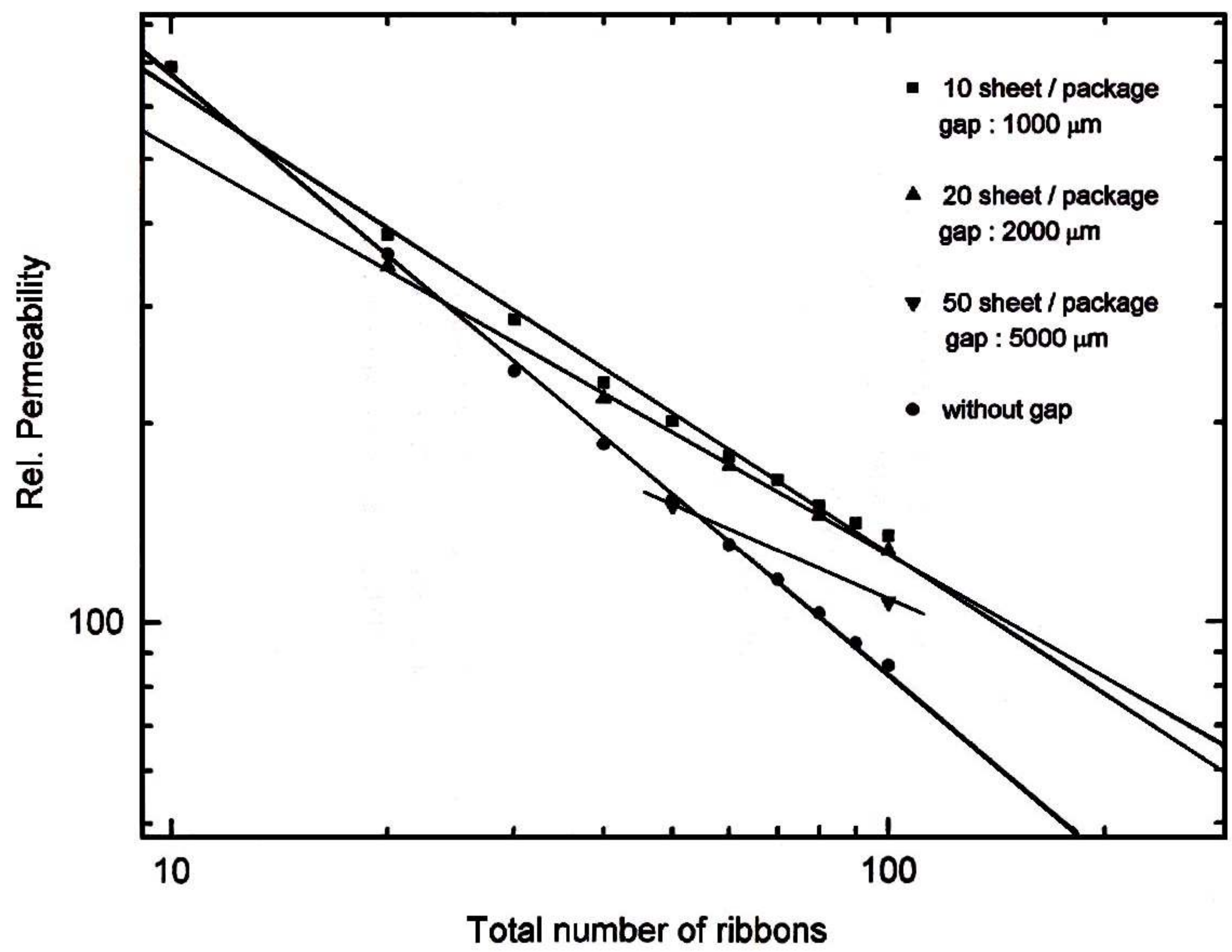

Relative permeability depending on the total number of ribbons for the different air gap between ribbons.

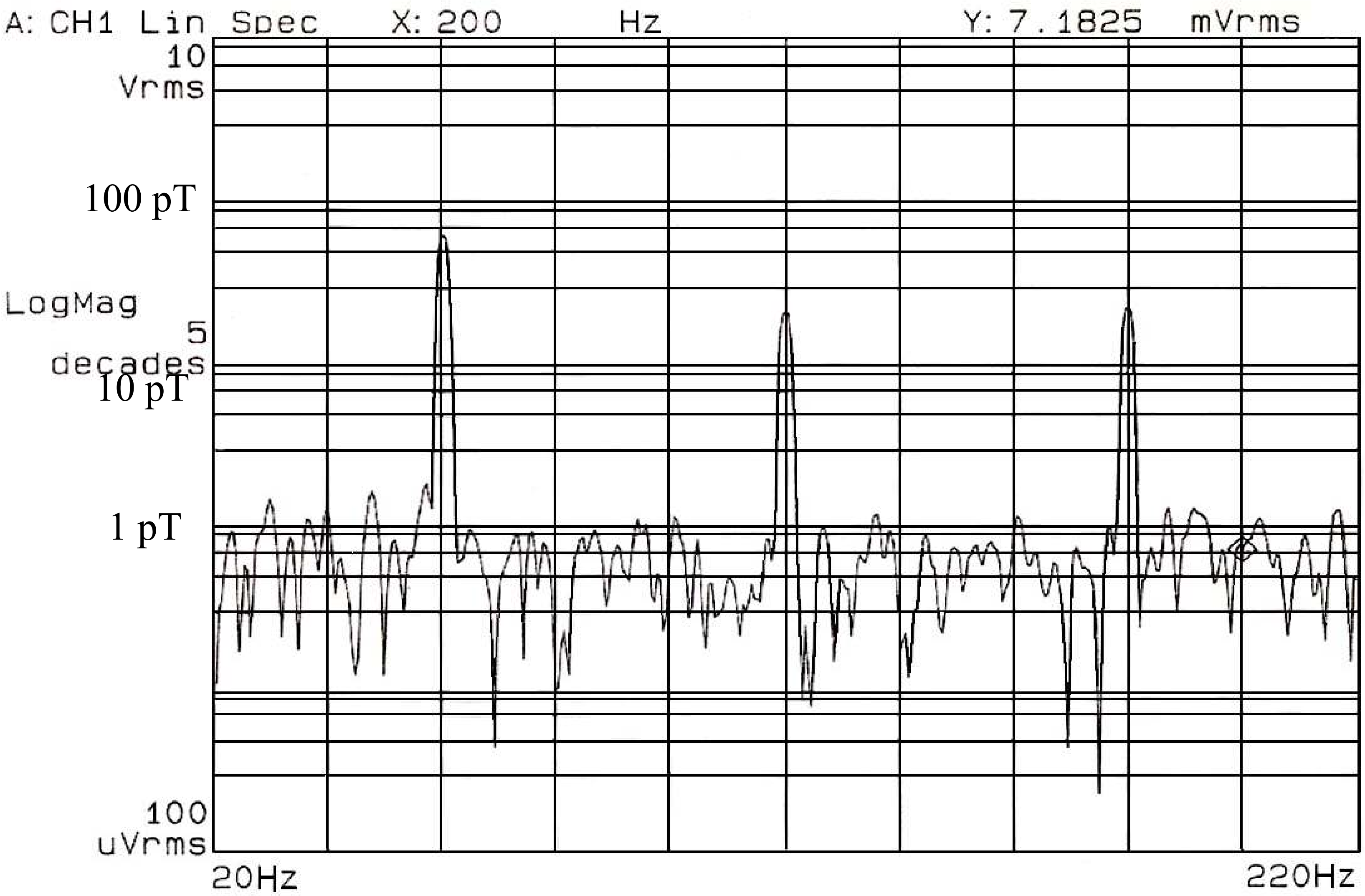

Noise spectrum of the developed search coil magnetometer.

Hall 효과

$$U_{HL} = \frac{R_H I}{t} B$$

$$E_H = -\frac{1}{ne} J_x B$$

$$R_H = -\frac{1}{ne}$$

$$R_H = \frac{P\mu_h^2 - n\mu_e^2}{e(n\mu_e + p\mu_h)^2}$$

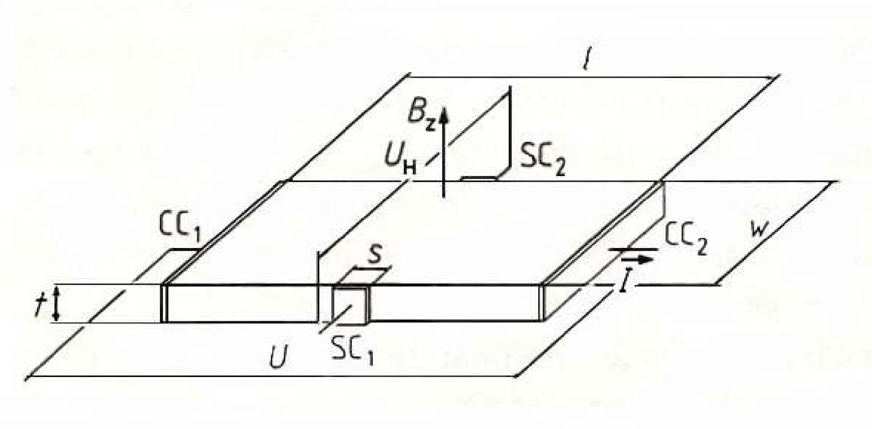

Rectangular Hall plate (cc_1,cc_2: current constant sc_1,sc_2: sensor constant *I*: bias current *U*: voltage drop ,U_H: Hall voltage

Physics : carrier concentration and kind of carrier measurement

Engineering : magnetic field measurement

Current Measurement

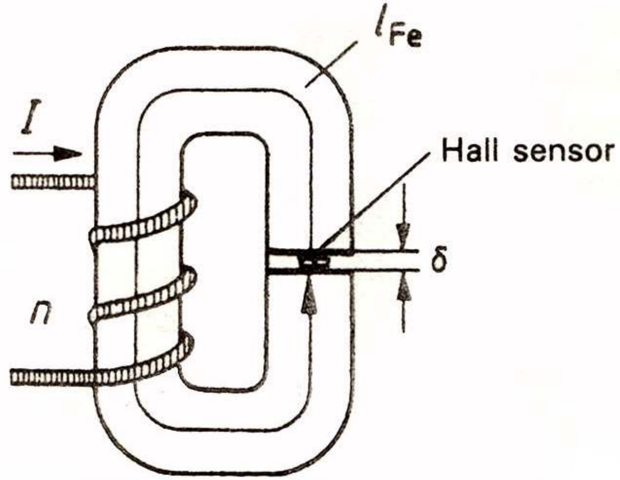

Arrangement for noninvasive current measurement using an iron core. The current to be measured produces a proportional magnetic field which can be measured in the air gap.

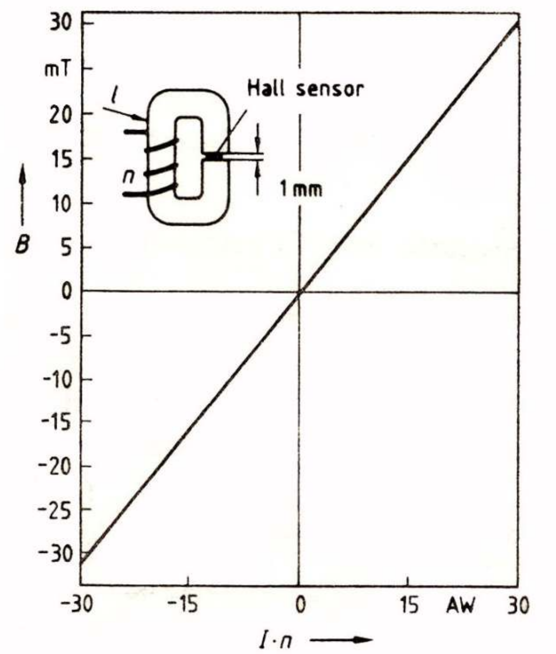

Characteristic curve produced by the current

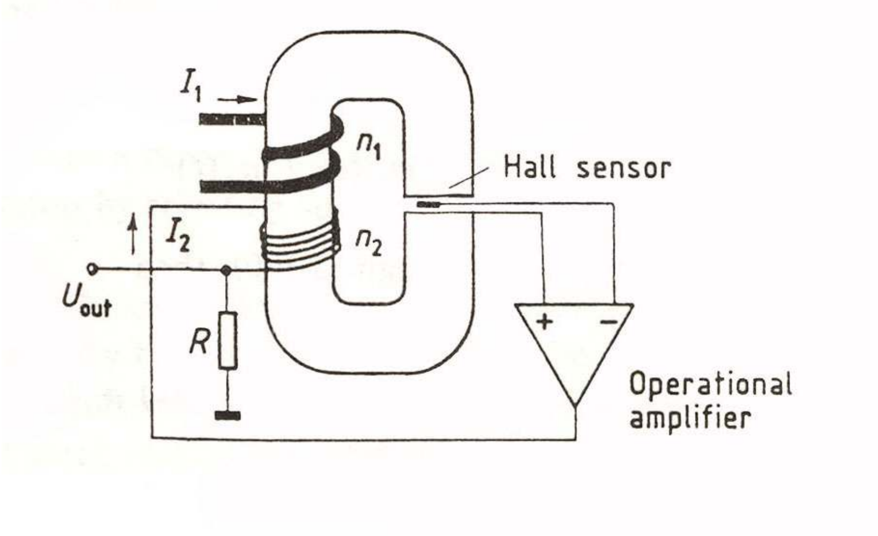

Arrangement for indirect noninvasive current measurement using the compensation principle. An iron core as represented in Figure 3-29 is held field free by injection a current into a compensating coil wound on the core which offsets the field generated by the current being measured. The Hall effect sensor in the air gap serves as a null indicator.

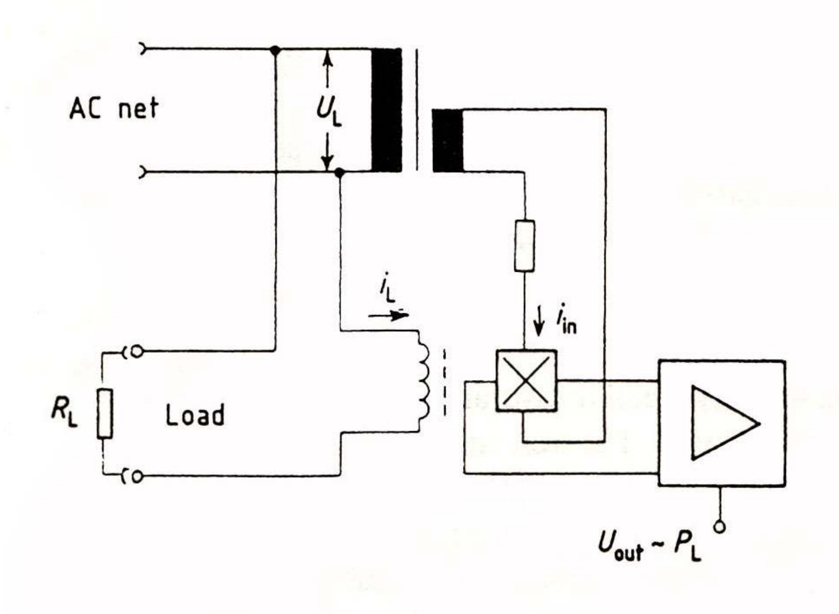

Circuit diagram for AC-power measurement using a Hall effect sensor.

DC Power Measurement

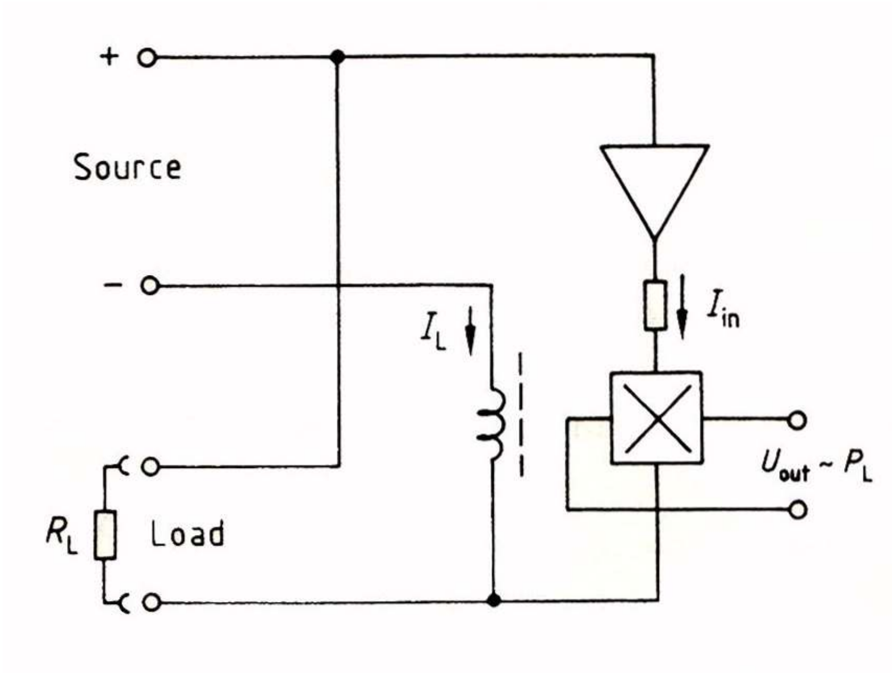

Circuit diagram for DC-power measurement using a Hall effect sensor.

Noncontact Position Sensing

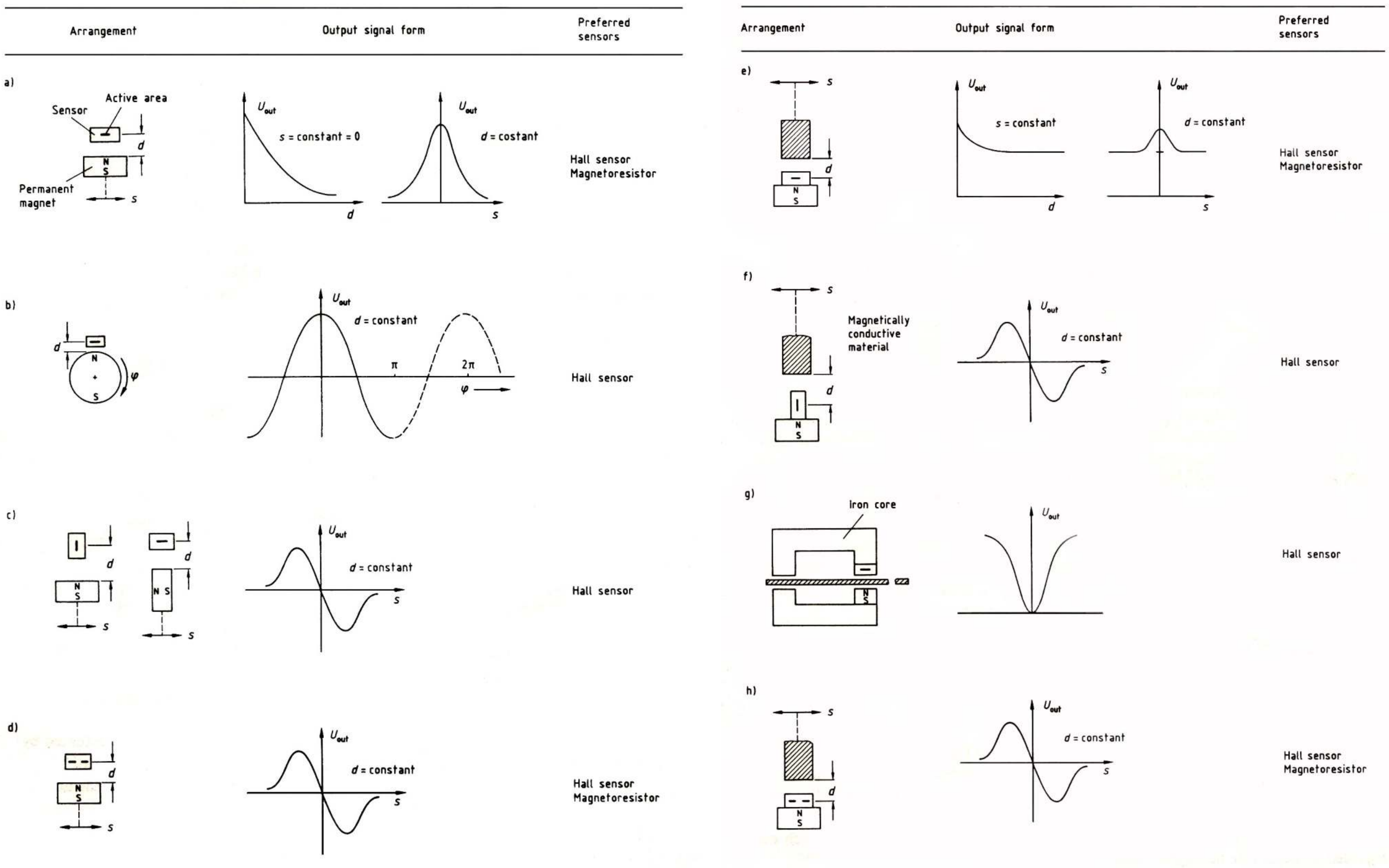

Current Sensor Based on Hall Sensor and Magnetic Core for Hybrid Vehicle

K.H. Yeon[1], S.D. Kim[1], and D. Son[2]
[1]Auto industry co.,14F Hanshin IT tower Guro Gu, Seoul, Korea
[2]Hannam University,Ojung dong 133, Daejeon Rep. of Korea

Current Sensor Based on Hall Sensor and Magnetic Core

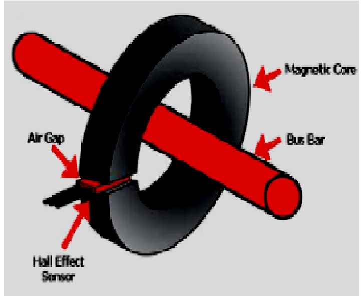

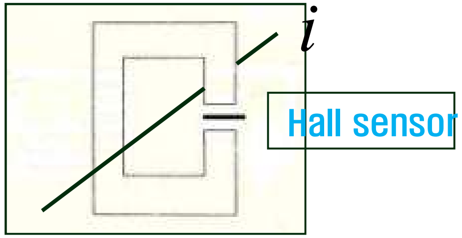

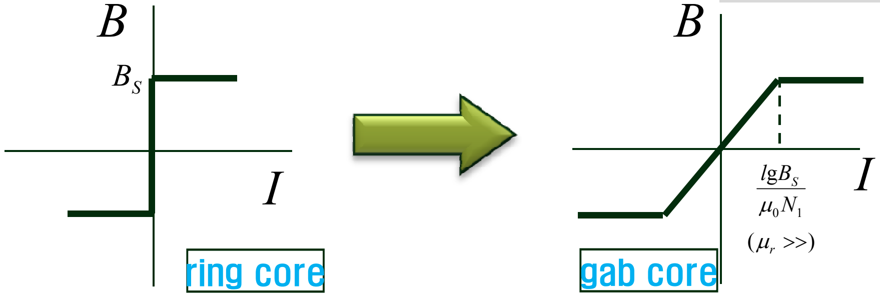

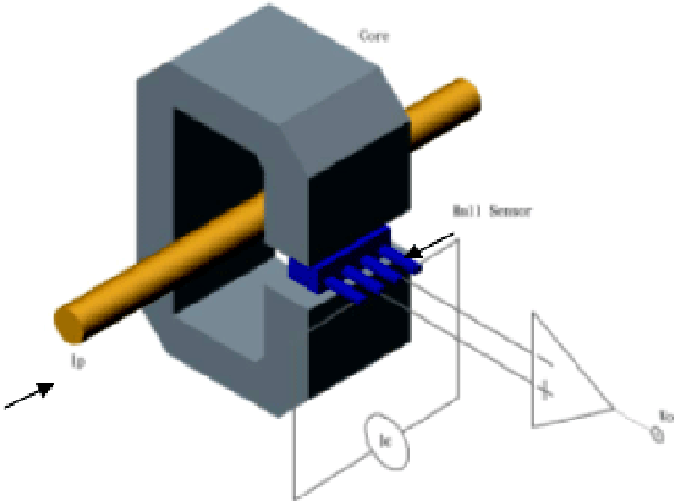

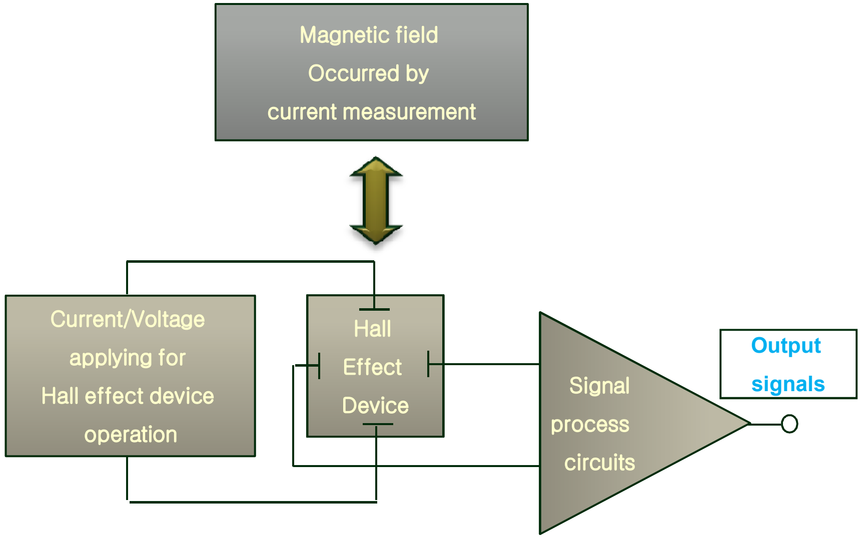

Developed Current Sensor

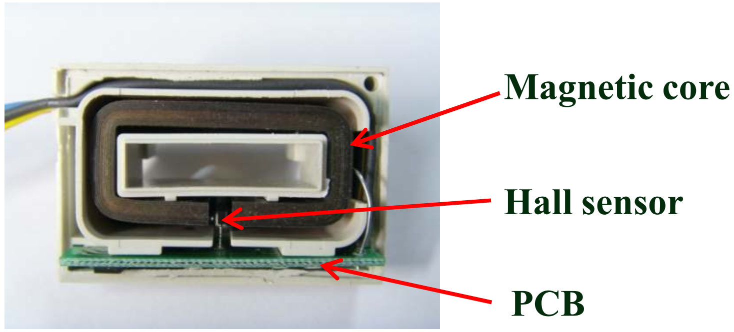

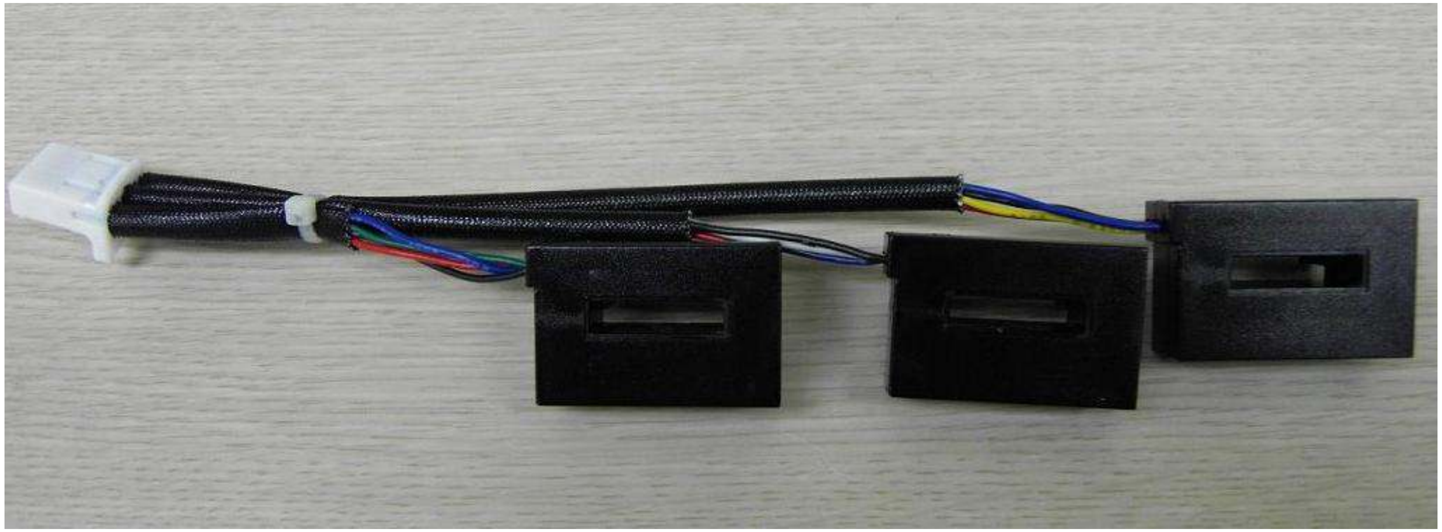

Characteristics of the Current Sensors

◆ Linearity of the sensor

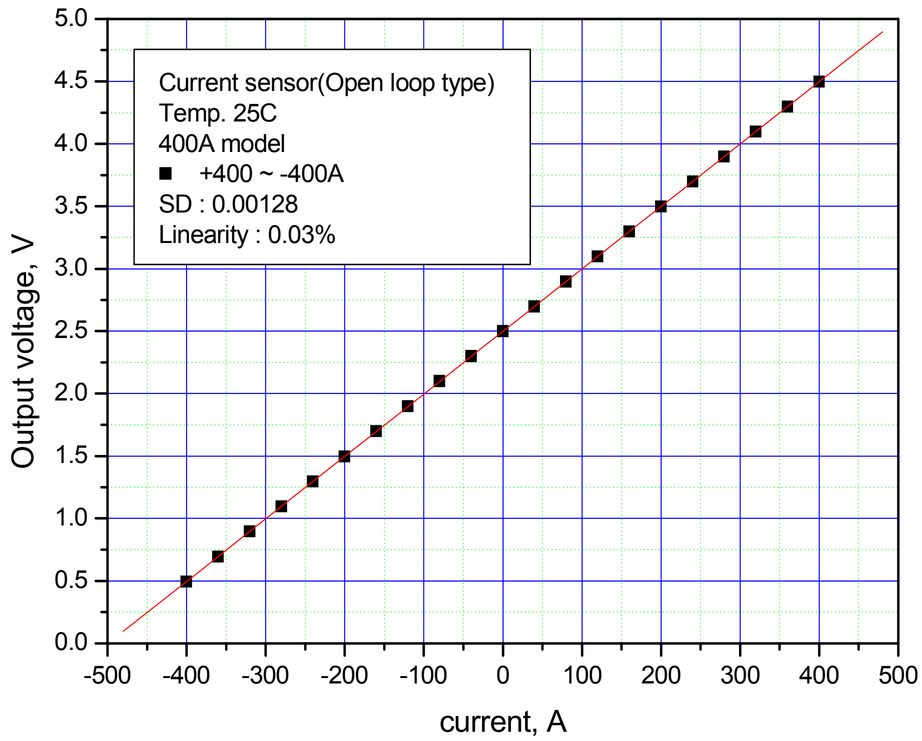

Temperature : 25℃
Linearity : 0.03%
Measuring range : -400A ~ +400A

1000A ,10 V power supply

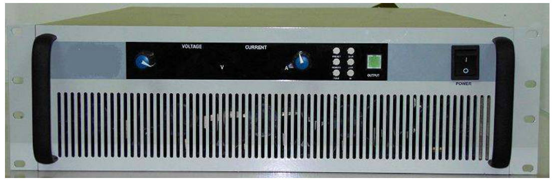

1000A Electronic Load

◆ Frequency bandwidth

Gain bandwidth : 3 MHz
Current : 10 A

Frequency bandwidth : 100 kHz

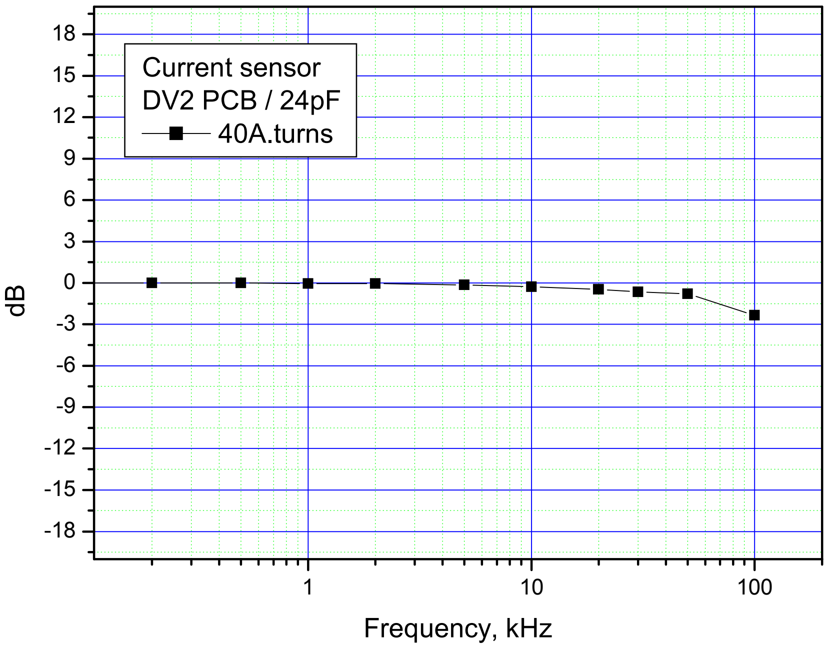

Sensor output voltage vs. frequency
at applied current of 40 A·turns.

Temperature : 25℃
Current : 40A.turns
Frequency range 100 Hz ~ 100 kHz

측정온도 : 25℃

주파수특성 : 30kHz 이상(3dB 기준)

측정전류 : 40A.turns(4A, 10턴)

측정주파수 : 100Hz ~ 100kHz

Magnetoresistance effect(AMR)

What is Magnetoresistance

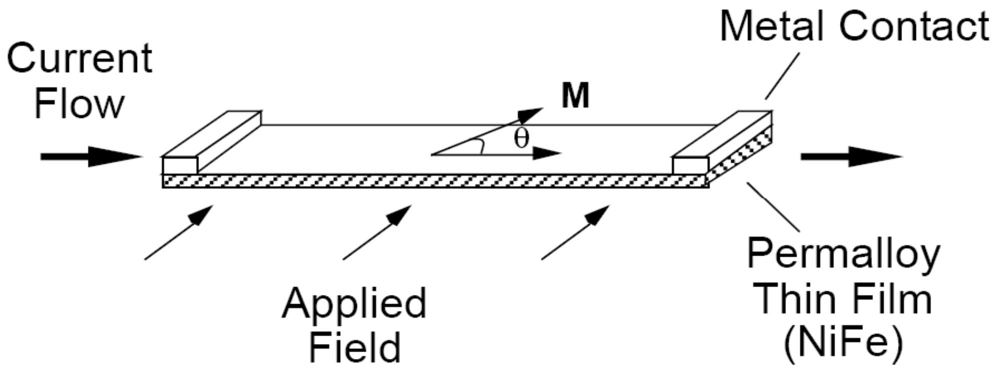

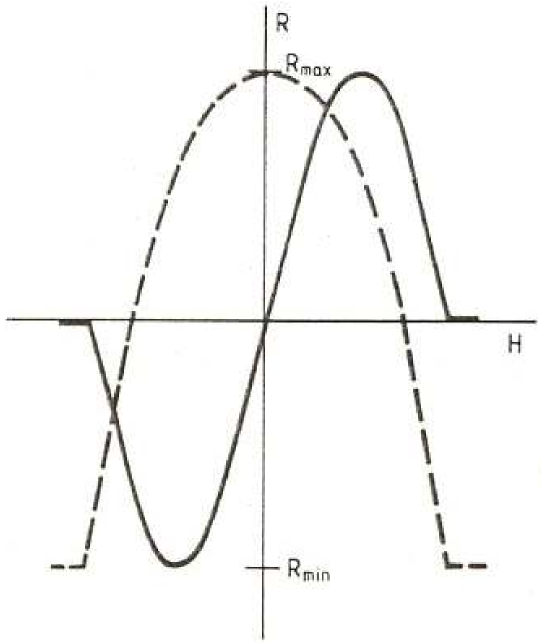

$$\Delta R_x \approx \Delta R_m (h_x^{\ 2} \cos 2\theta + h_x \sqrt{1 - h_x^{\ 2}} \sin 2\theta - \frac{1}{2} \cos 2\theta$$

$$\Delta \rho / \rho \approx 2 - 3\%$$

New effect: GMR, CMR and GMI

$$\Delta \rho / \rho \geq 10\%$$

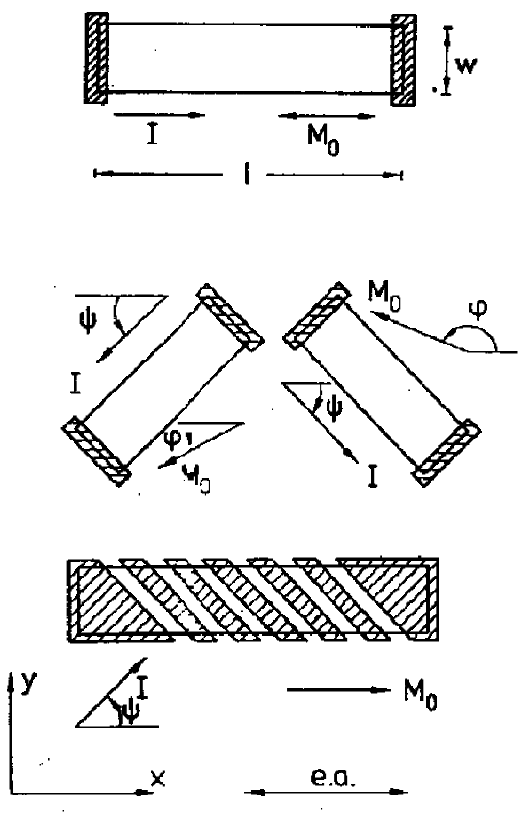
w
I
M0
l
ψ
I
M0
φ
φ1
M0
ψ
I
y
I
ψ
M0
x
e.a.

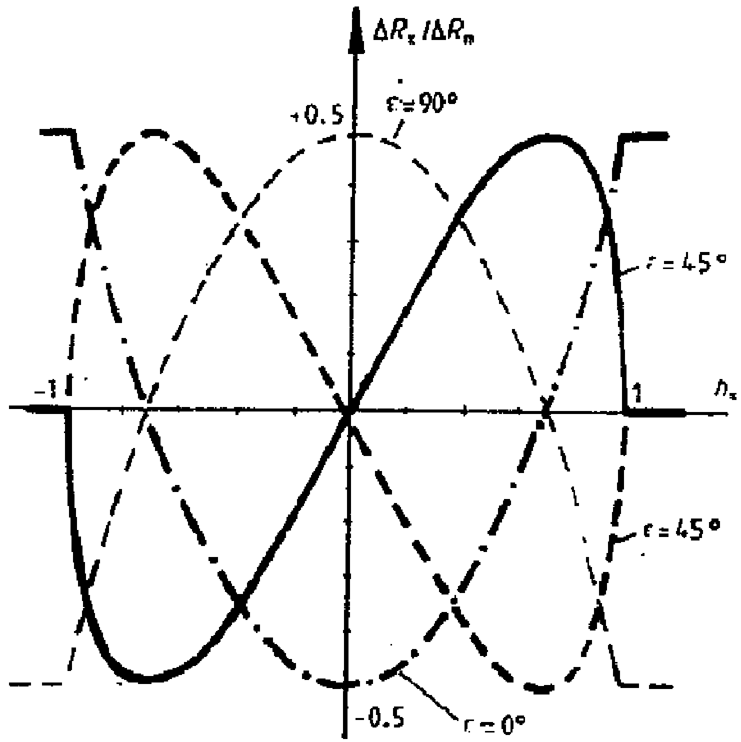
ΔRx/ΔRm
+0.5
ε=90°
ε=45°
-1
1
hx
ε=45°
-0.5
ε=0°

SENSiTEC
MagnetoResistive Sensors

AFF755B
MagnetoResistive Field Sensor

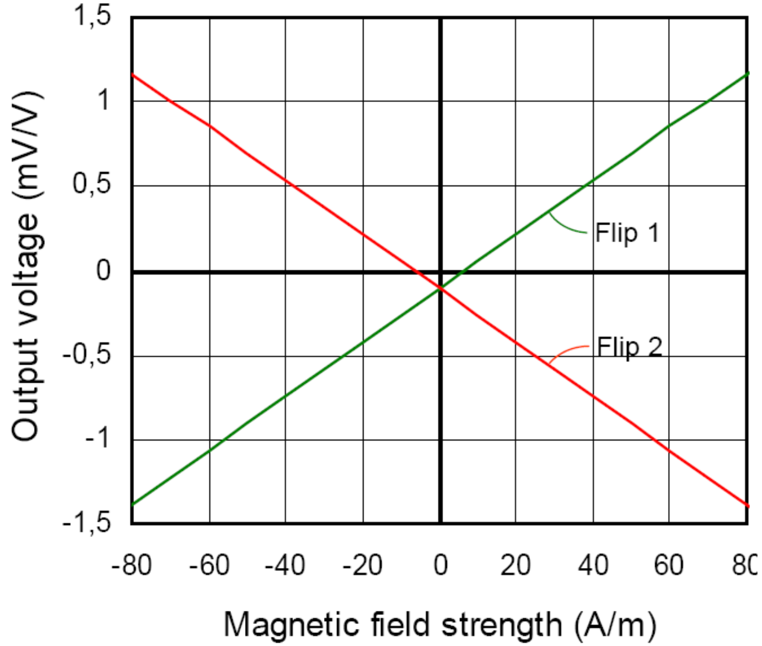

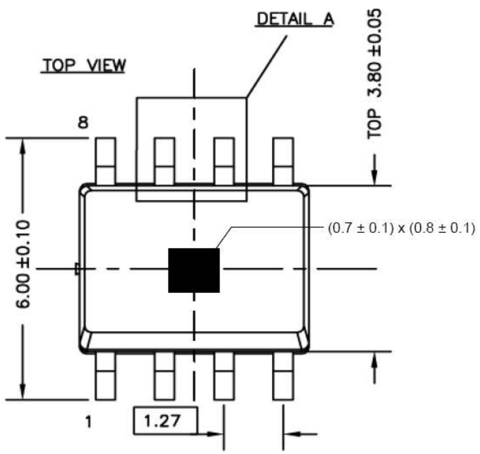

Package outline of SO8-housing.

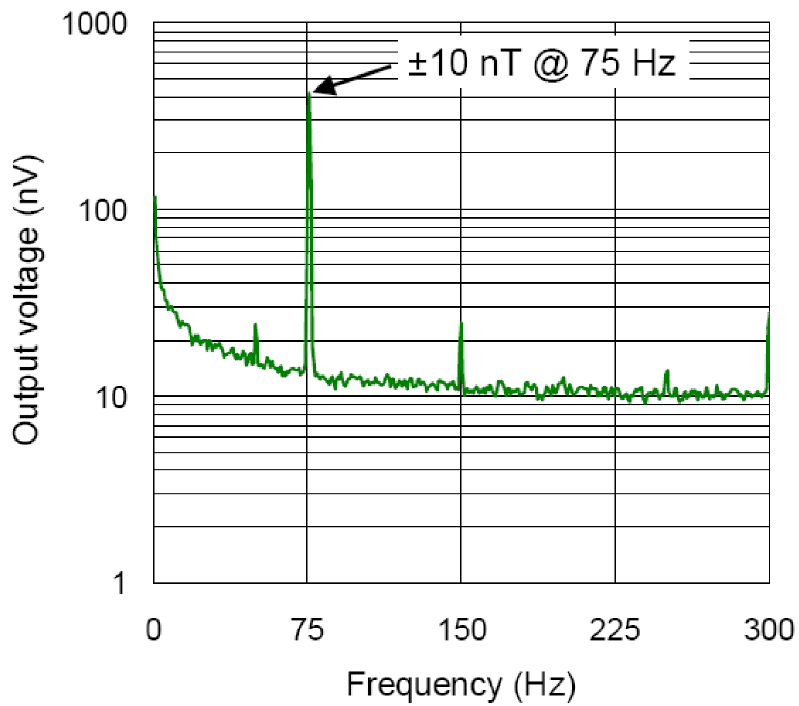

Two bridge configuration for rotational angle measurement

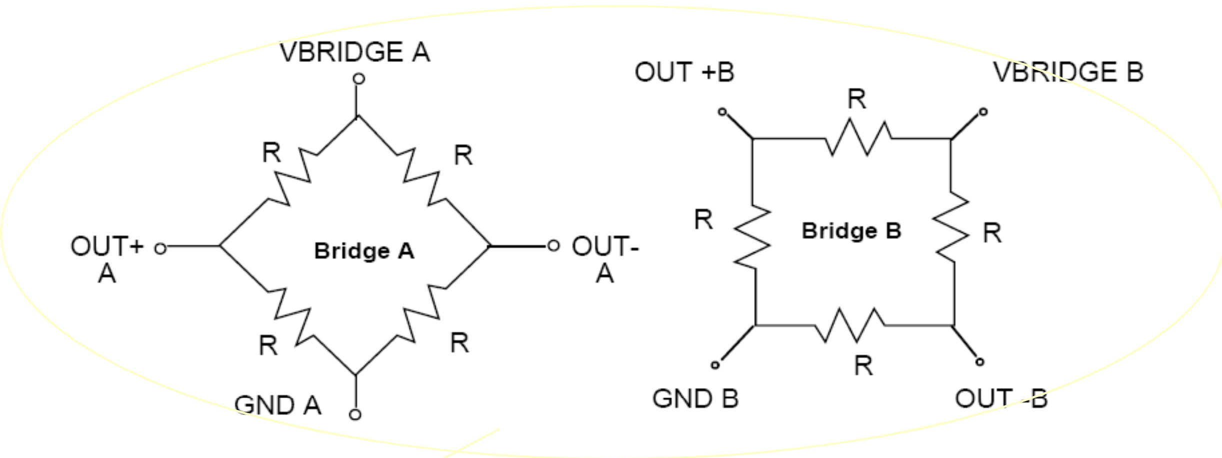

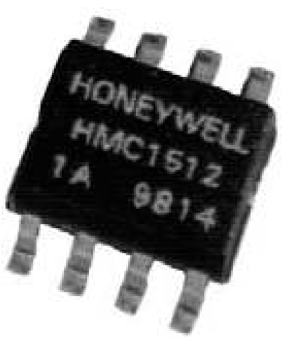

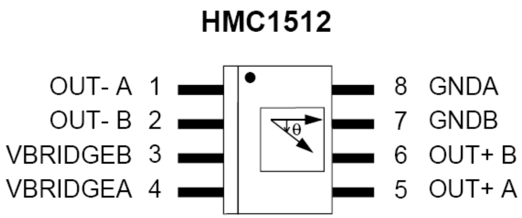

output voltage vs. magnetic field angle

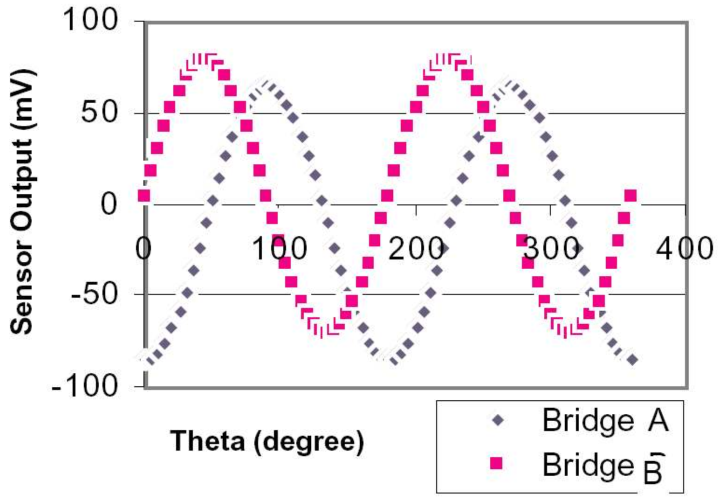

measurement angle more than 180º

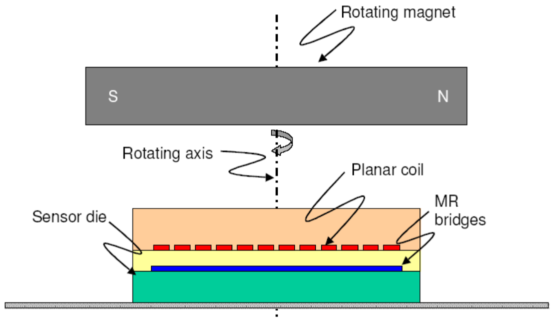

Sensor element and magnet set up for rotational measurement

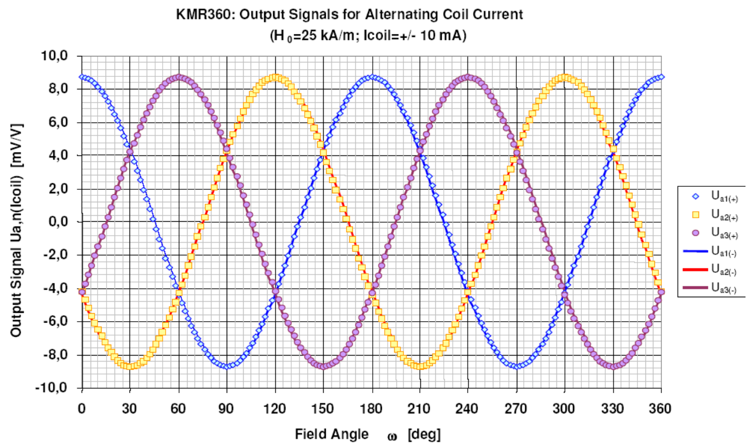

Typical output signal curves without (solid) and with (dashed) coil field for KMR360

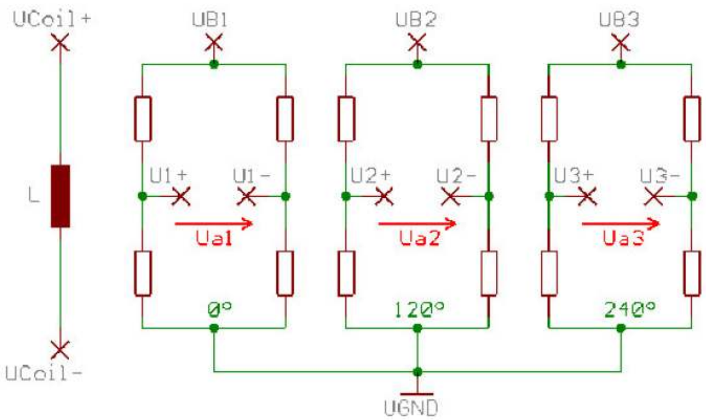

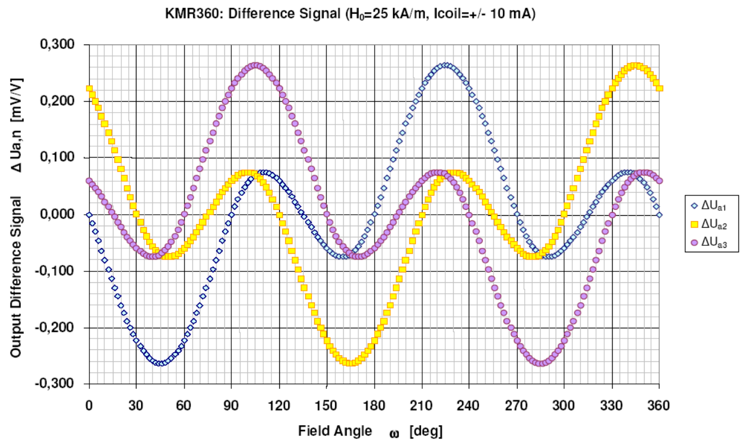

Signal change due to additional coil field

자동차 Engine Management System

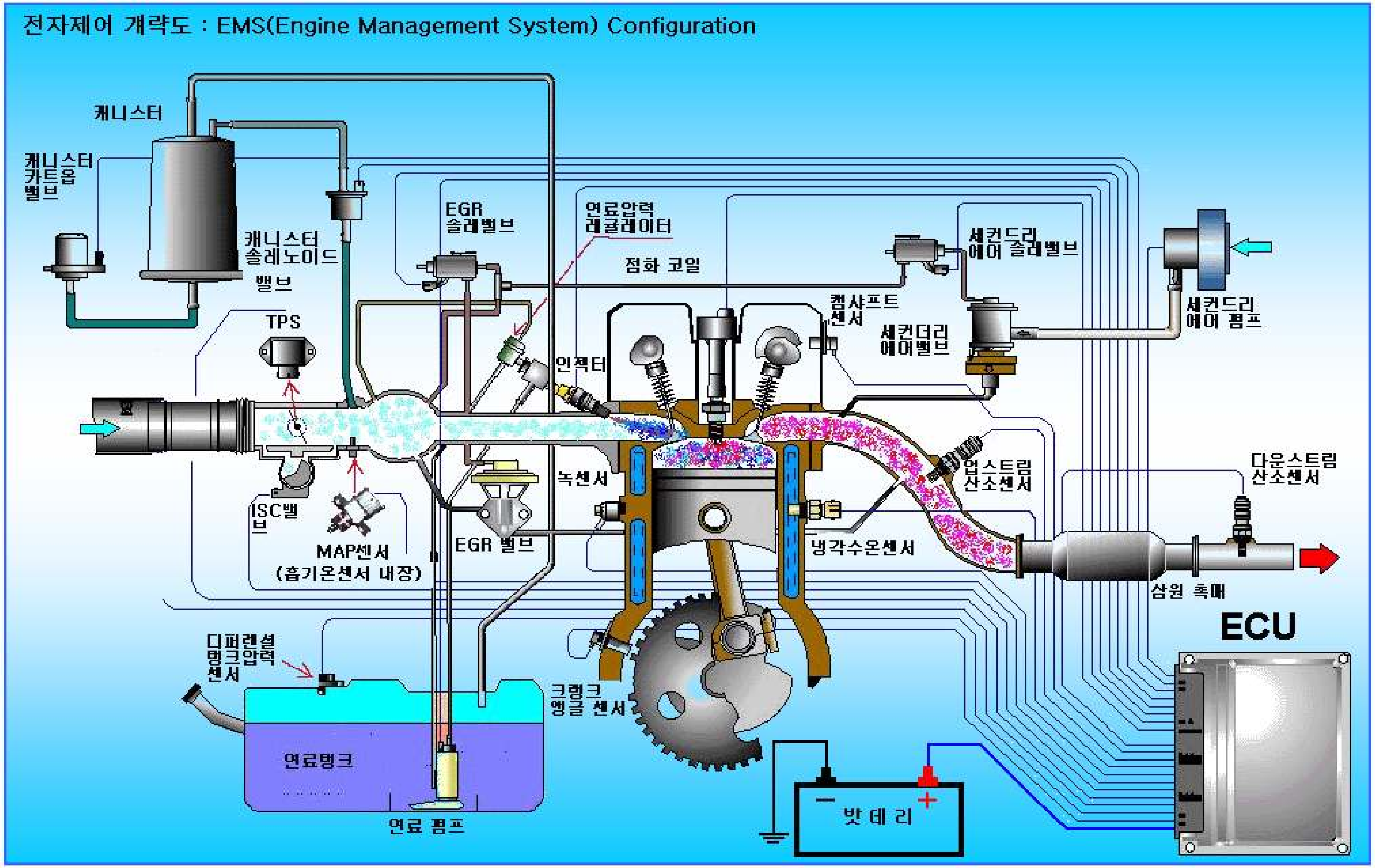

CTS®

Non-Contacting Position Sensors

581 Series

Typical Applications: Throttle & Pedal Position

Features / Benefits:

- Temperature Stable
- 10-12 Bit Resolution
- Recommend for High Thermal Shock, Water Spray/Immersion and Vibration Applications
- Adaptable for Multiple, Redundant Outputs
- Ultimate Performance at an Affordable Price
- Adaptable to most Automotive Sensor Applications
- Electronic Non-Contacting Solution where Potentiometer Devices are not Acceptable
- Mates with Framatome® Connector, Code 1 Black

TYPICAL SPECIFICATIONS

ELECTRICAL

Supply Voltage (V_S):	5 V ±10% Regulated
Supply Current (I_S):	2-6 mA Typical; 15 mA Max.
Output (V_O) Typical:	5% to 95%, 7% of V_S
Recommend Circuit Load (R_L, C_L) Pull-up:	20 K Ω Minimum, 0.01µF
Rotational Travel Electrical:	90° Standard, 110° Maximum
Independent Linearity:	±1% of V_S at 25°C
Step Response, 90% V_O:	<5 ms
EMI (Electromagnetic Radiated Immunity):	<50 mv Shift from 1 MHz to 2 GHz at 100 V/m & 200 V/m

Inductive and Eddy Current

Sensors Excited by Permanent Magnets

$$U(t) = -N \cdot \mathrm{d}\phi / \mathrm{d}\, t$$

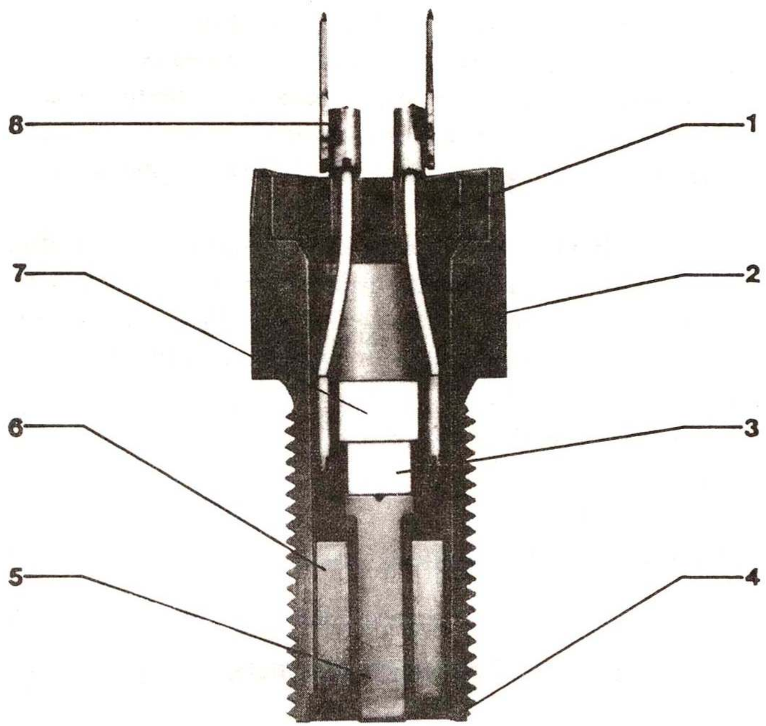

construction of an inductive sensor (courtesy VDO Adolf Schindling AG).

1) **constant socket,**
2) **terminal package,**
3) **permanent magnet,**
4) **cap,**
5) **soft magnetic core,**
6) **coil,**
7) **plate,**
8) **blade connector.**

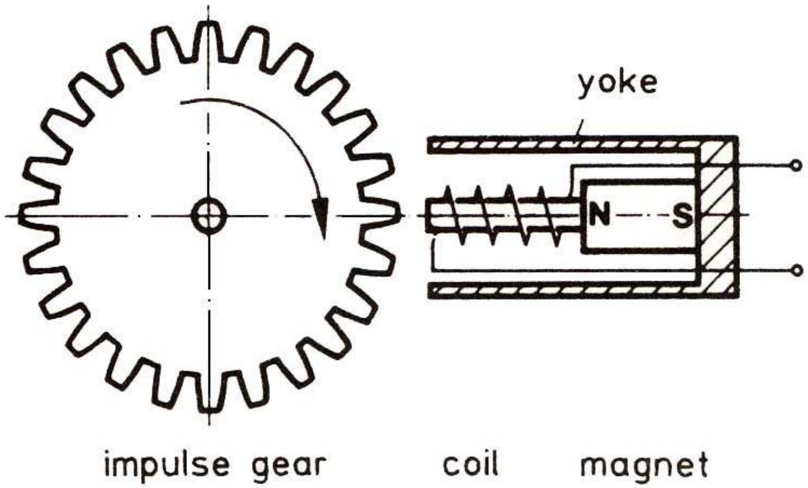

Sensor with yoke.

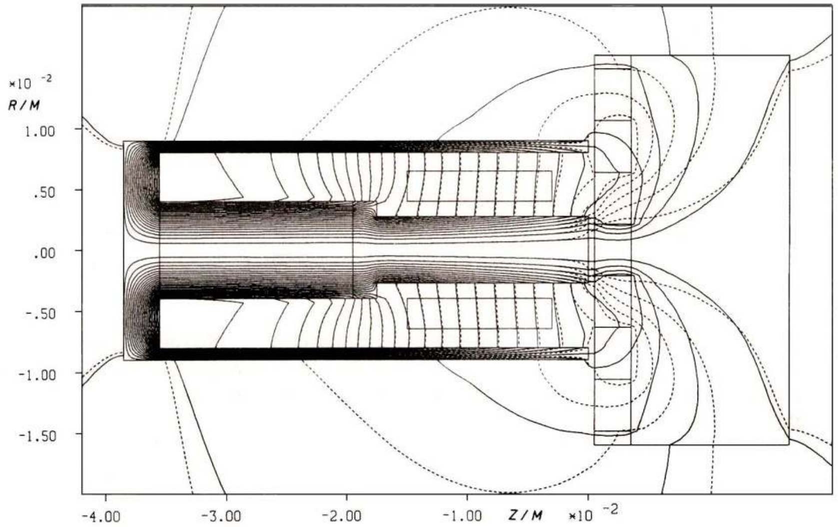

Change in the magnetic flux with varying air gap. Continuous lines: minimum air gap; dashed lines: maximum air gap.

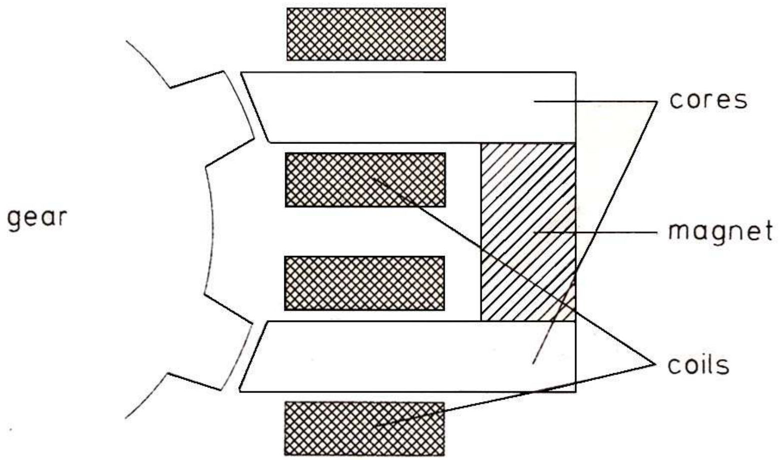

C-shaped sensor.

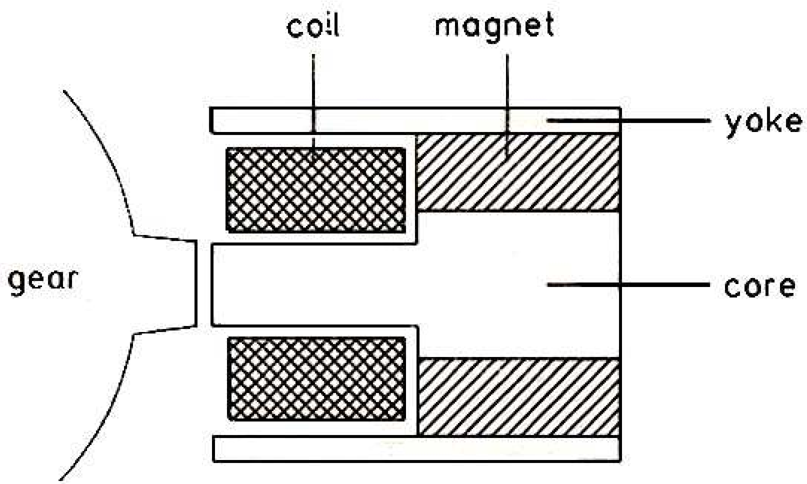

Sensor with radially magnetized permanent magnet.

Signal Conditioning

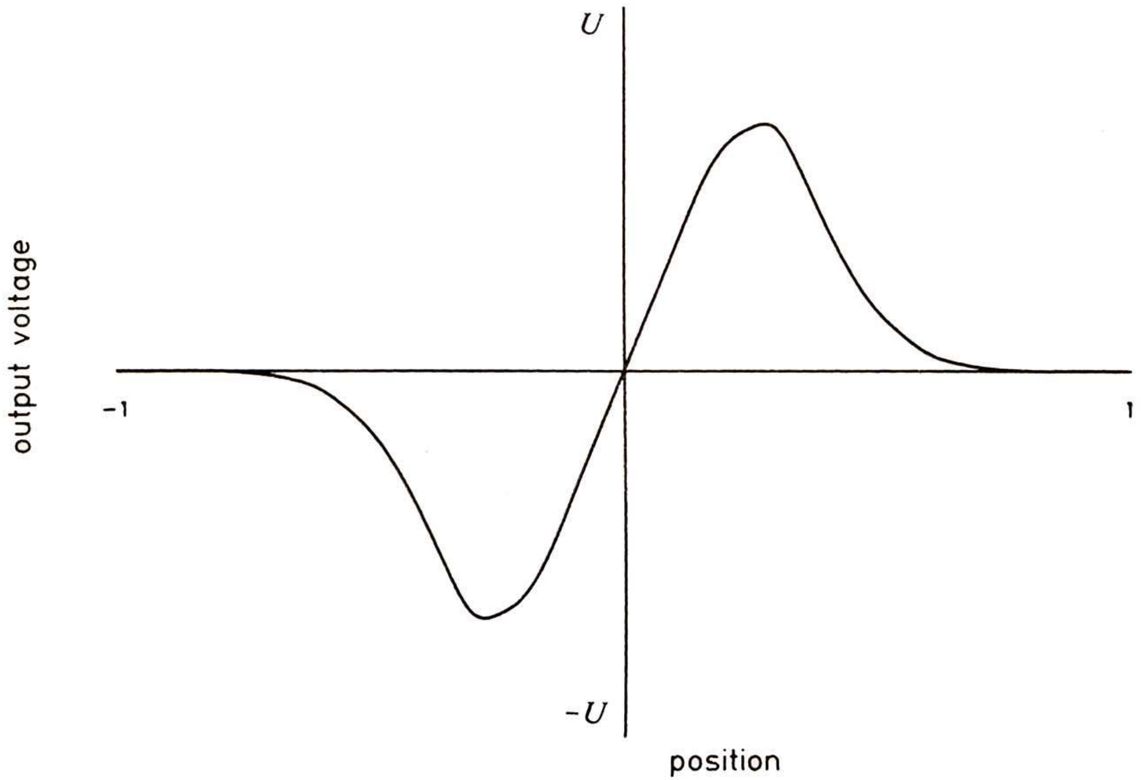

Output voltage *U* of a DC-excited sensor with permanent magnets, when a single iron object passes by.

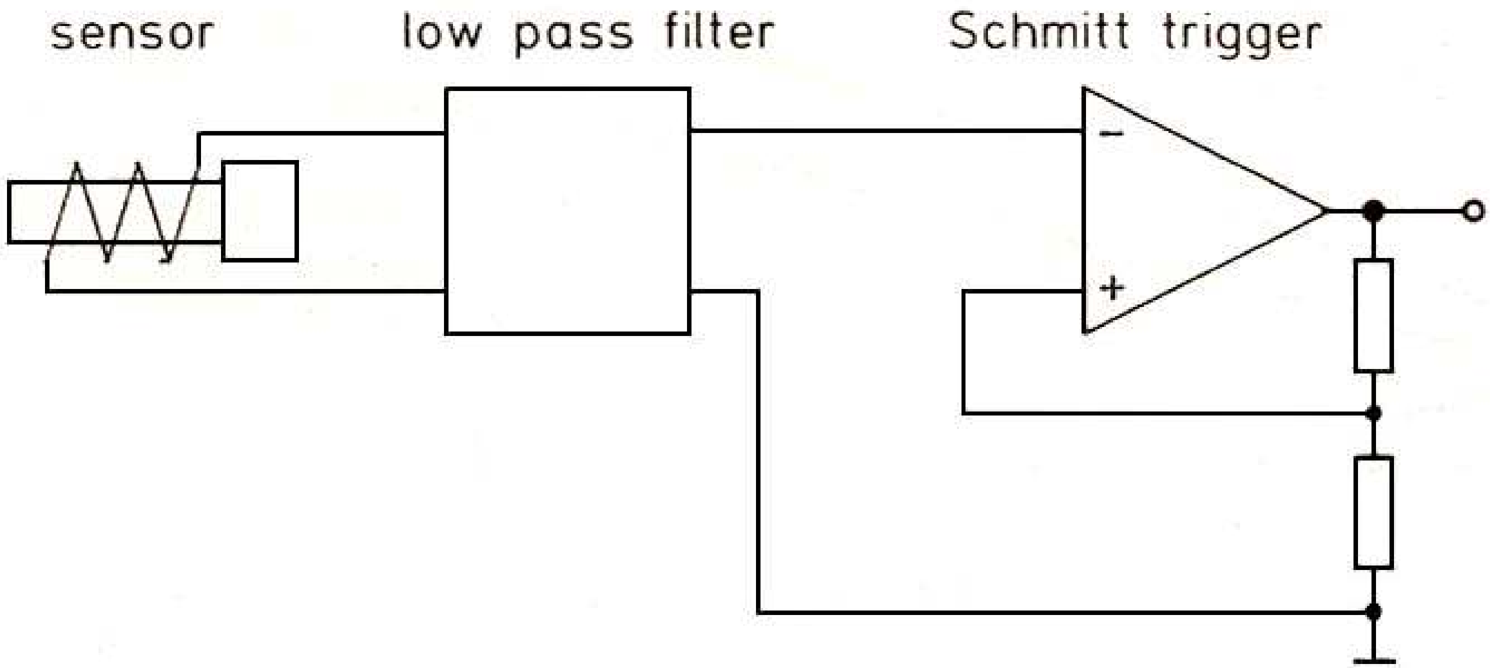

Schematic electrical diagram of an inductive sensor.

AC-Excited Sensors for Linear Movement

Linear Variable Differential Transformer

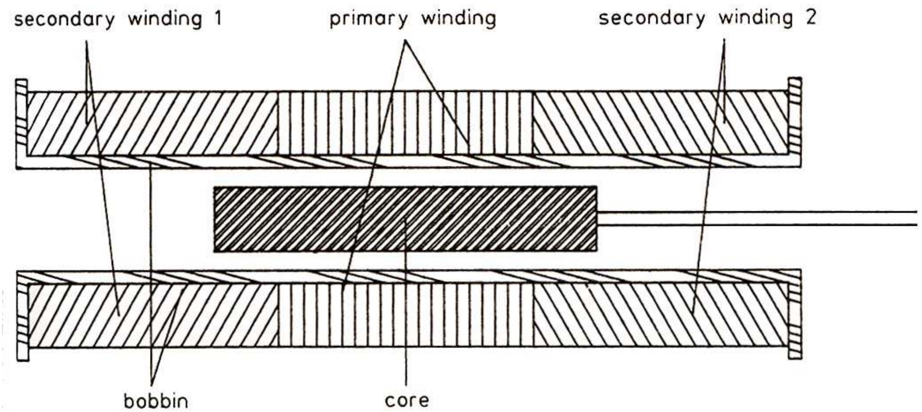

Principle of construction of an LVDT.

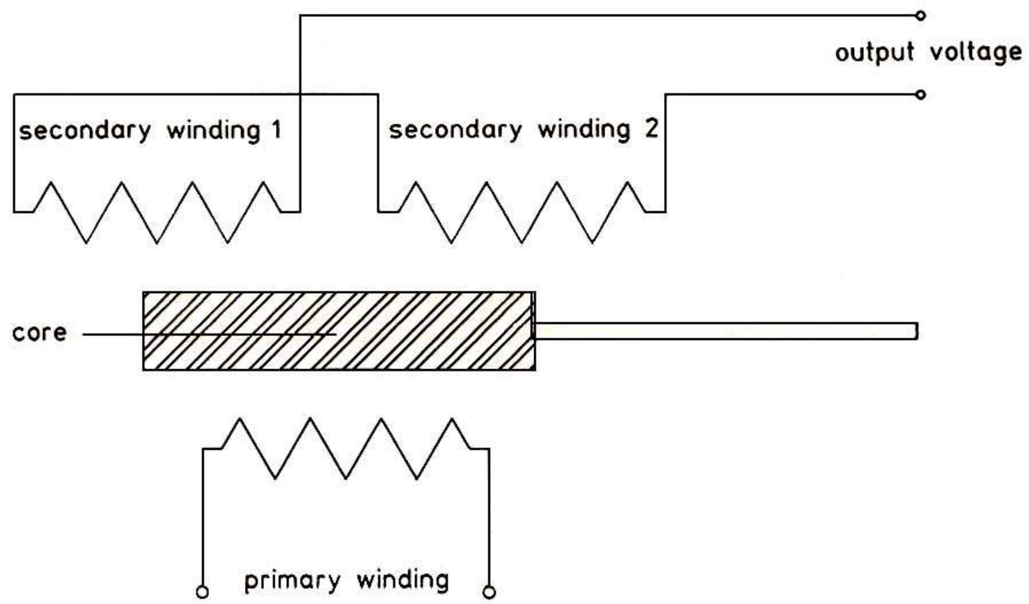

Electrical circuit of an LVDT.

$$U = -N \cdot \mathrm{d}\phi / \mathrm{d}\,t = -M \cdot \mathrm{d}I / \mathrm{d}\,t$$

$$U = U_2 - U_1 = M_2 \cdot \mathrm{d}I / \mathrm{d}\,t - M_1 \cdot \mathrm{d}I / \mathrm{d}\,t$$

$$U = (M_2 - M_1) \cdot \mathrm{d}I / \mathrm{d}\,t$$

$$M = M_2 - M_1 = M(x)$$

$$U = M(x) \cdot \mathrm{d}I / \mathrm{d}\,t \qquad M(x) = \frac{U}{\mathrm{d}I / \mathrm{d}\,t}$$

a)

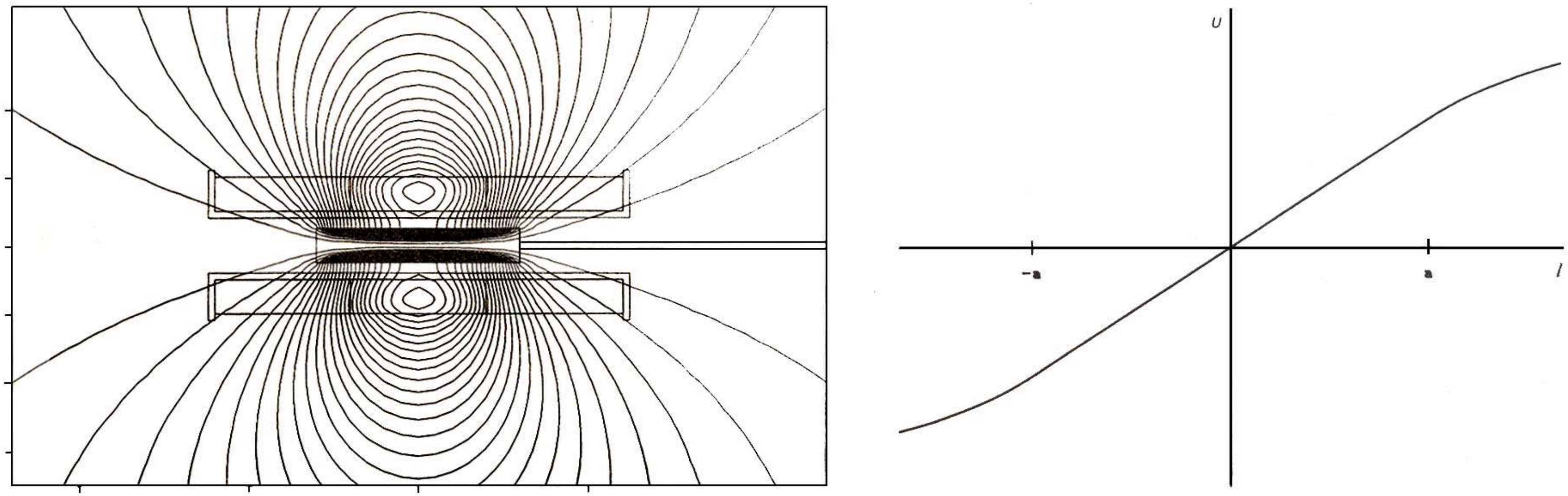

b)

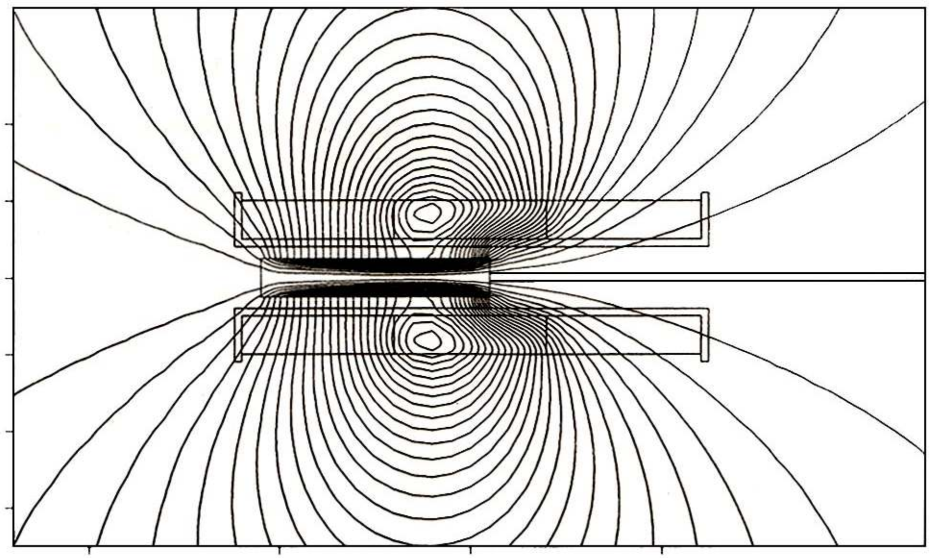

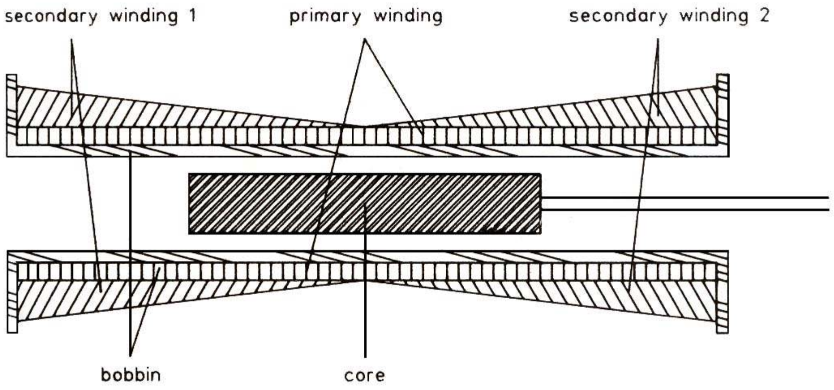
secondary winding 1
primary winding
secondary winding 2
bobbin
core

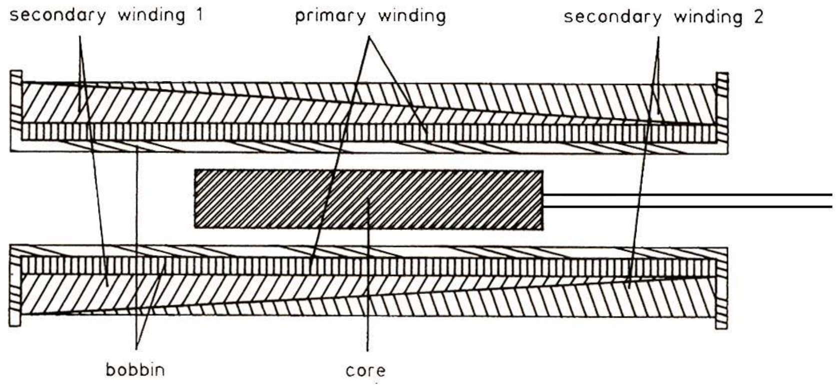
secondary winding 1
primary winding
secondary winding 2
bobbin
core

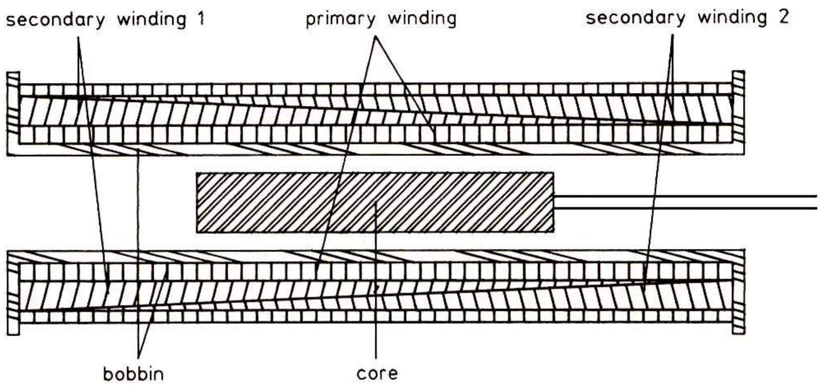
secondary winding 1
primary winding
secondary winding 2
bobbin
core

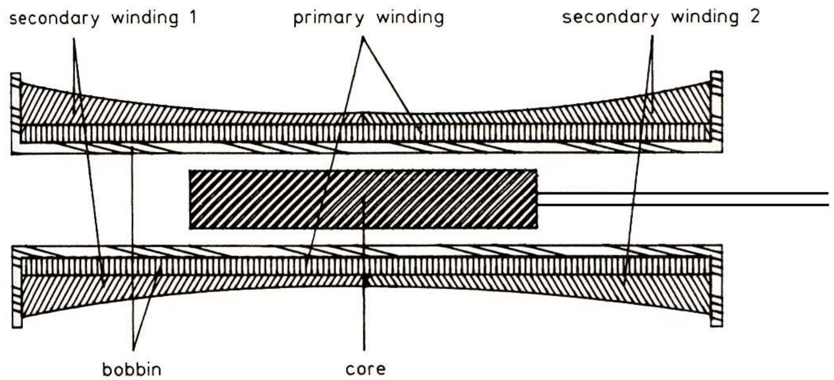
secondary winding 1
primary winding
secondary winding 2
bobbin
core

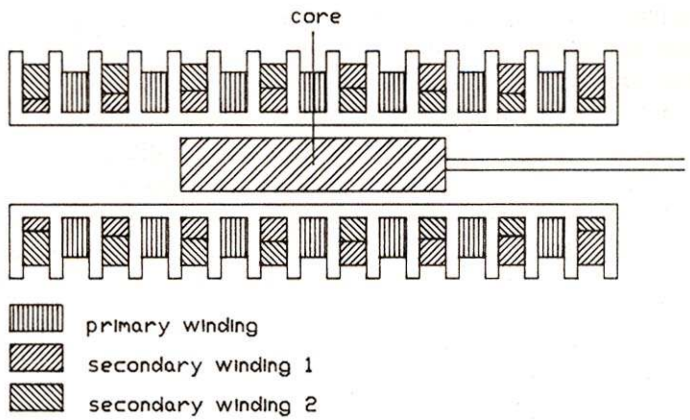
core
primary winding
secondary winding 1
secondary winding 2

Signal Conditioning

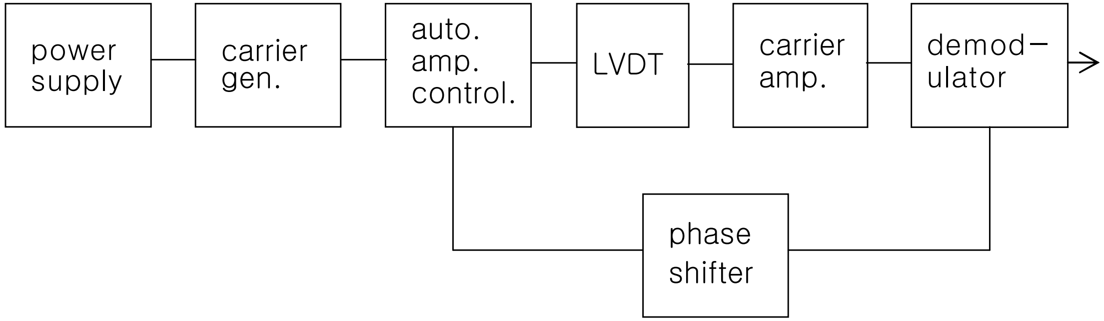

Block diagram of a carrier amplifier system.

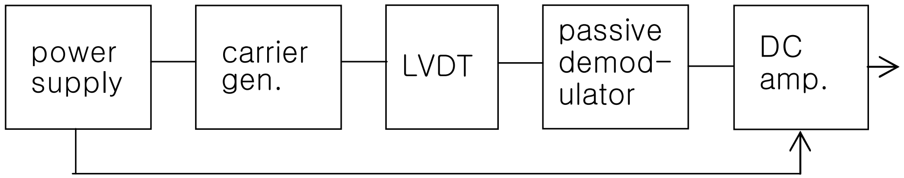

Block diagram of a DC amplifier system.

Variable Inductive Sensors

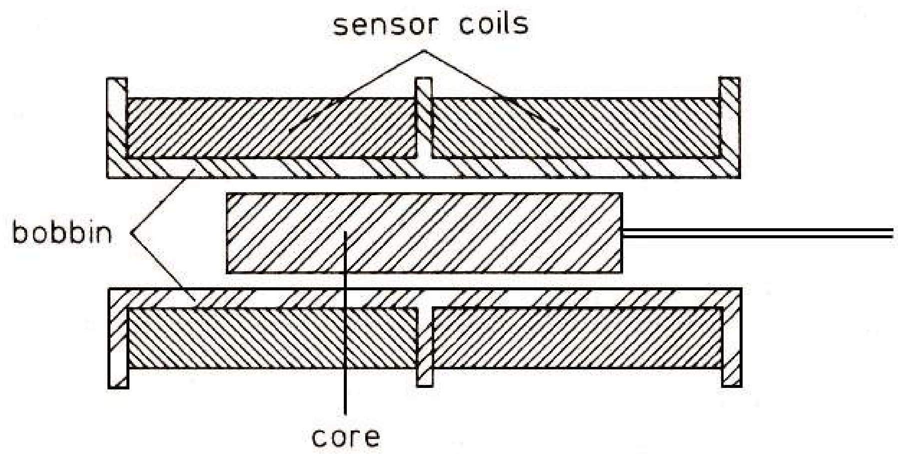

Principle of construction of the VLP sensor.

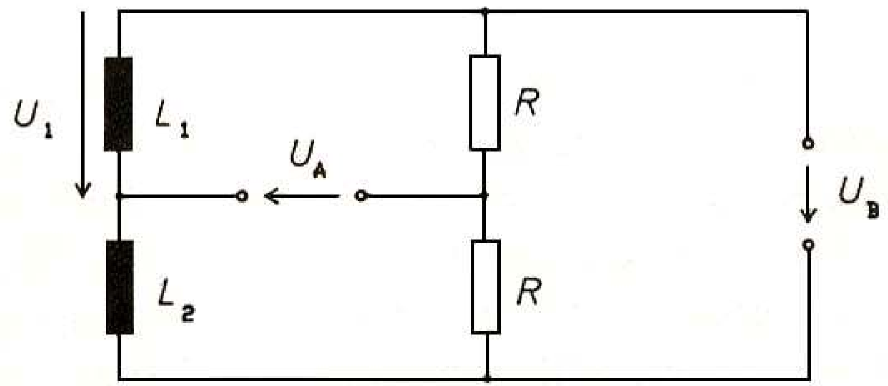

Principle of a bridge circuit.

$$L = \mu_0 \cdot \mu_r \cdot N^2 \cdot A / l$$

$$U_A = U_1 - U_B / 2$$

$$U_A = U_B \cdot (\mathrm{i}\omega L_1/(\mathrm{i}\omega L_1 + \mathrm{i}\omega L_2) - 1/2$$

$$U_A = U_B \cdot (L + \Delta L/((L + \Delta L) + (L - \Delta L)) - 1/2)$$

$$U_A = U_B \cdot ((L + \Delta L)/2L - 1/2)$$

$$U_A = 1/2 \cdot U_B \cdot \Delta L / L$$

$$\Delta L = \mathrm{d}\,L / \mathrm{d}l \cdot \Delta l$$

$$U_A / U_B = 1/(2L) \cdot \mathrm{d}\,L / \mathrm{d}l \cdot \Delta l$$

Applications and Properties

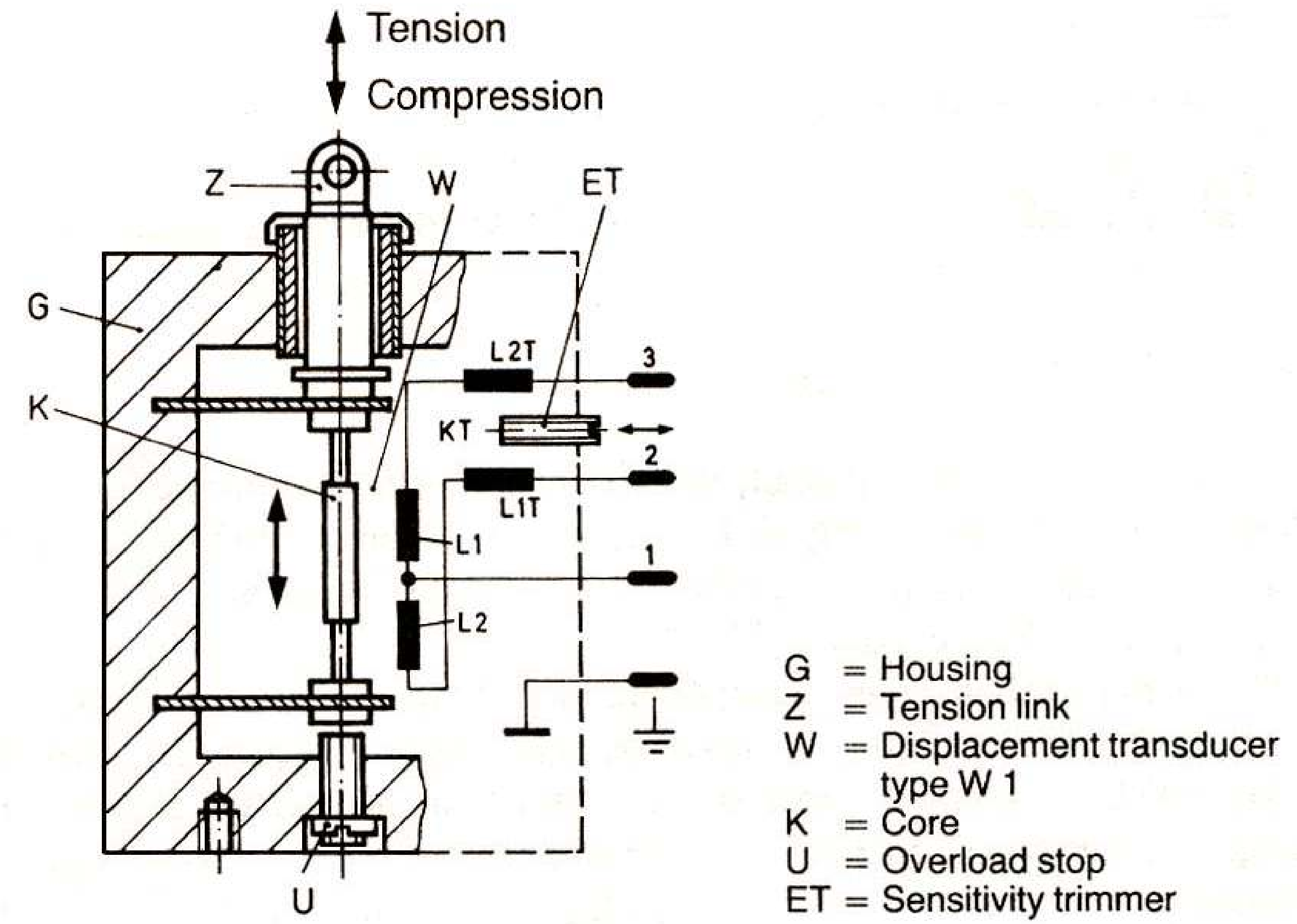

Principle of a construction of a force transducer (courtesy Hottinger Baldwin Messtechnik)

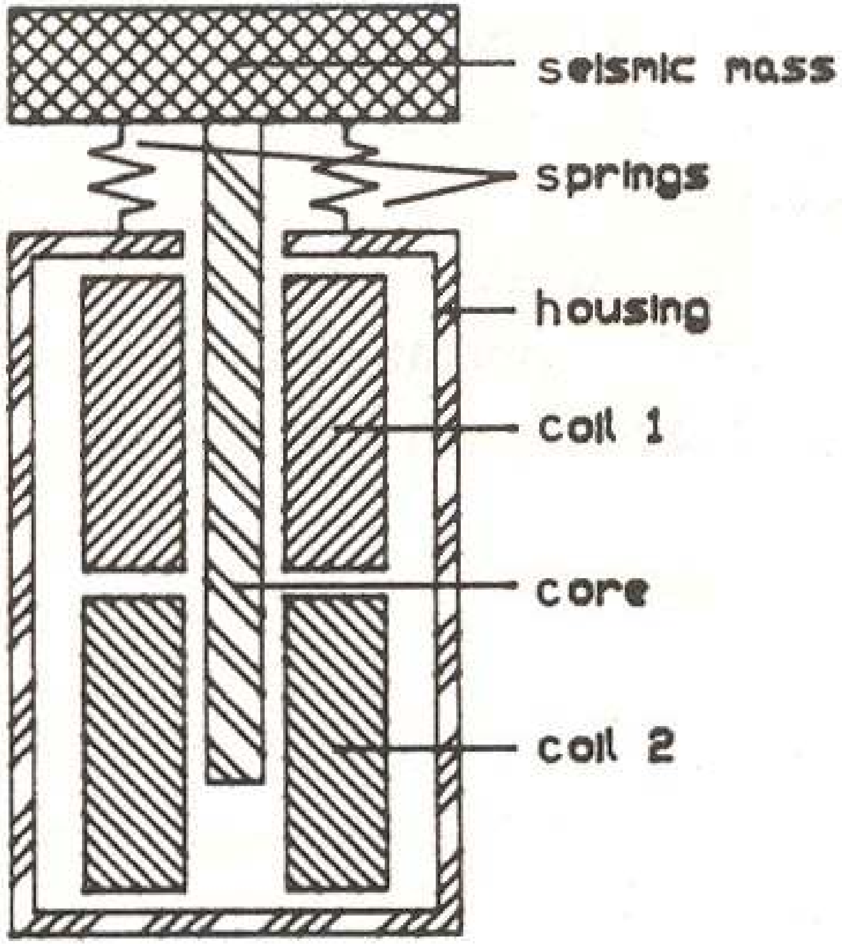

Vibration/acceleration sensor.

Signal Conditioning

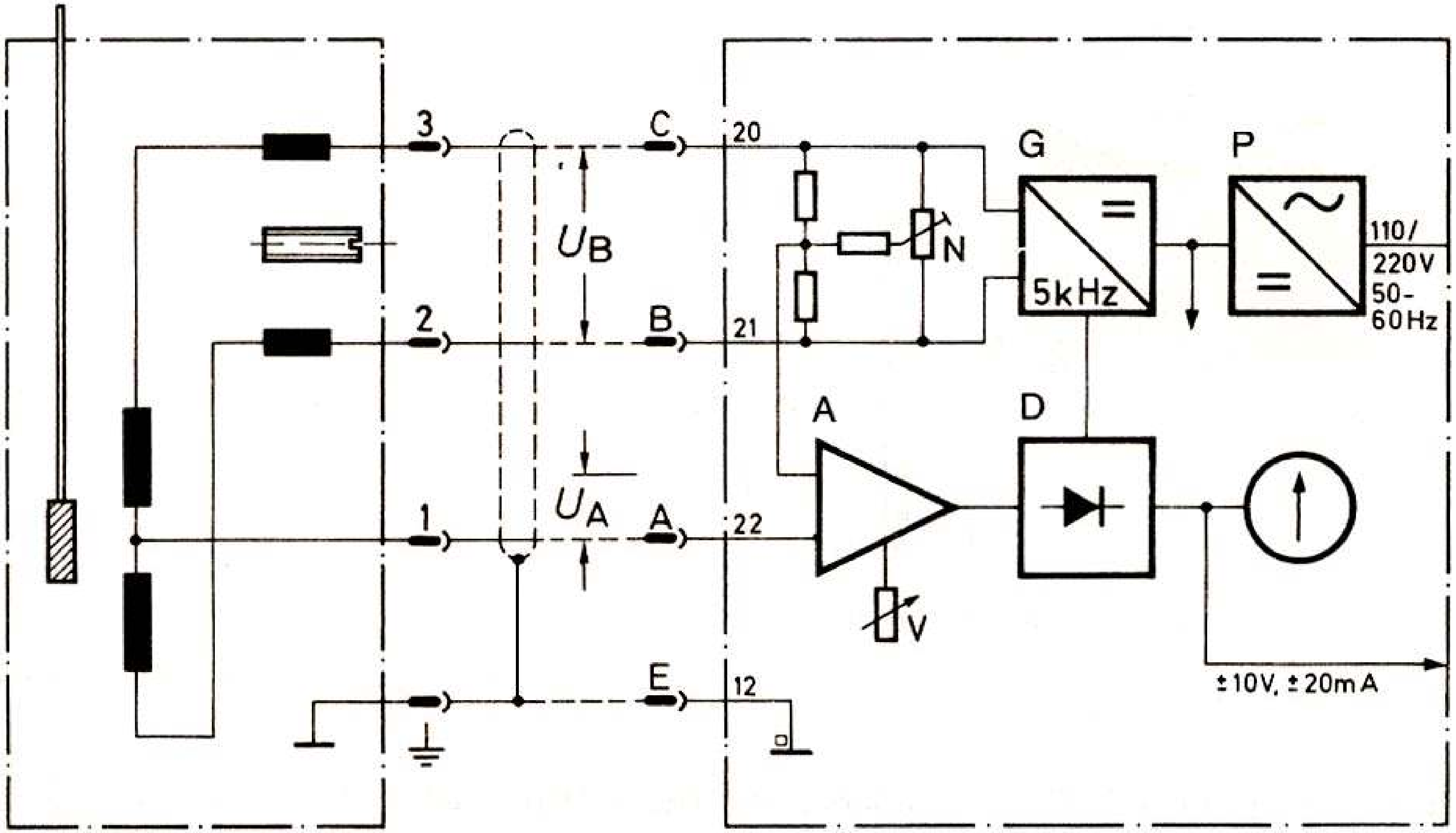

Schematic electrical diagram of a force transducer connected with an amplifier (courtesy Hottinger Baldwin Messtechnik GmbH).

Variable Gap Sensors

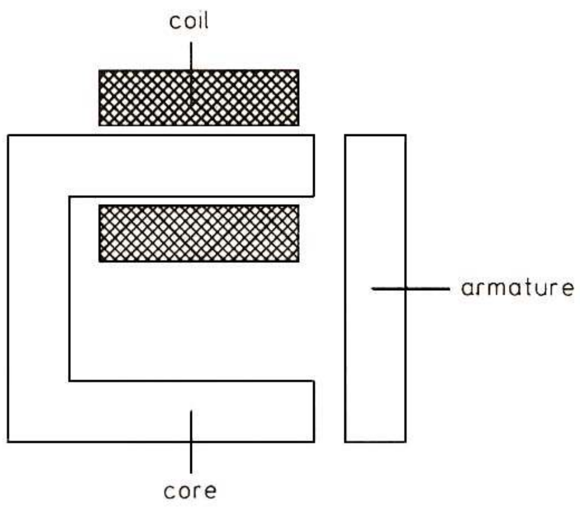

$$L = \mu_0 \cdot N^2 \cdot A / (l_{Fe} / \mu_{Fe} + l_L / \mu_L)$$

$$L_{max} = \mu_0 \cdot N^2 \cdot \mu_{Fe} \cdot A / l_{Fe}$$

Construction of a variable gap sensor.

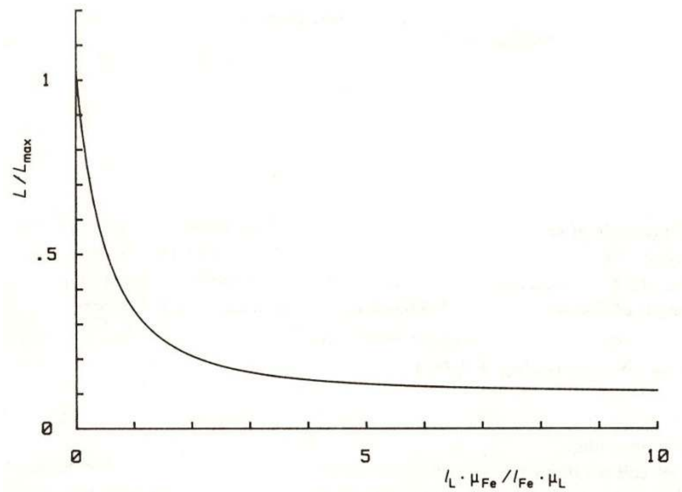

Characteristic of a variable gap sensor.

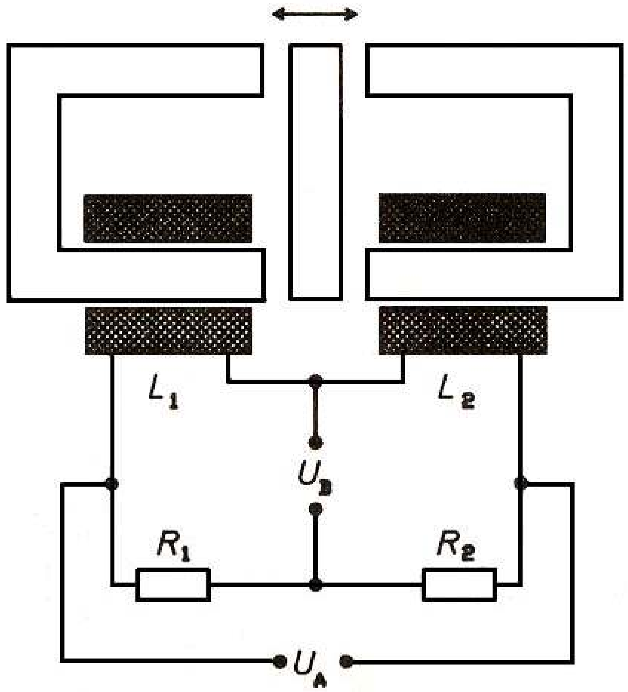

Construction of a differential cross-anchor sensor.

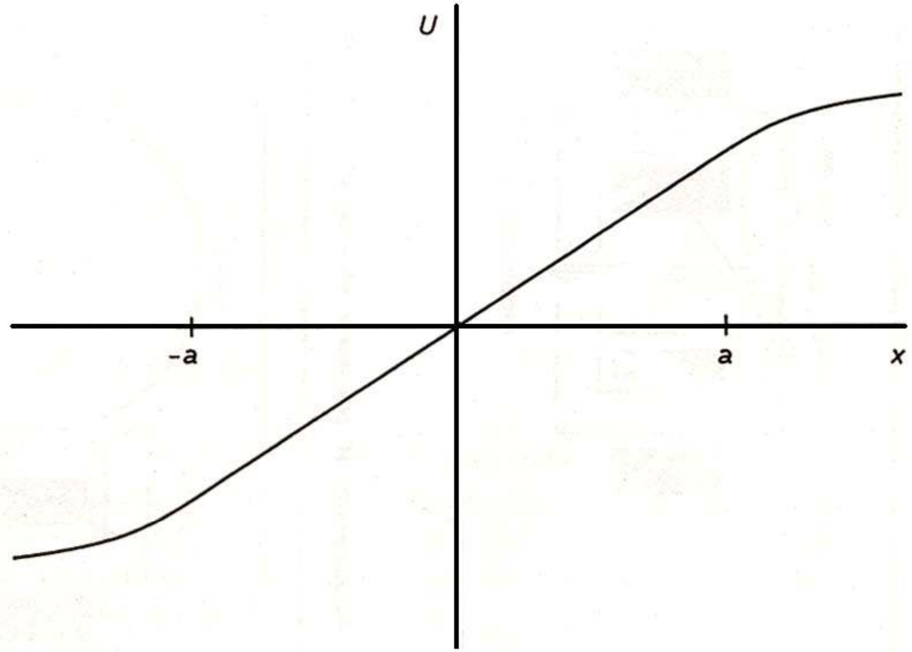

Output voltage U versus core position x. ± a : limits of the linear rage.

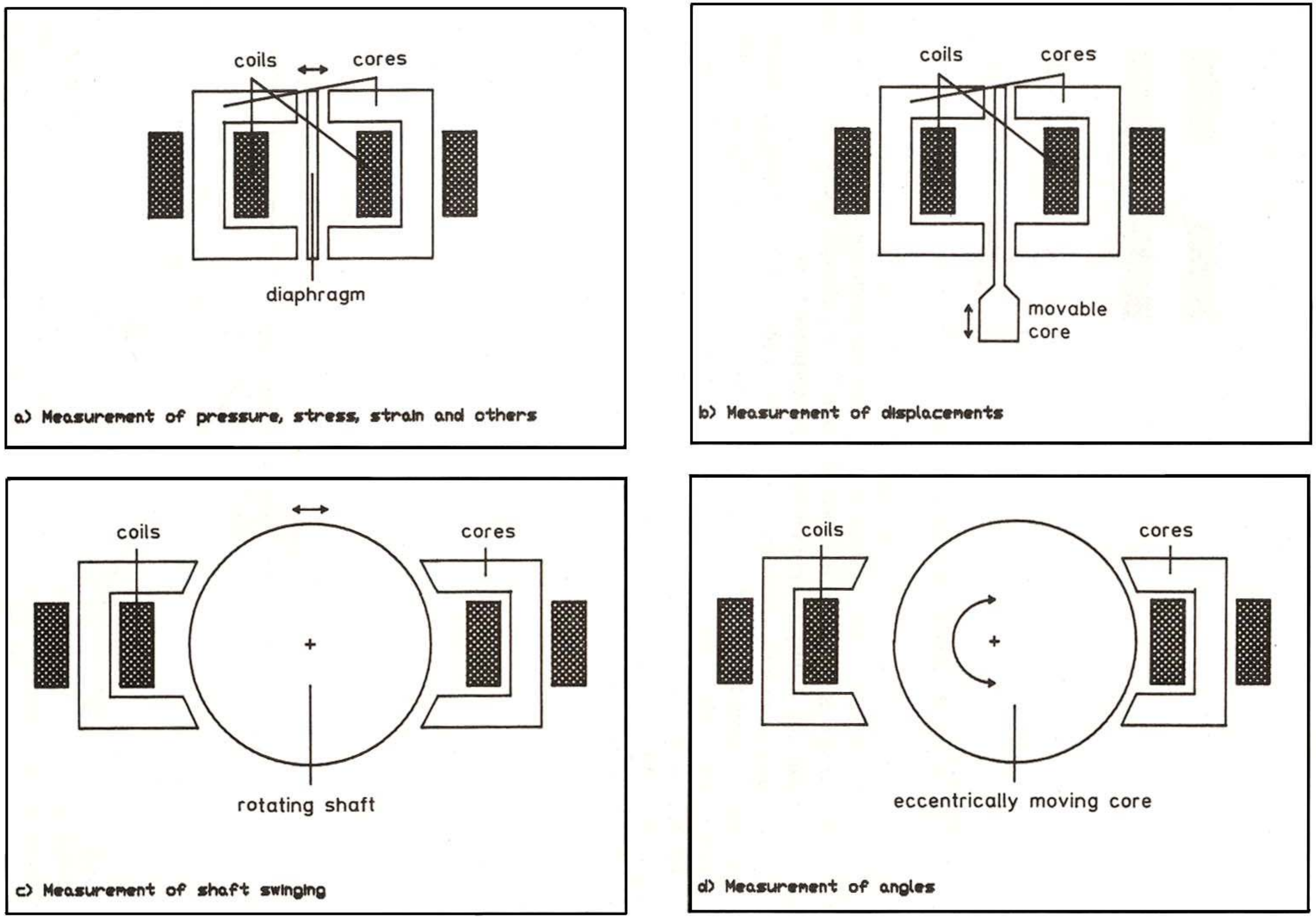

a) Measurement of pressure, stress, strain and others

b) Measurement of displacements

c) Measurement of shaft swinging

d) Measurement of angles

Applications of differential cross-anchor sensors.

AC-excited Sensors for Rotary Movements

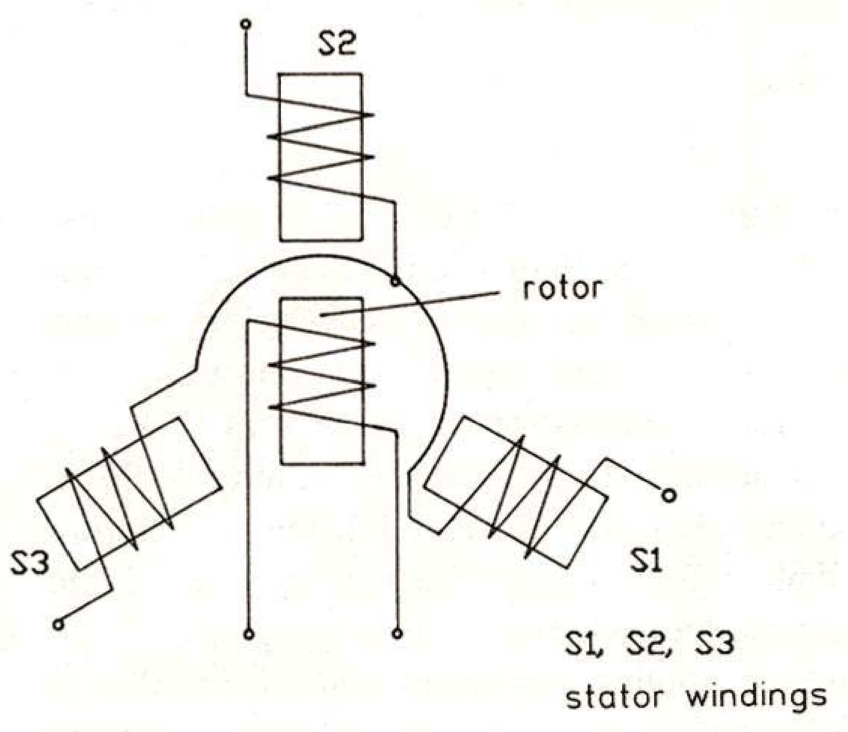

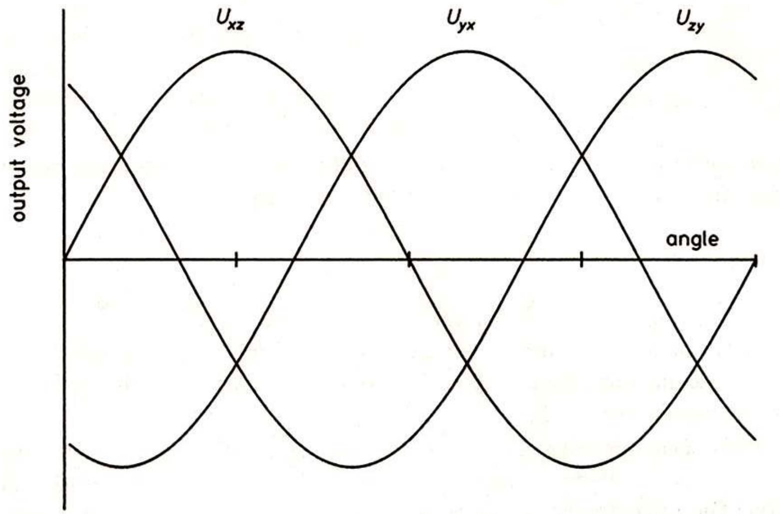

$$U_{yx} = U_{x0} - U_{y0} = U_1 \cdot K \cdot \sqrt{3} \cdot \sin(\alpha - 120°)$$

$$U_{zy} = U_{y0} - U_{z0} = U_1 \cdot K \cdot \sqrt{3} \cdot \sin(\alpha - 240°)$$

$$U_{xz} = U_{z0} - U_{x0} = U_1 \cdot K \cdot \sqrt{3} \cdot \sin\alpha$$

Principle of construction of a synchro.

$$U_{y0} = K \cdot U_1 \cdot \cos\alpha$$

$$U_{z0} = K \cdot U_1 \cdot \cos(\alpha - 120°)$$

$$U_{x0} = K \cdot U_1 \cdot \cos(\alpha - 240°)$$

Application to the Torque Sensor

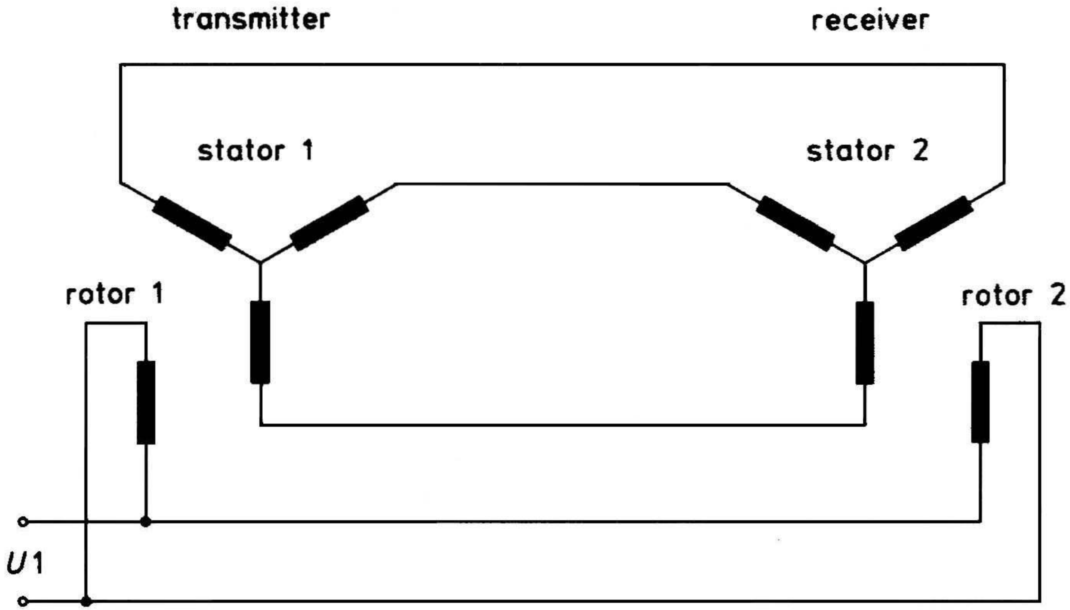

Principle of construction of a torque-type synchro.

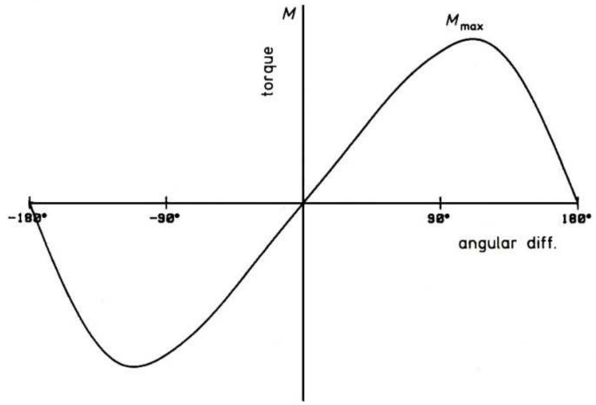

Torque versus angular difference.

$$M \sim K \cdot \sin(\alpha_t - \alpha_r)$$

$$U_r \sim U_1 \cdot \cos(\alpha_t - \alpha_r)$$

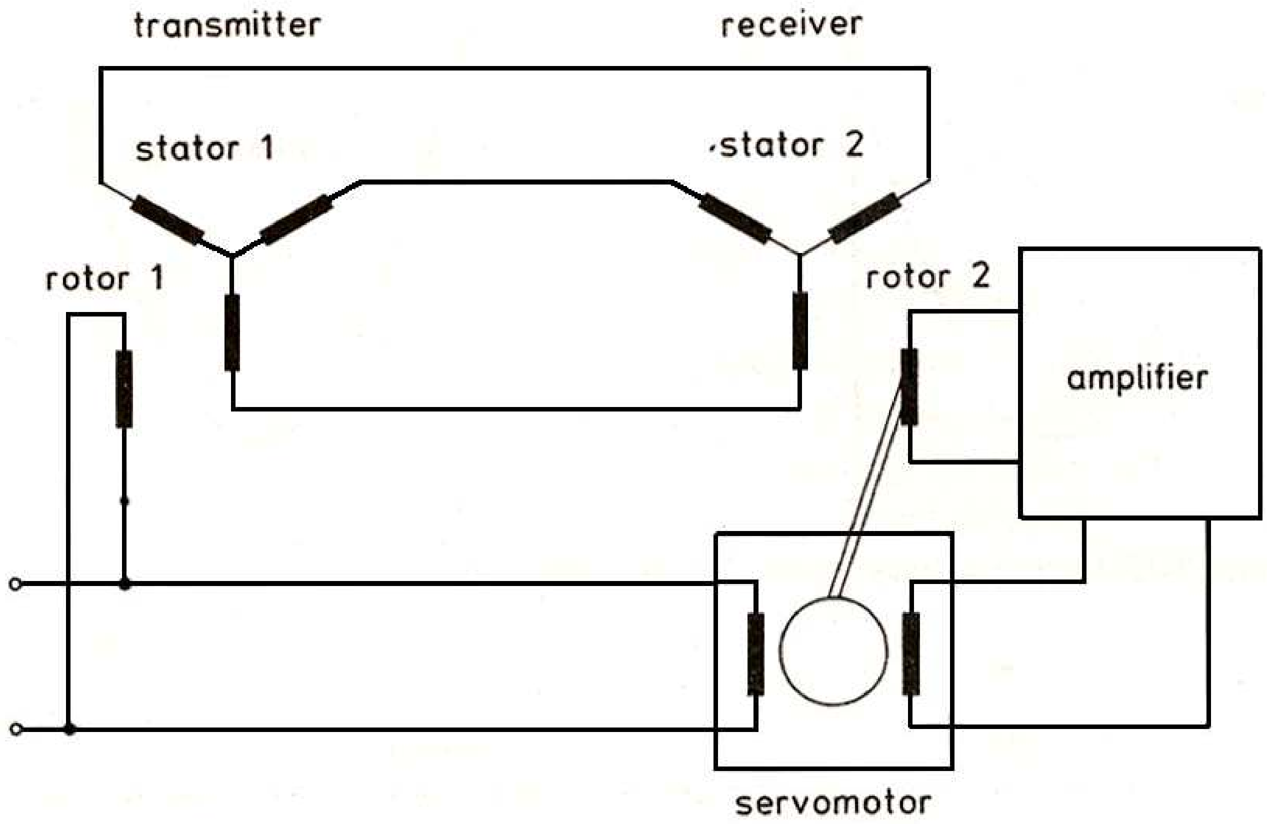

Principle of construction of a control-type sensor.

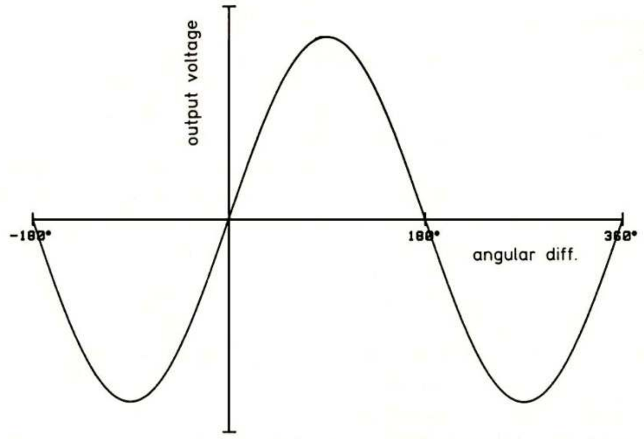

Output voltage versus angular difference.

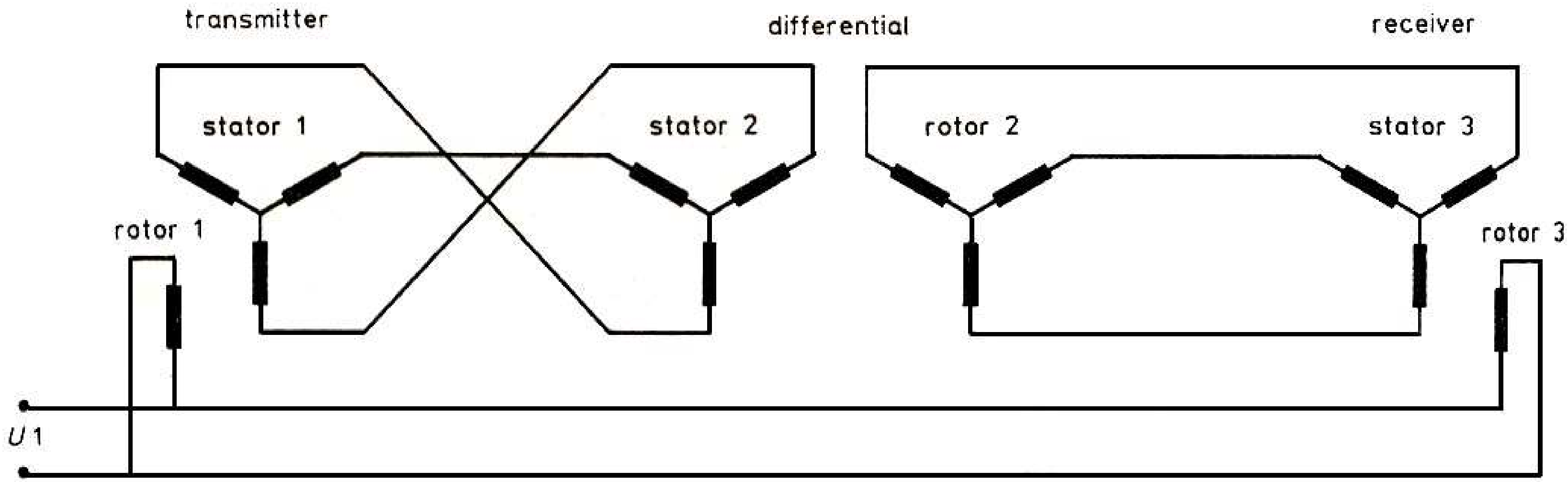

Principle of construction of a differential sychro.

Eddy Current Sensors

$$\text{curl } E = -\mathrm{d}B / \mathrm{d}t$$

$$\text{curl } H = J$$

$$\text{div } B = 0$$

$$\boldsymbol{B} = \mu\boldsymbol{(H)} \cdot \boldsymbol{H}$$

$$\boldsymbol{J} = \sigma\boldsymbol{(E)} \cdot \boldsymbol{E}$$

$$\boldsymbol{B} = \text{curl } \boldsymbol{A}$$

$$\boldsymbol{E} = -\mathrm{d}\boldsymbol{A}/\mathrm{d}t$$

$$\boldsymbol{J} = \sigma(-\mathrm{d}\boldsymbol{A}/\mathrm{d}t)$$

$$\text{curl curl } \boldsymbol{A}/\mu = -\sigma \mathrm{d}\boldsymbol{A}/\mathrm{d}t$$

$$(1/\mu)(\text{curl curl } \boldsymbol{A}) = -i\sigma\omega\boldsymbol{A}$$

$$(1/\mu)(\Delta\boldsymbol{A}) = i\sigma\omega\boldsymbol{A}$$

Eddy Current Tachometer

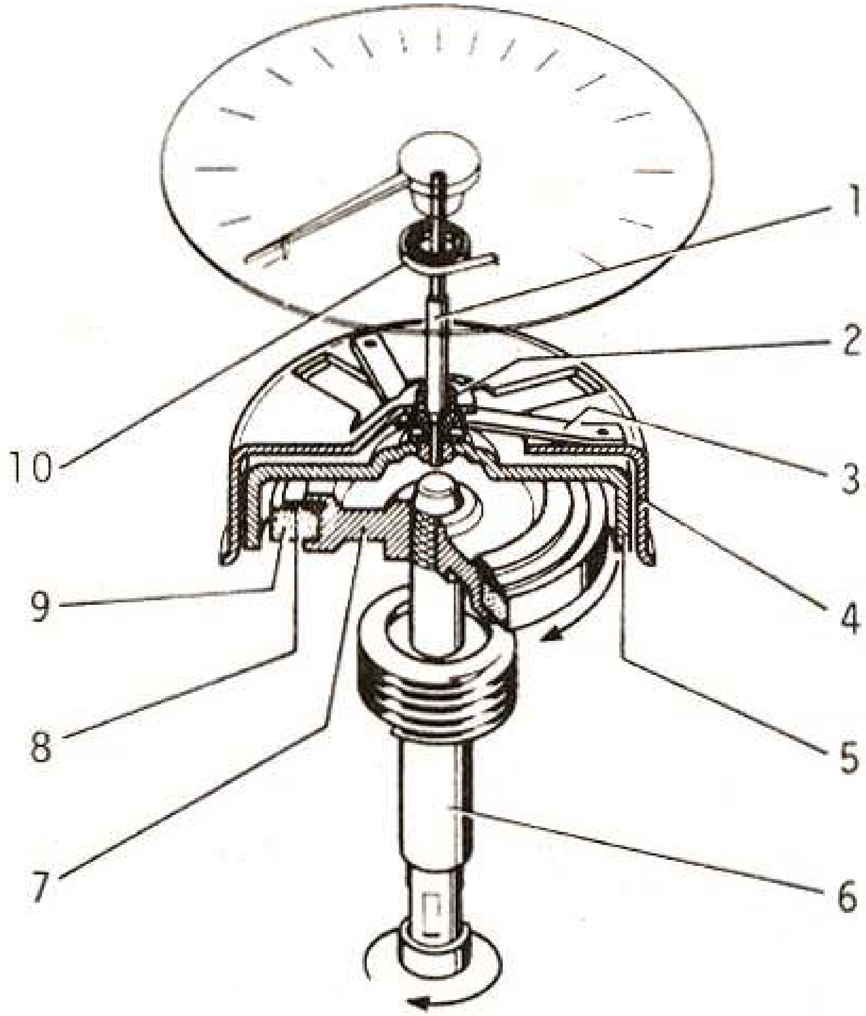

Construction of a speedometer (courtesy VDO Adolf Schinding AG). 1) spindle, 2) bearing, 3) holding spring, 4) iron yoke, 5) eddy current cup, 6) shaft of the magnet, 7) support of the magnet, 8) temperature compensation, 9) permanent magnet, 10) torsion spring.

Proximity Sensors

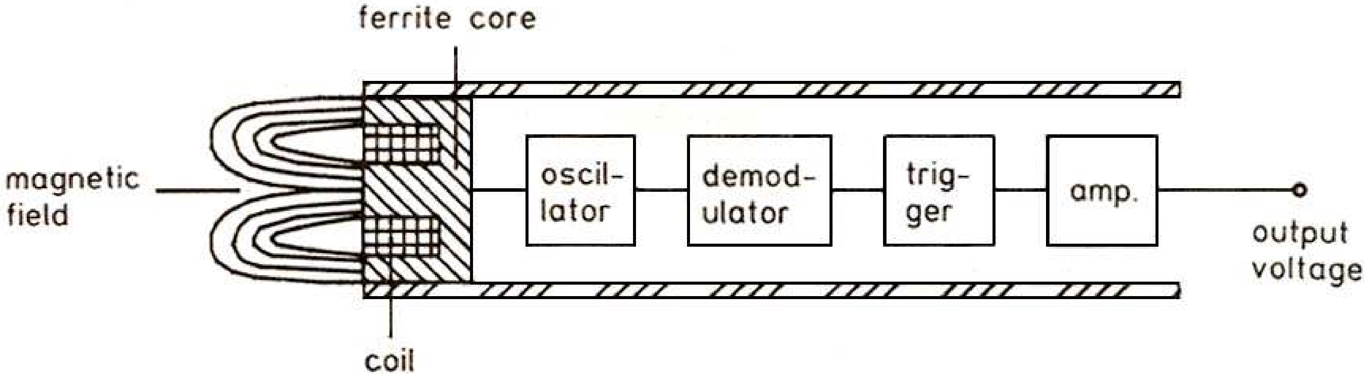

Schematic diagram of a proximity sensor.

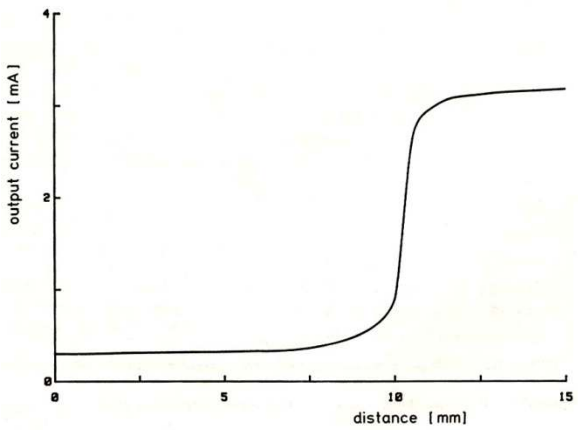

Output current of a proximity switch versus distance

Inductive Flowmeters

$$F = q \cdot (\upsilon \times \boldsymbol{B})$$

$$F = q \cdot E$$

$$E = \upsilon \times B$$

$$U = E\mathrm{ds} = (\upsilon \times \boldsymbol{B})$$

$$U = \boldsymbol{d} \cdot (\upsilon \times \boldsymbol{B})$$

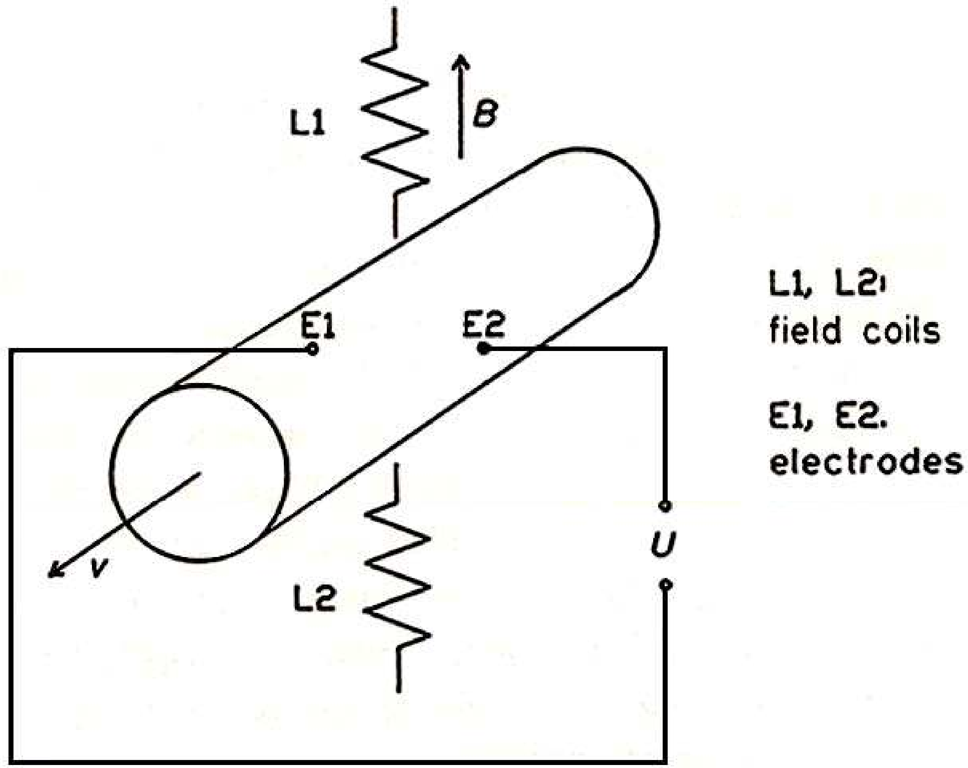

$$U = K \cdot d \cdot \upsilon \cdot \boldsymbol{B}$$

Development of magnetic phase detection sensor for steam generator tube

Dirac Son[1], Kwan-Sang Ryu[2], Duck-Gun Park[3]

[1]Hannam University, Daejeon, Rep. of Korea
[2]Korea Research Institute of Standards and Science, Daejeon, Rep. of Korea
[3]Korea Atomic Energy Research Institute, Daejeon, Rep. of Korea

Introduction

The layout of pressurized water reactor (PWR) components

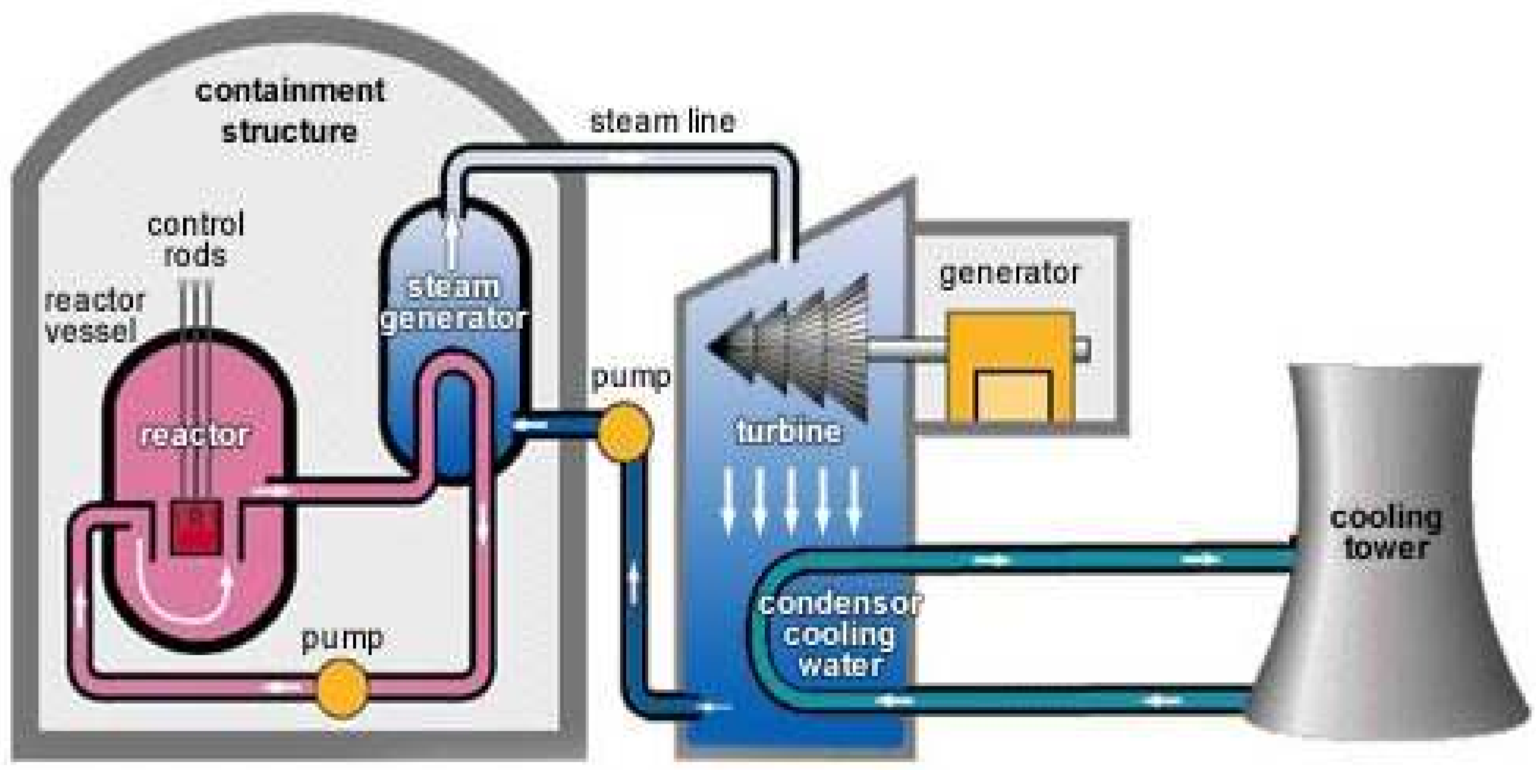

Primary side
(radioactive side)

Secondary side (non-radioactive side)

The Structure of SG(Steam Generator)
(degradation mechanism)

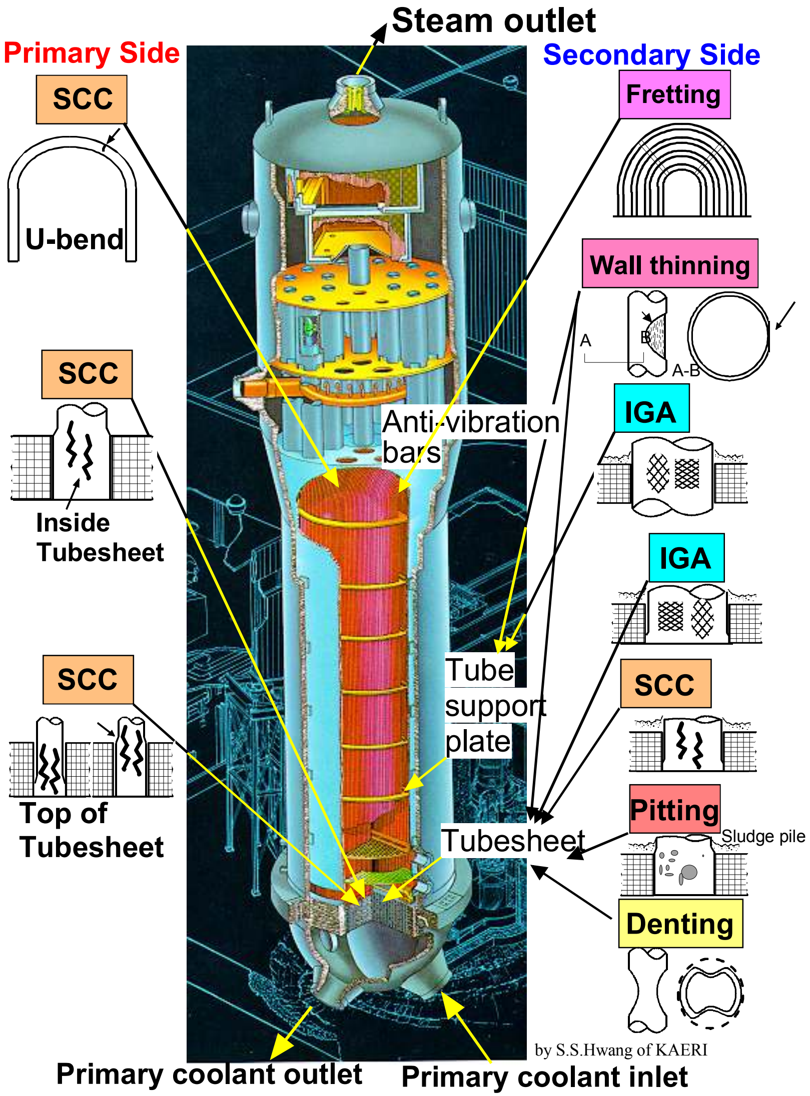

In commercial power plants SG:
- height up to 21 m
- weight up to 800 tons
- 2~4 sets of SG were installed
- SG can contain from 3,000 to 16,000 tubes, each about 20 mm in diameter.

The SGT is made of nickel based Inconel alloy, which is composed of 75% Ni, 16.5%Cr and 8.15%Fe

- Degradation mechanism : corrosion, pitting, denting, inter granular attack

- Inspection : Eddy current Testing(ECT

Permeability Variation Clusters (PVC)
(Ferro-magnetic phase)

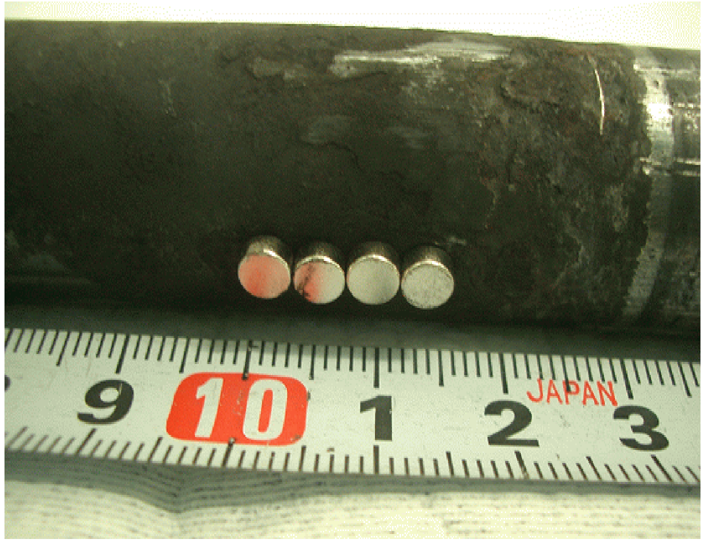

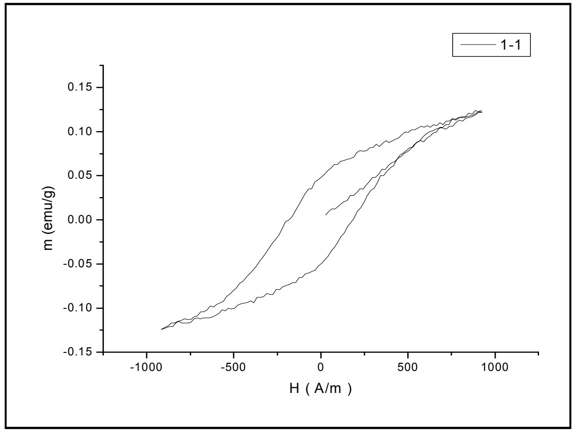

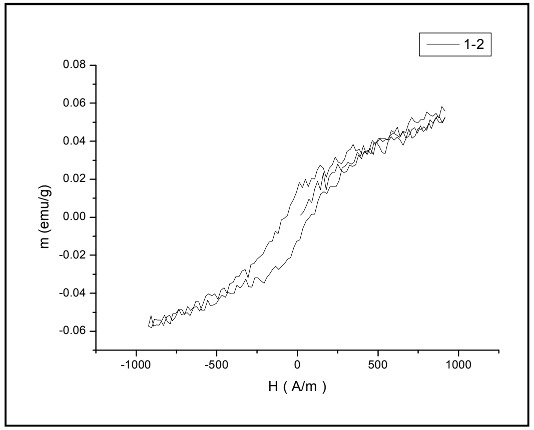

The hystresis loop in the fragment of PVC parts of Kori-1 retired SG tube

How can we detect magnetic phase (PVC)selectively from the flaws in SGT

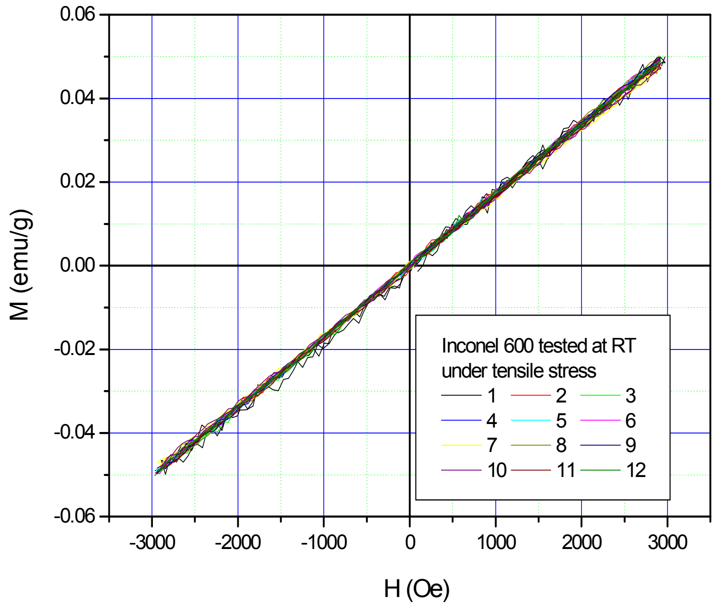

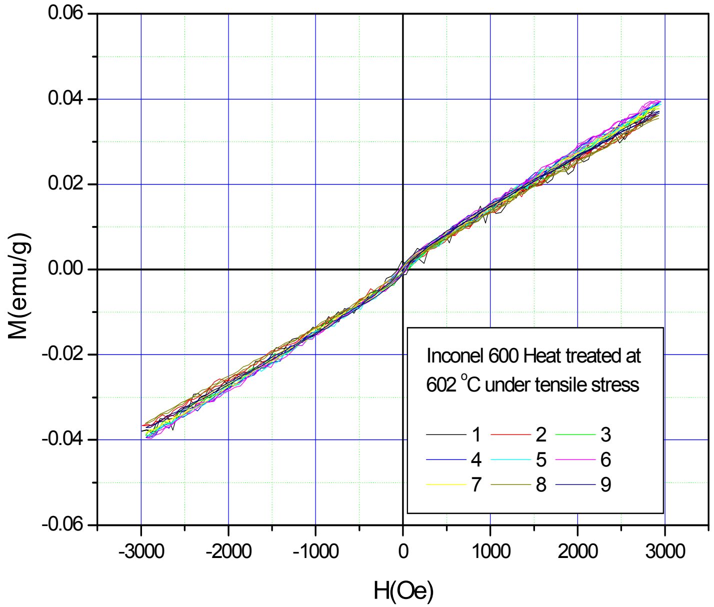

The hysteresis loop of the tensile tested specimen at room temperature (a), and tensile tested at high temperature (b).

The magnetic phase can be created under the high temperature and pressure conditions, which is correspond to the stress corrosion cracking in the SG tube in the NPP

(Bruemmer, S.M.; Charlot, L.A. & Henager, C.H. (1988). *Corrosion*, 782).

Principle of ECT

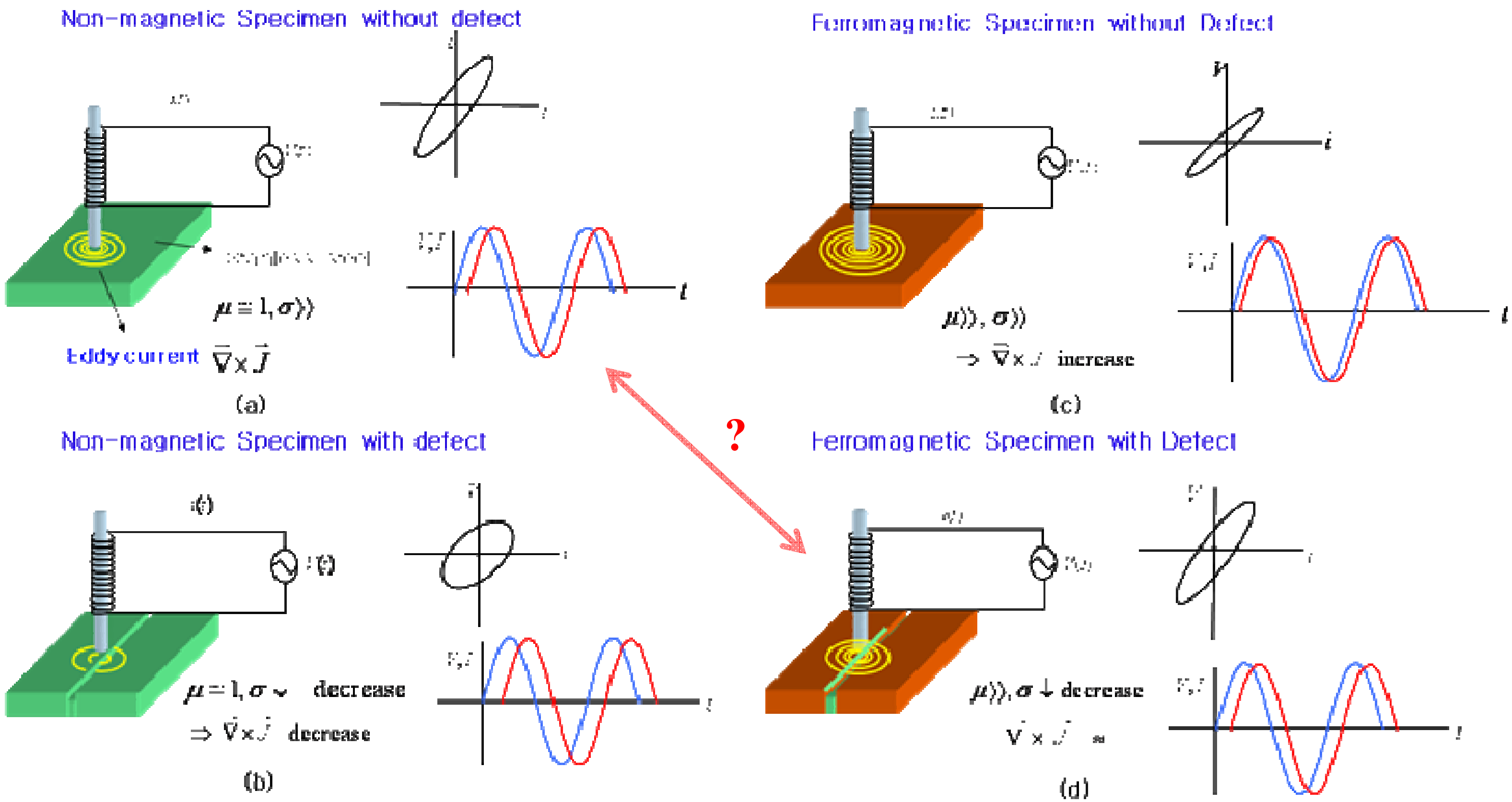

If we can separate magnetic phase selectively from the flaws using magnetic sensor, the reliability of EC in SGT inspection will be greatly enhanced

Design of Magnetic Sensor for PVC

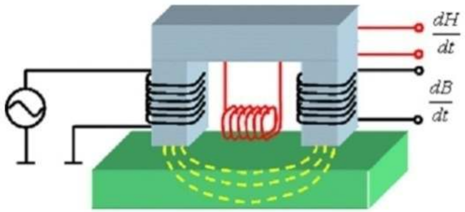

Structure of the permeability sensor

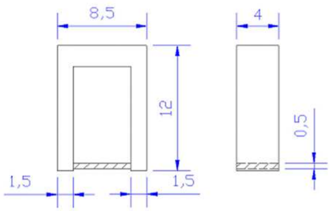

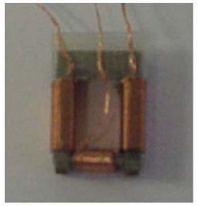

Dimension and photograph of U-shape sensing yoke

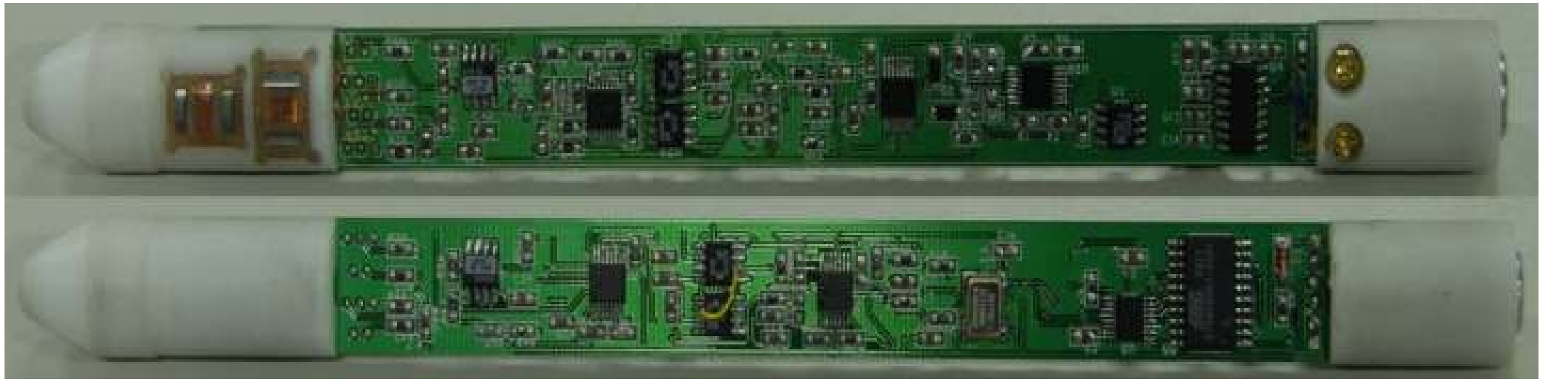

Photograph of the completed sensor, front side (above) and rear side (bottom)

Electronic Circuit of Magnetic Sensor

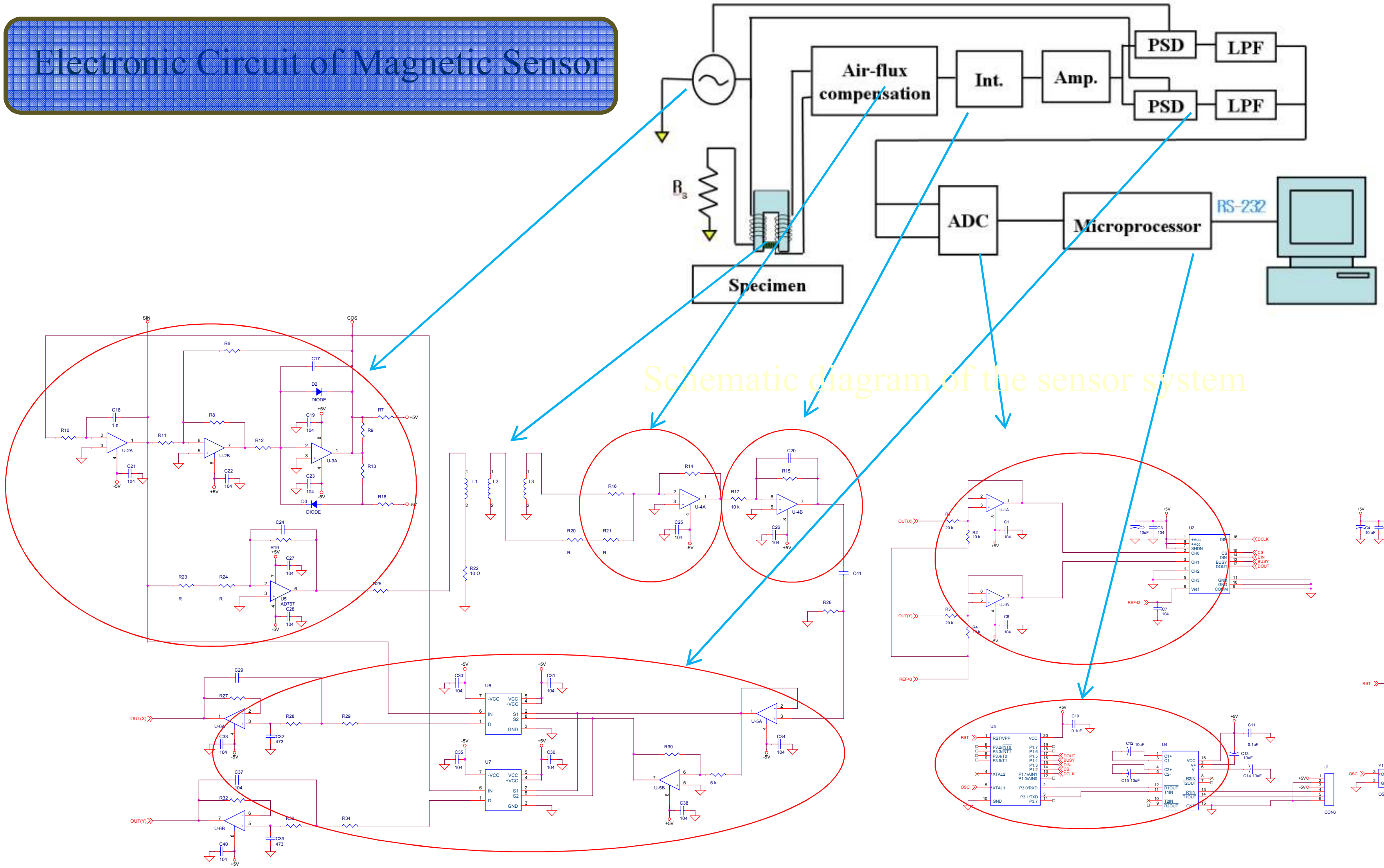

Electronic circuit diagram of the magnetic sensor

Experimental Setup for Magnetic Sensor

Photograph of the completed measuring system data acquisition software in PC and probe scanning system.

Reference material

Scanning System

Software LabVIEW

Reference Material (1) : Normal defects and PVCs

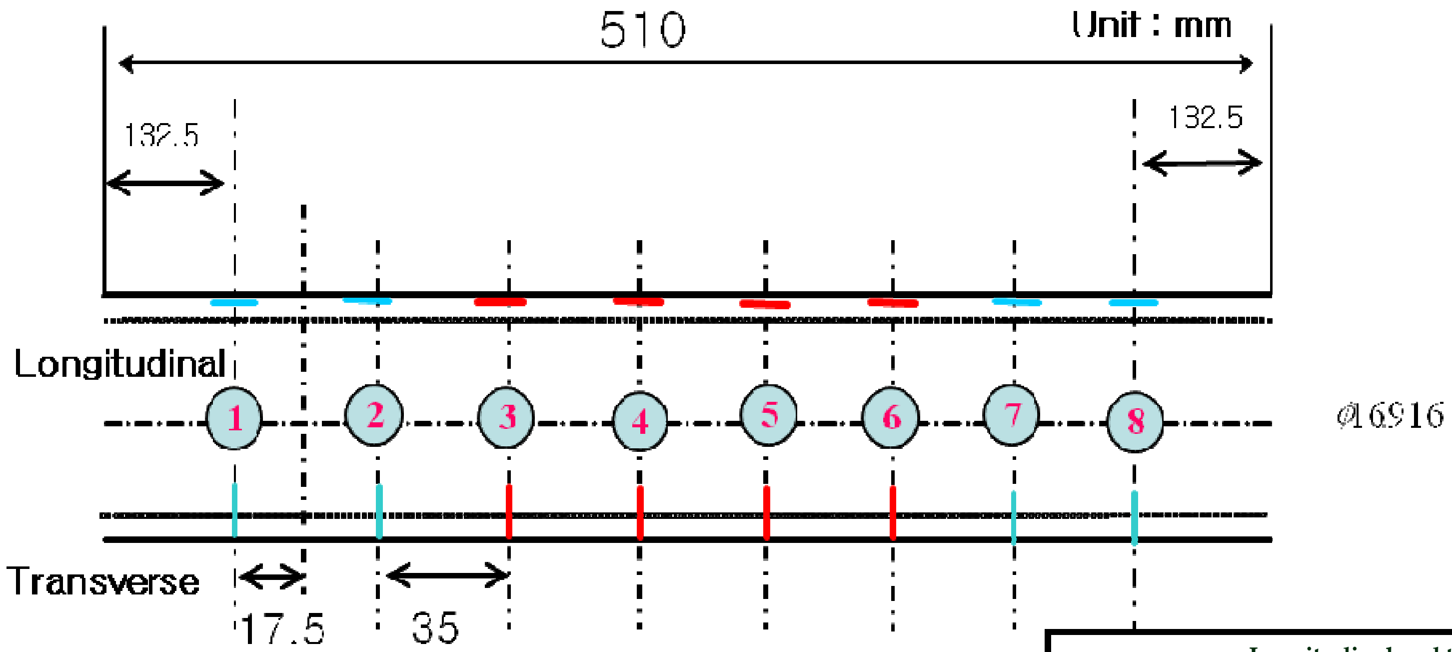

- 1 and 2 are inner defects,
- 3,4,5, and 6 are outer defects with PVC,
- 7 and 8 are inner defects

Longitudinal and transverse defects

Def.#	W	L	D	Remarks
1	0.2	5.00	0.213 (20 %)	Inner defects
2	0.2	5.00	0.427 (40 %)	
3	0.2	5.00	0.213 (20 %)	Outer defects PVC(1018)
4	0.2	5.00	0.427 (40 %)	
5	0.2	5.00	0.639 (60 %)	
6	0.2	5.00	0.852 (80 %)	
7	0.2	5.00	0.639 (60 %)	Inner defects
8	0.2	5.00	0.852 (80 %)	

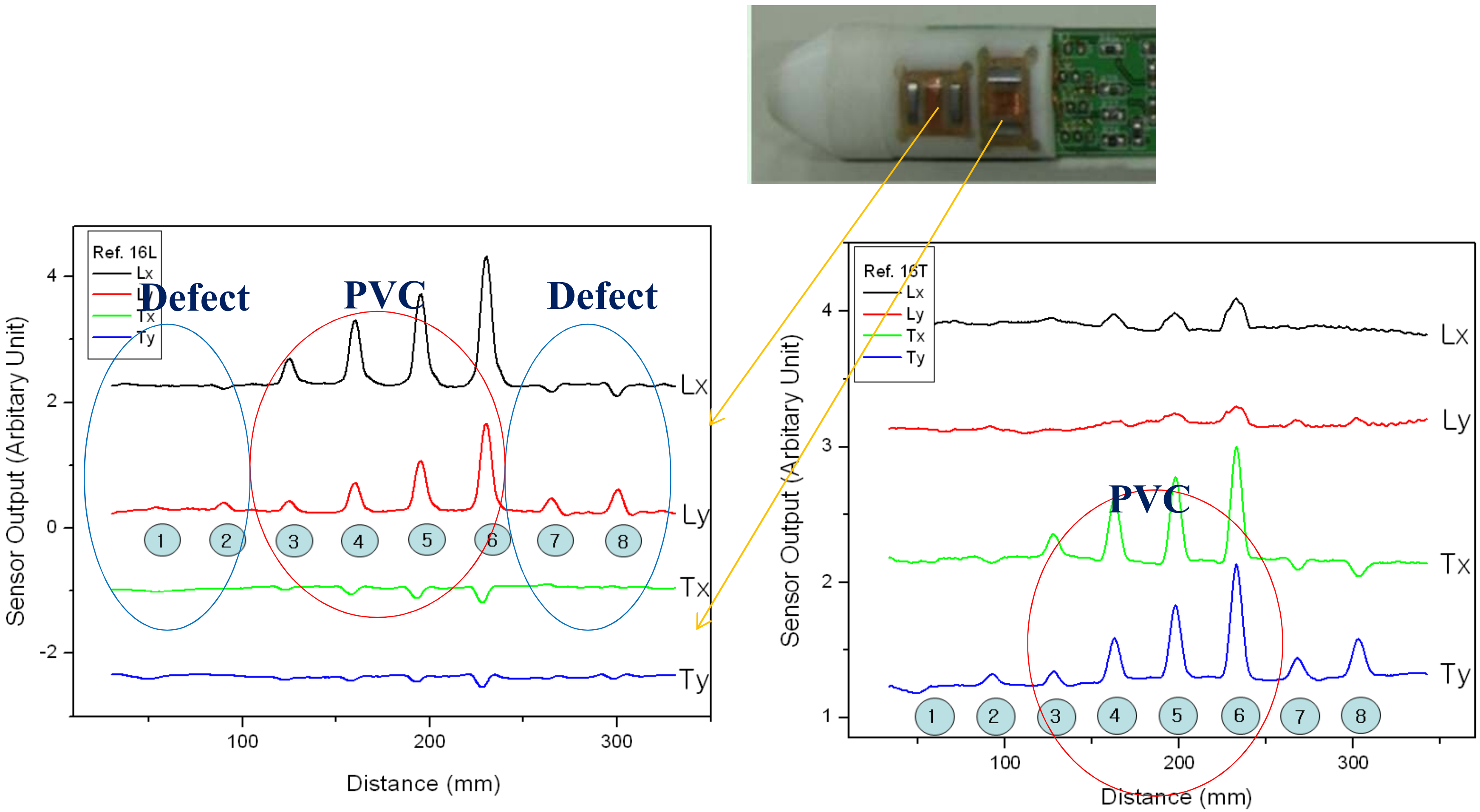

For longitudinal defects and PVC

For circumferential defects and PVC

We can distinguish PVCs and defects, and longitudinal and circumferential defects

!! ECT is very difficult to detect circumferential defects

Flux-gate Magnetometer

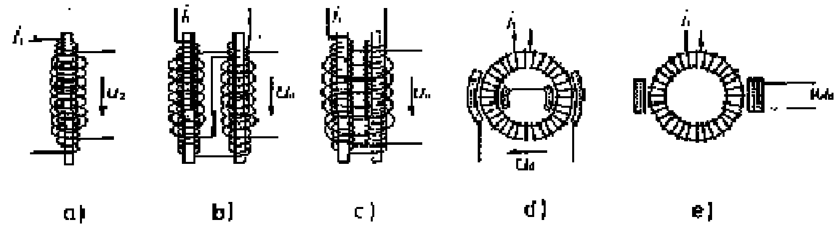

Verschiedene Sonden nach dem Prinzip der Unsymmetrie in der Magnetisierung

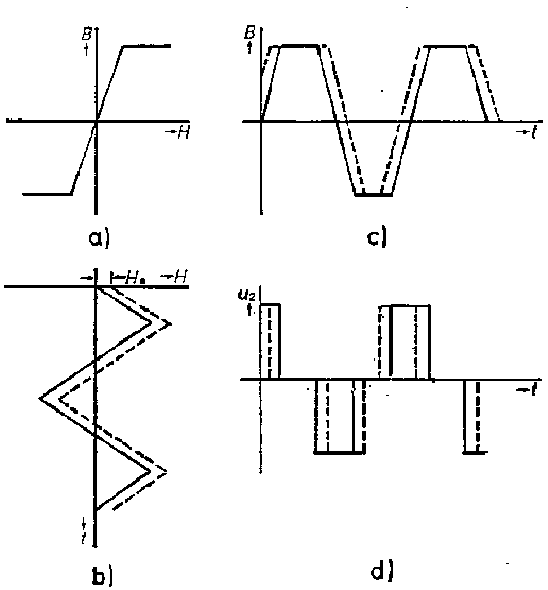

One core sensor

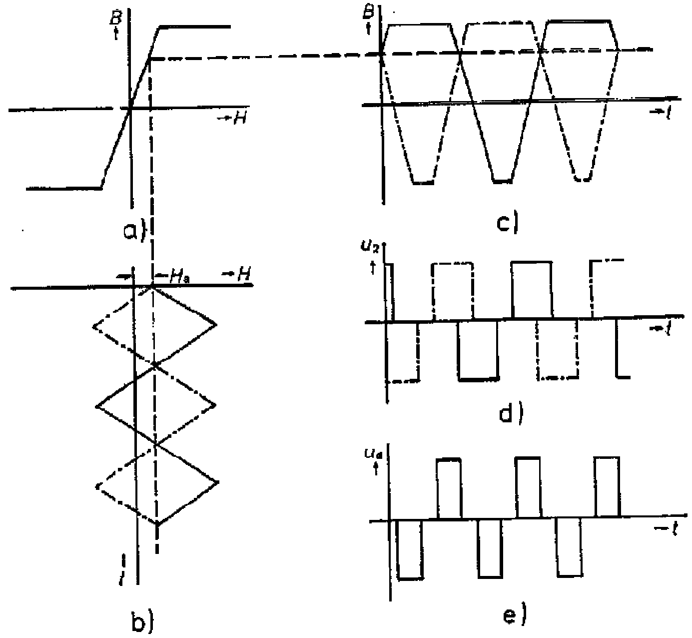

Two core sensor

3-축 flux-gate Magnetometer의 계략도

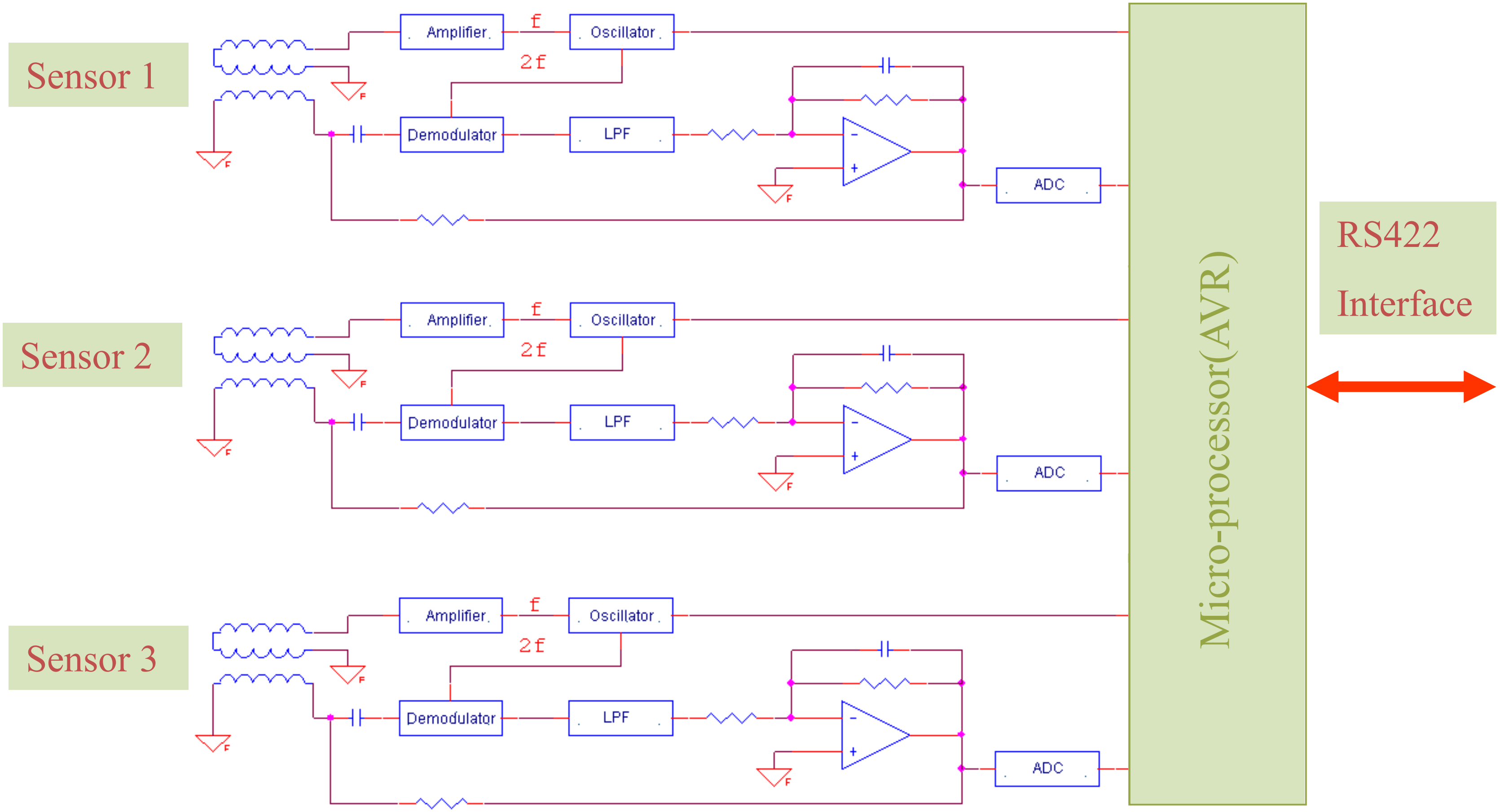

Sensorpia Co.

조립된 마그네토미터의 사진

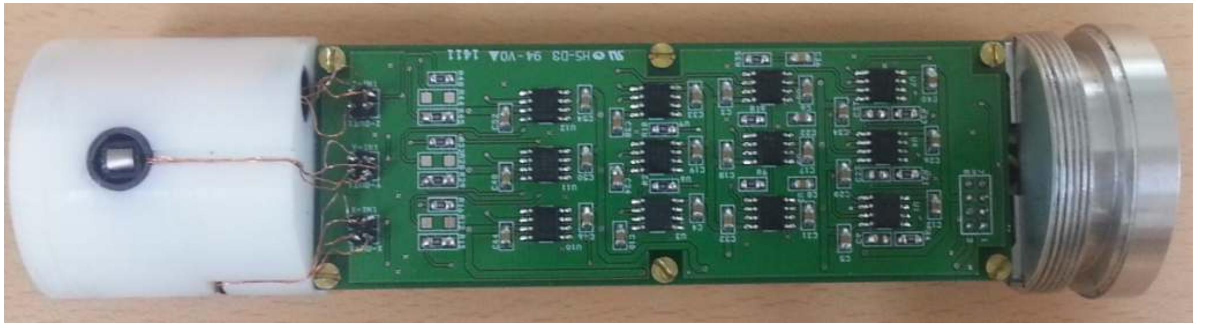

Analog PCB

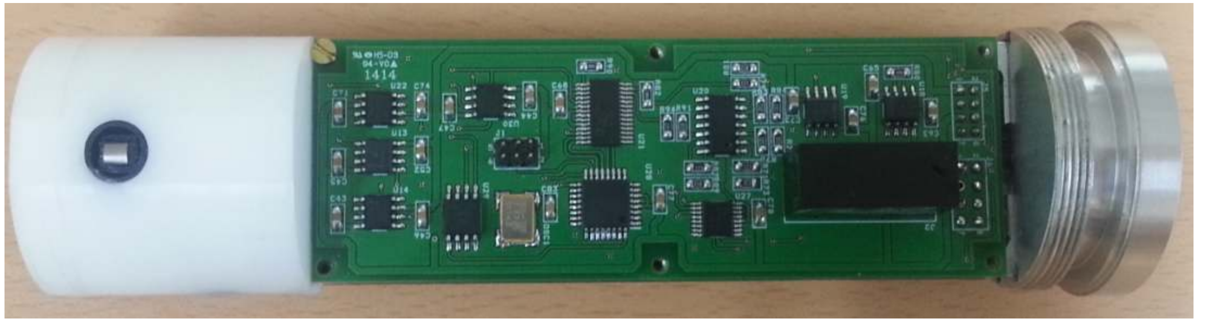

Digital PCB

Sensorpia Co.

선형도(linearity)

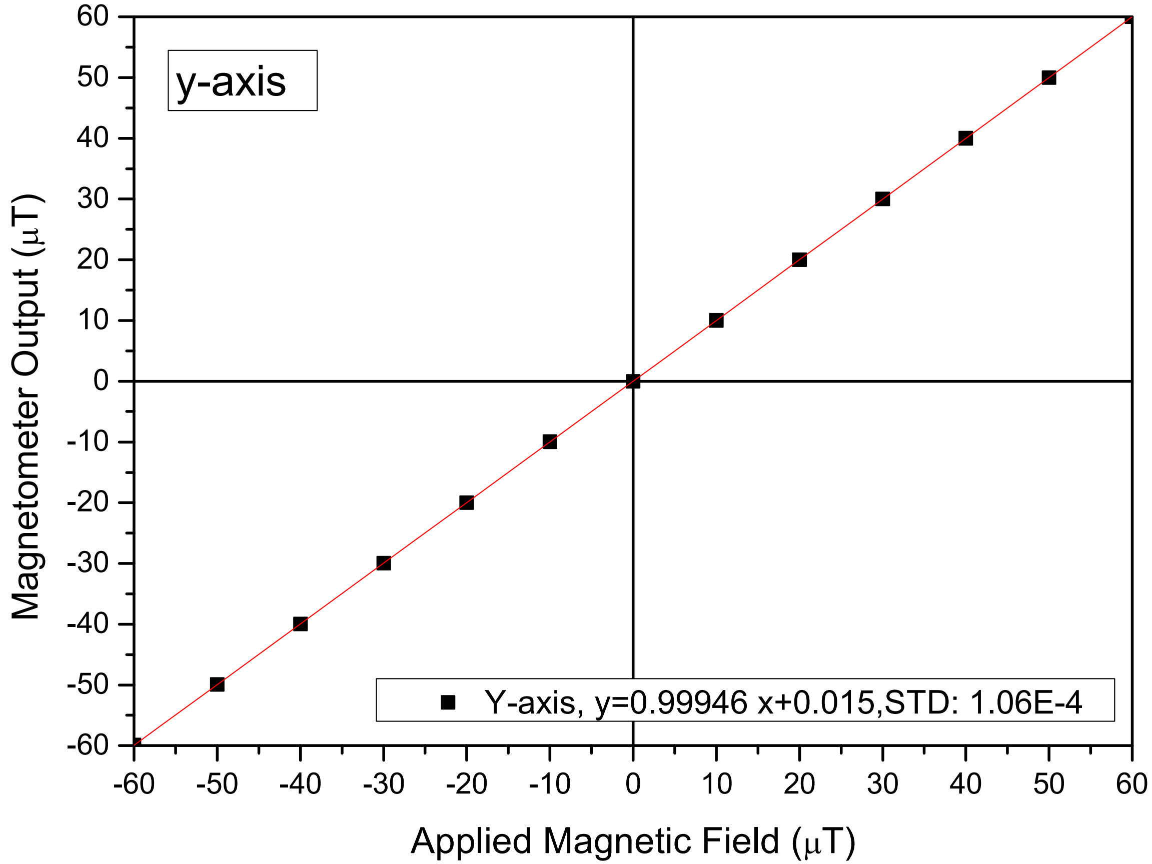

마그네토미터의 noise 특성

Sensorpia Co.

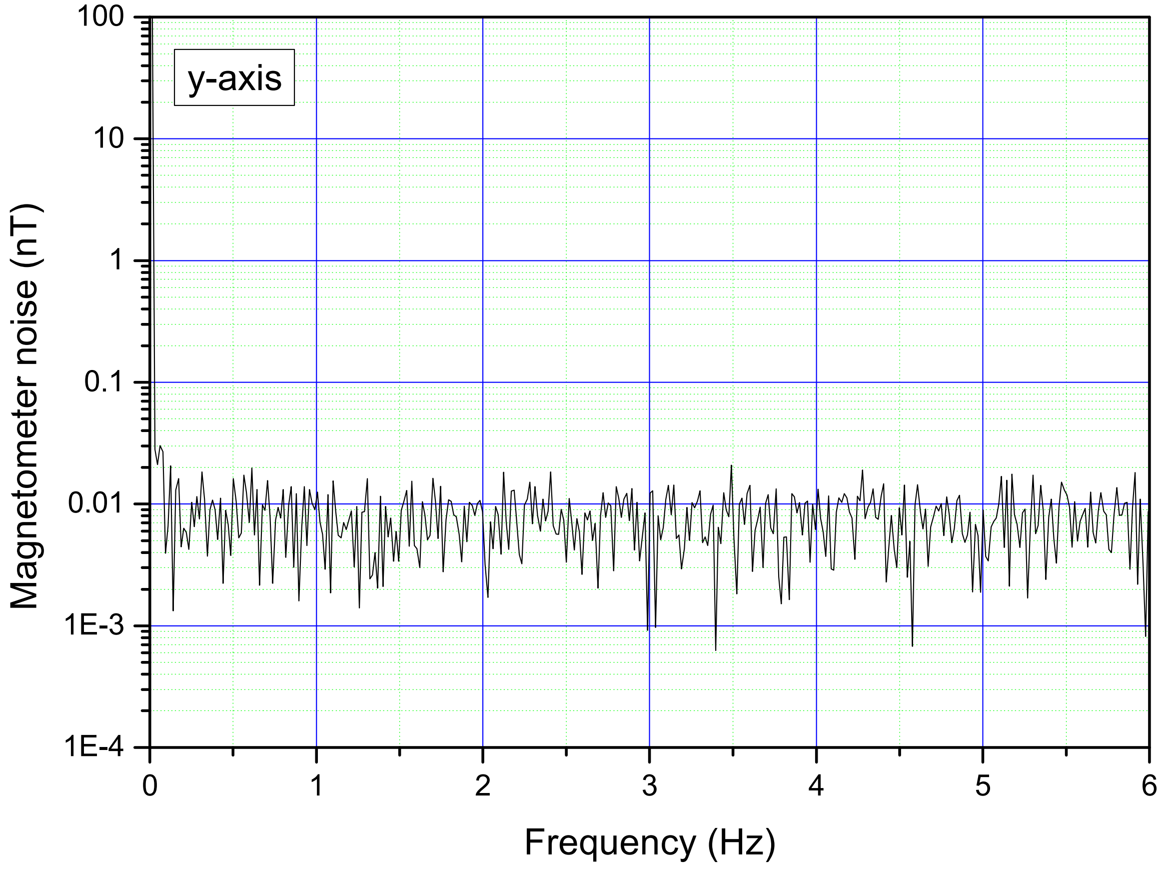

Magnetometer for KoDSAT

Photograph of KoDSAT

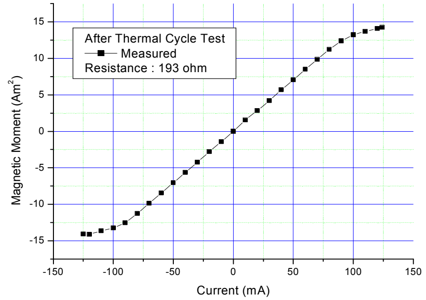

Photograph of Magnetic torquer

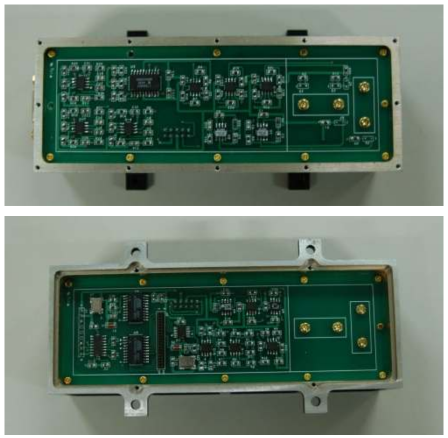

Photograph of 3-axis Fluxgate Magnetometer

Application of magnetometer

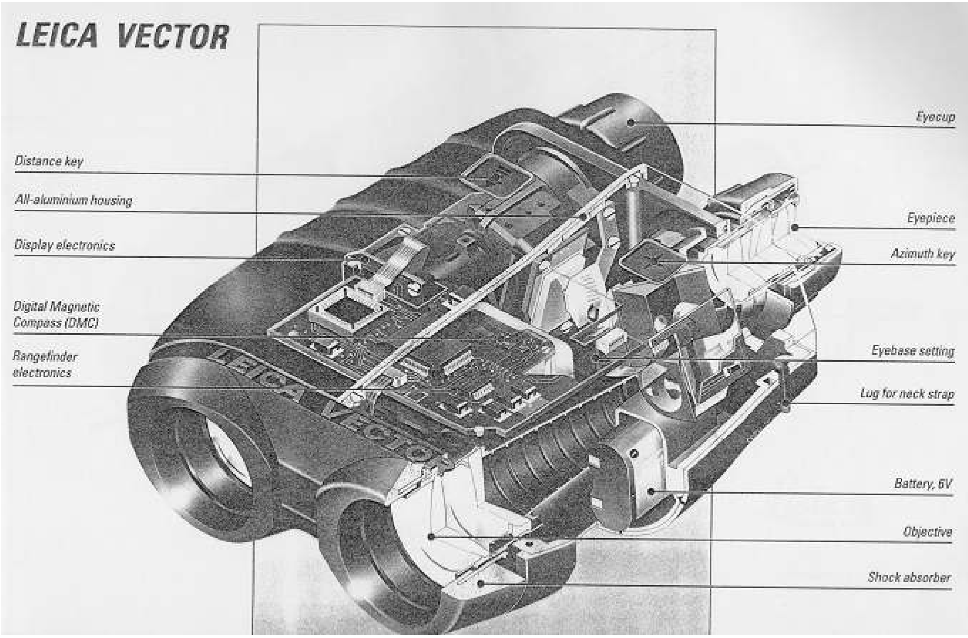

Telescope with direction indication

Moon magnetic field measurement

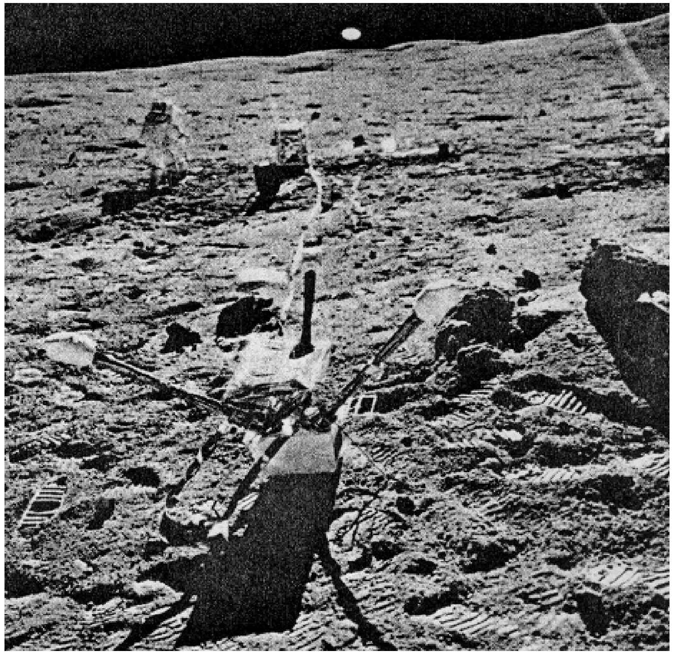




Joule Effect (Magnetostriction)

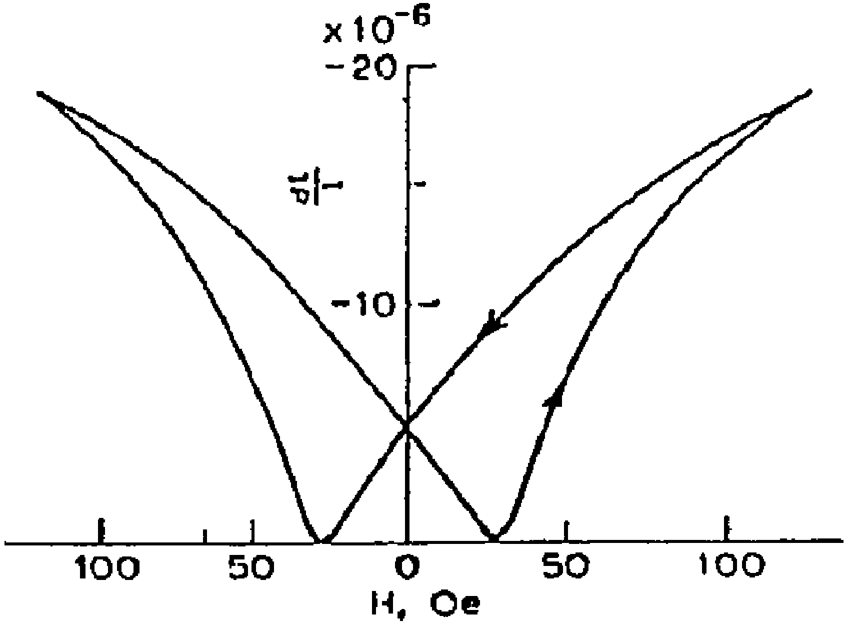

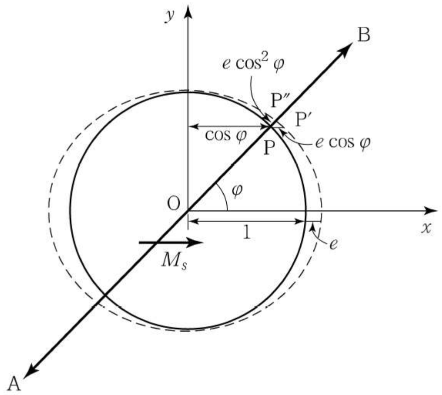

$$\frac{\Delta l}{l} = e\cos^2\varphi$$

$$\frac{\Delta\ell}{\ell} + \frac{\Delta a}{a} + \frac{\Delta b}{b} = 0$$

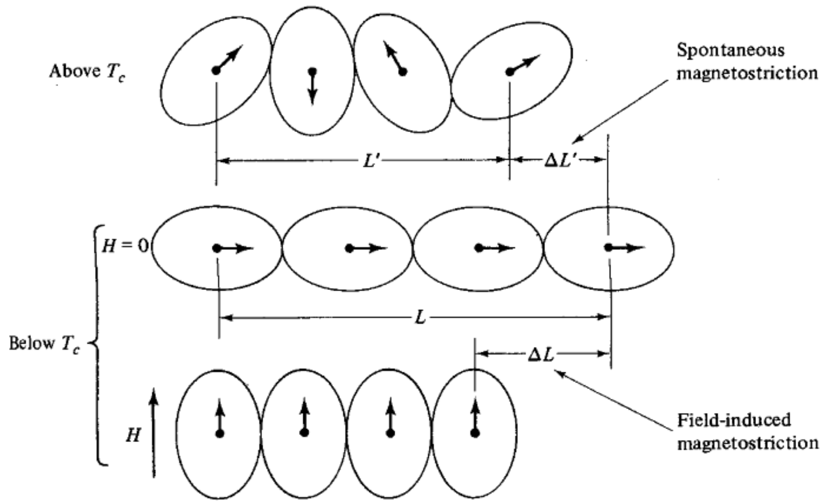

Actuator using Terfenol-D

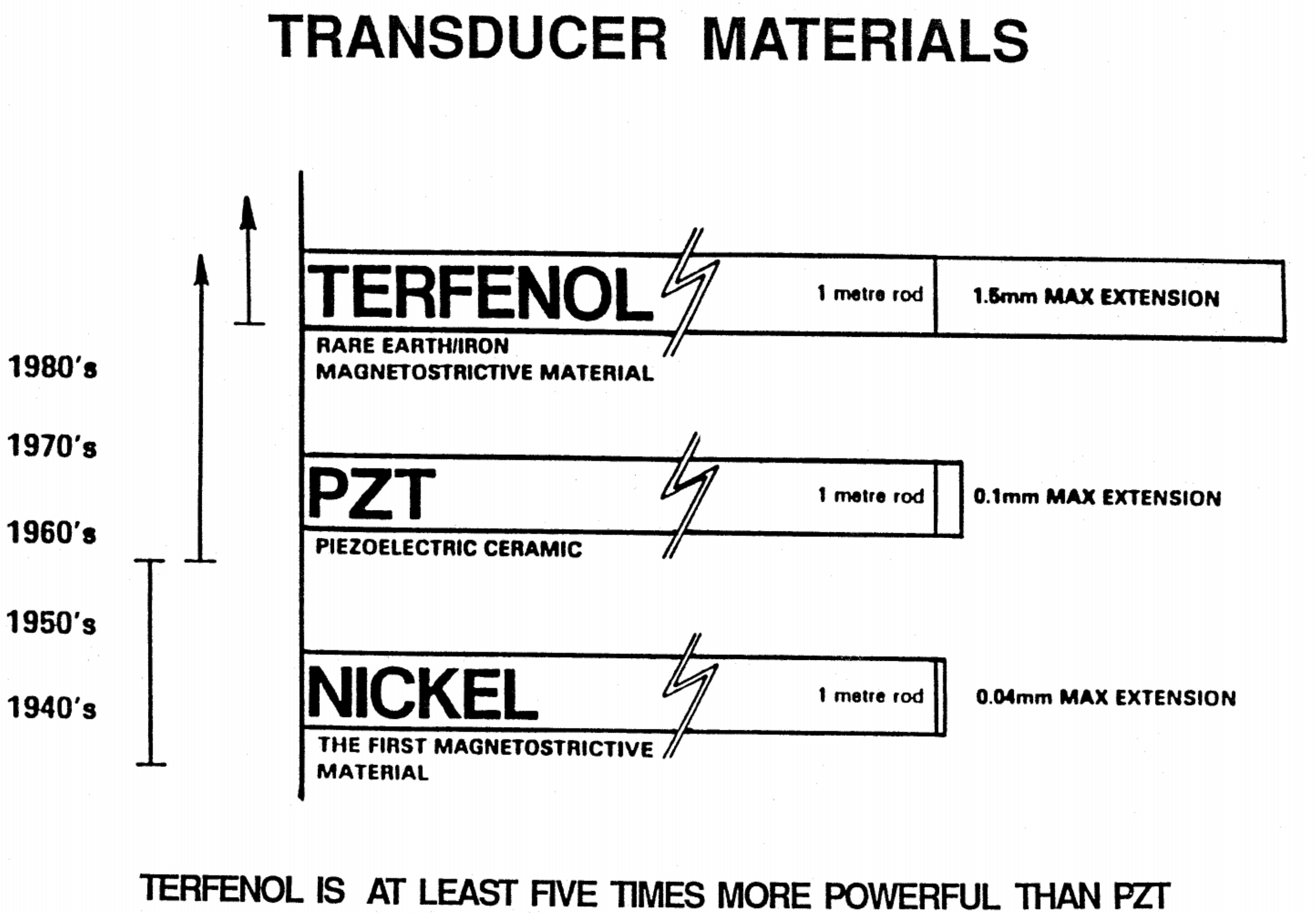

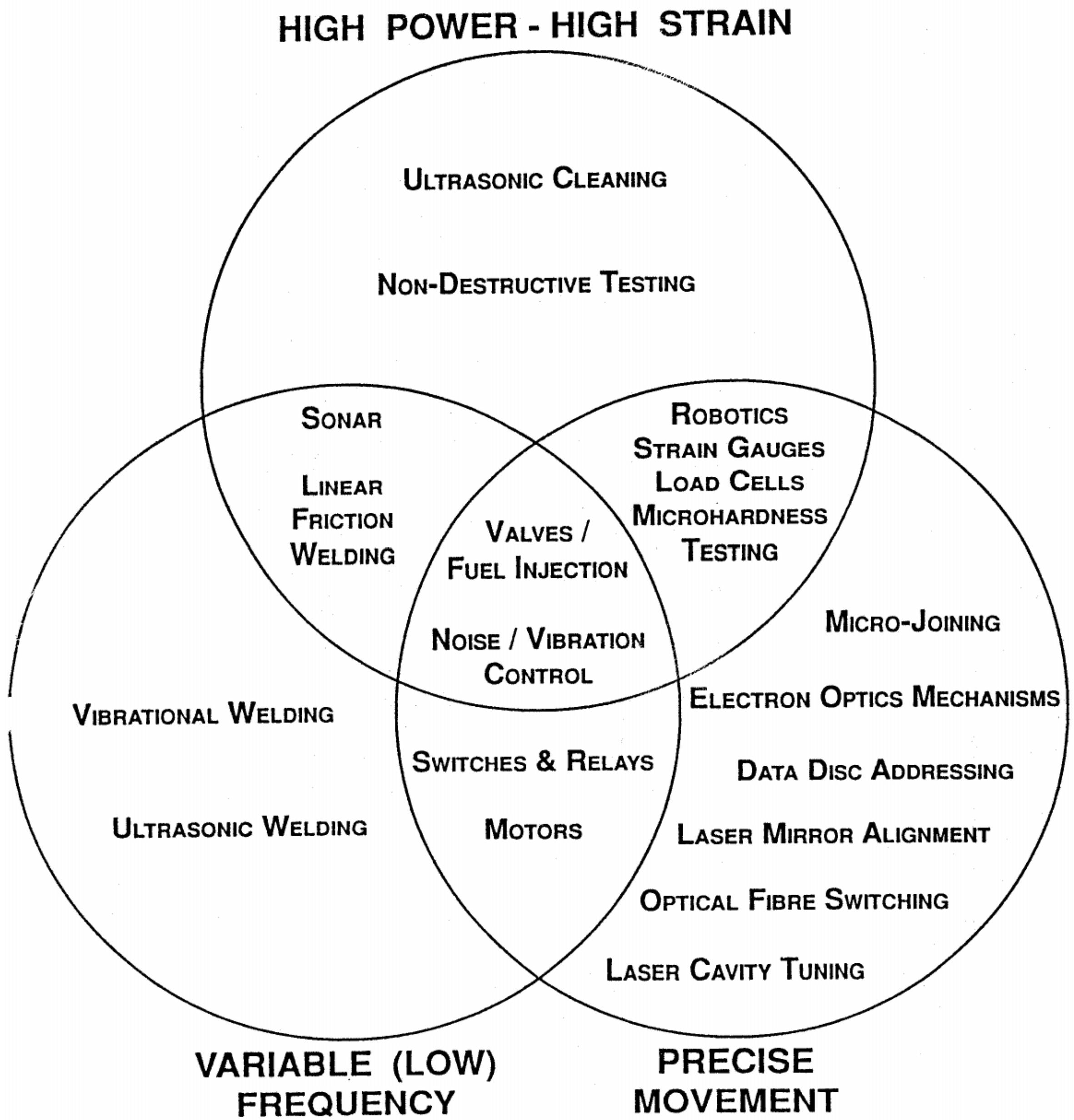
HIGH POWER - HIGH STRAIN
ULTRASONIC CLEANING
NON-DESTRUCTIVE TESTING
SONAR
LINEAR FRICTION WELDING
ROBOTICS
STRAIN GAUGES
LOAD CELLS
MICROHARDNESS TESTING
VALVES / FUEL INJECTION
NOISE / VIBRATION CONTROL
MICRO-JOINING
VIBRATIONAL WELDING
ELECTRON OPTICS MECHANISMS
SWITCHES & RELAYS
DATA DISC ADDRESSING
ULTRASONIC WELDING
MOTORS
LASER MIRROR ALIGNMENT
OPTICAL FIBRE SWITCHING
LASER CAVITY TUNING
VARIABLE (LOW) FREQUENCY
PRECISE MOVEMENT

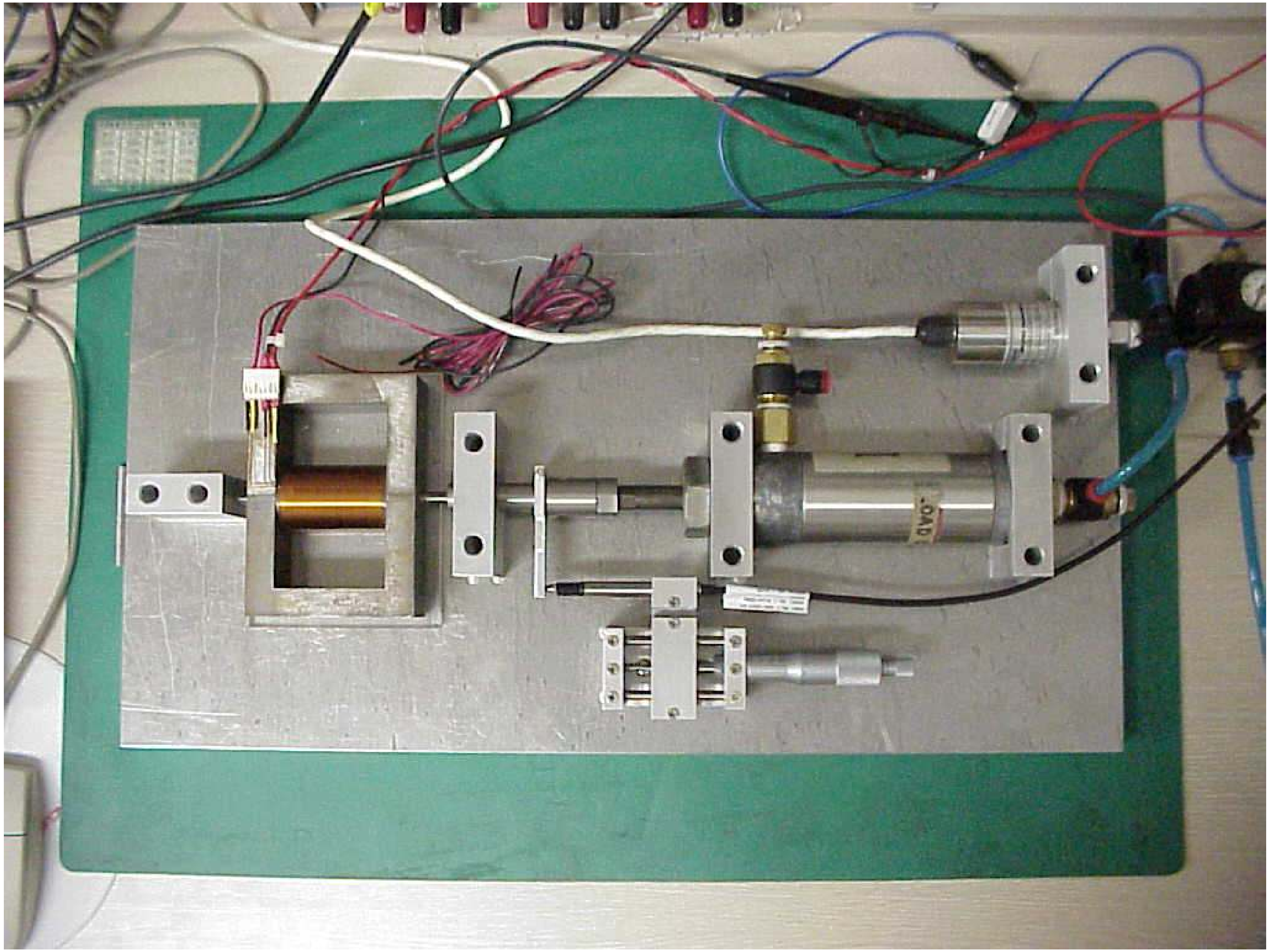

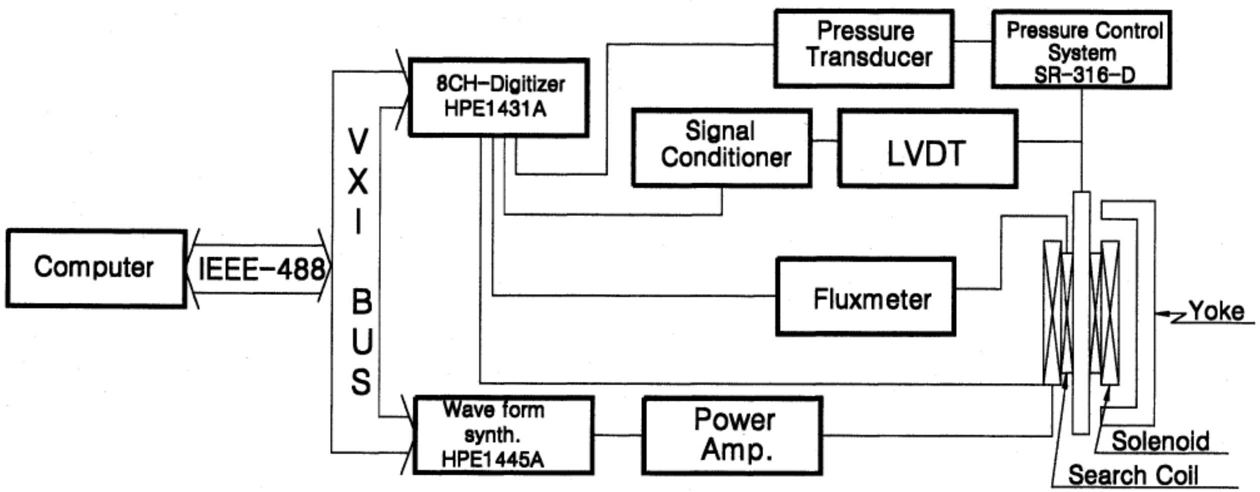
Pressure Transducer
Pressure Control System SR-316-D
8CH-Digitizer HPE1431A
Signal Conditioner
LVDT
Computer
IEEE-488
VXI BUS
Fluxmeter
Yoke
Wave form synth. HPE1445A
Power Amp.
Solenoid
Search Coil

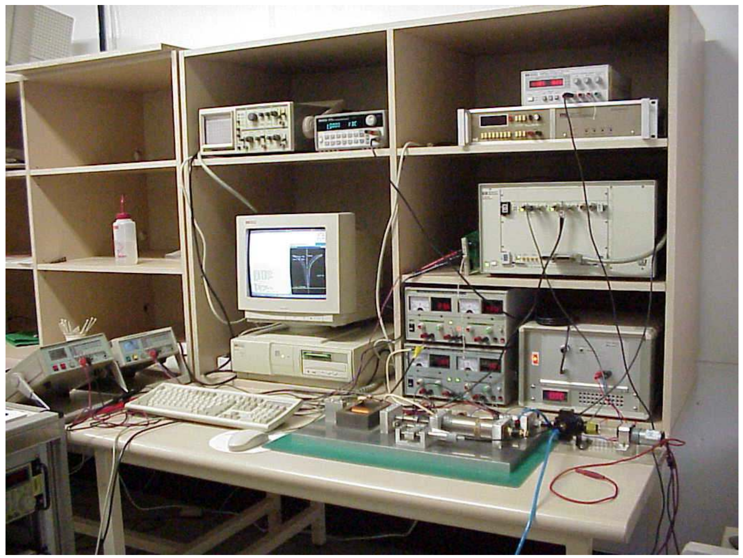

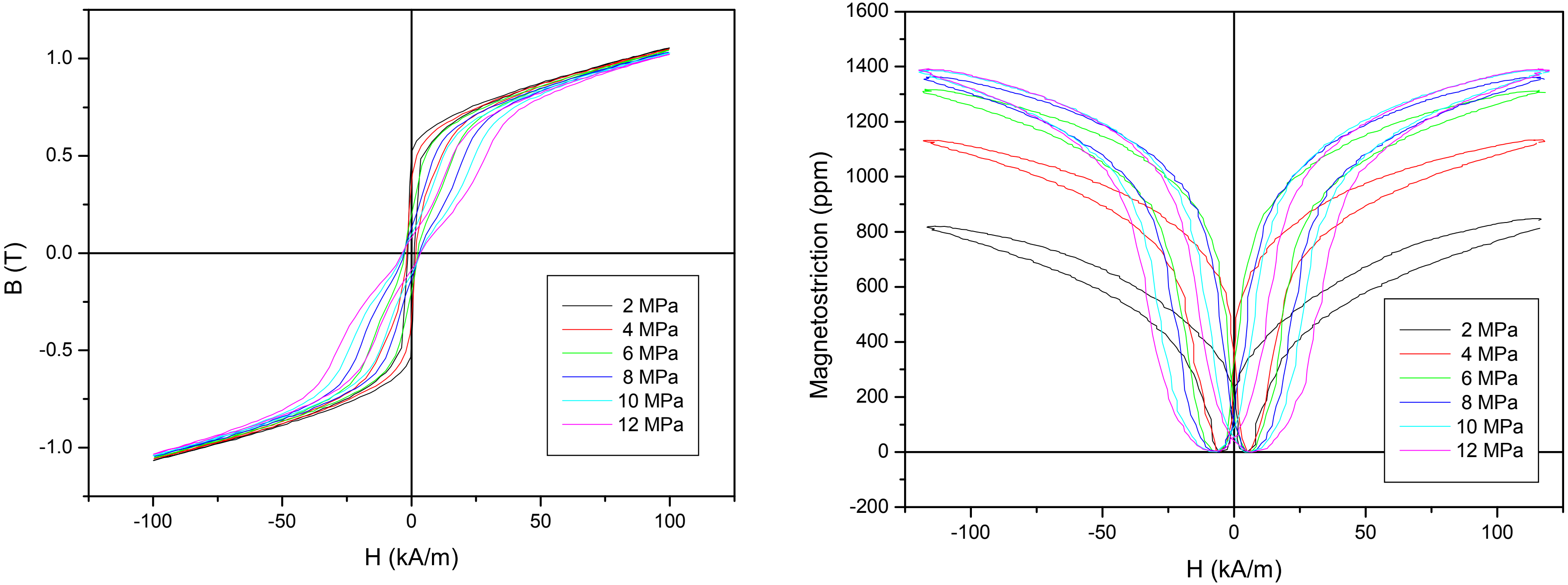

B (T)
1.0
0.5
0.0
-0.5
-1.0
-100
-50
0
50
100
H (kA/m)
2 MPa
4 MPa
6 MPa
8 MPa
10 MPa
12 MPa
Magnetostriction (ppm)
1600
1400
1200
1000
800
600
400
200
0
-200
-100
-50
0
50
100
H (kA/m)
2 MPa
4 MPa
6 MPa
8 MPa
10 MPa
12 MPa

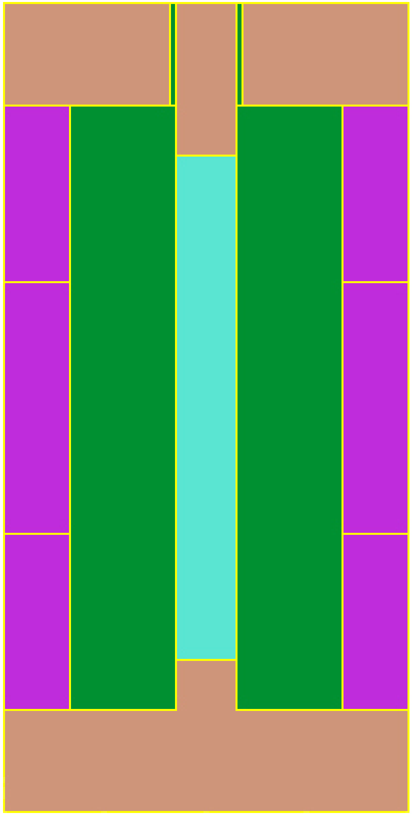

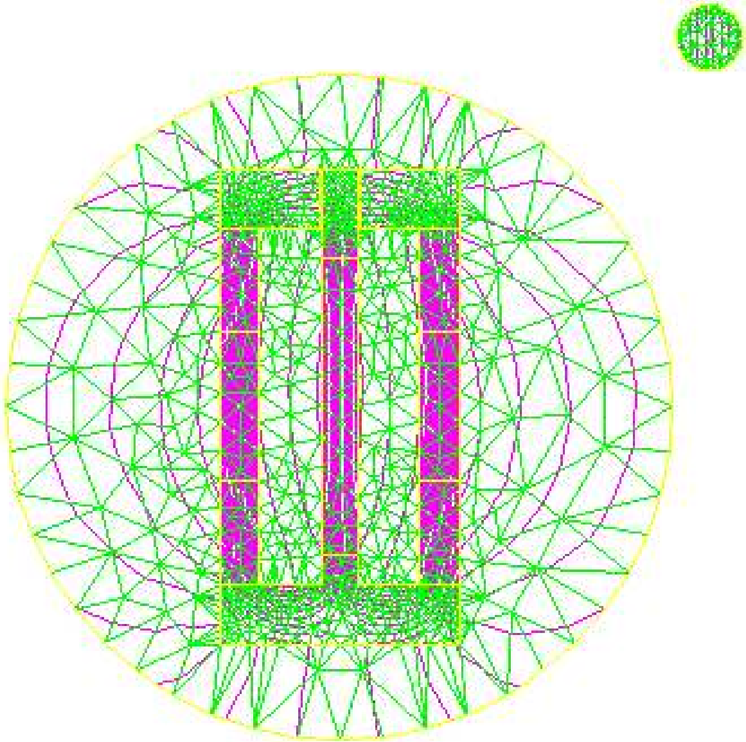

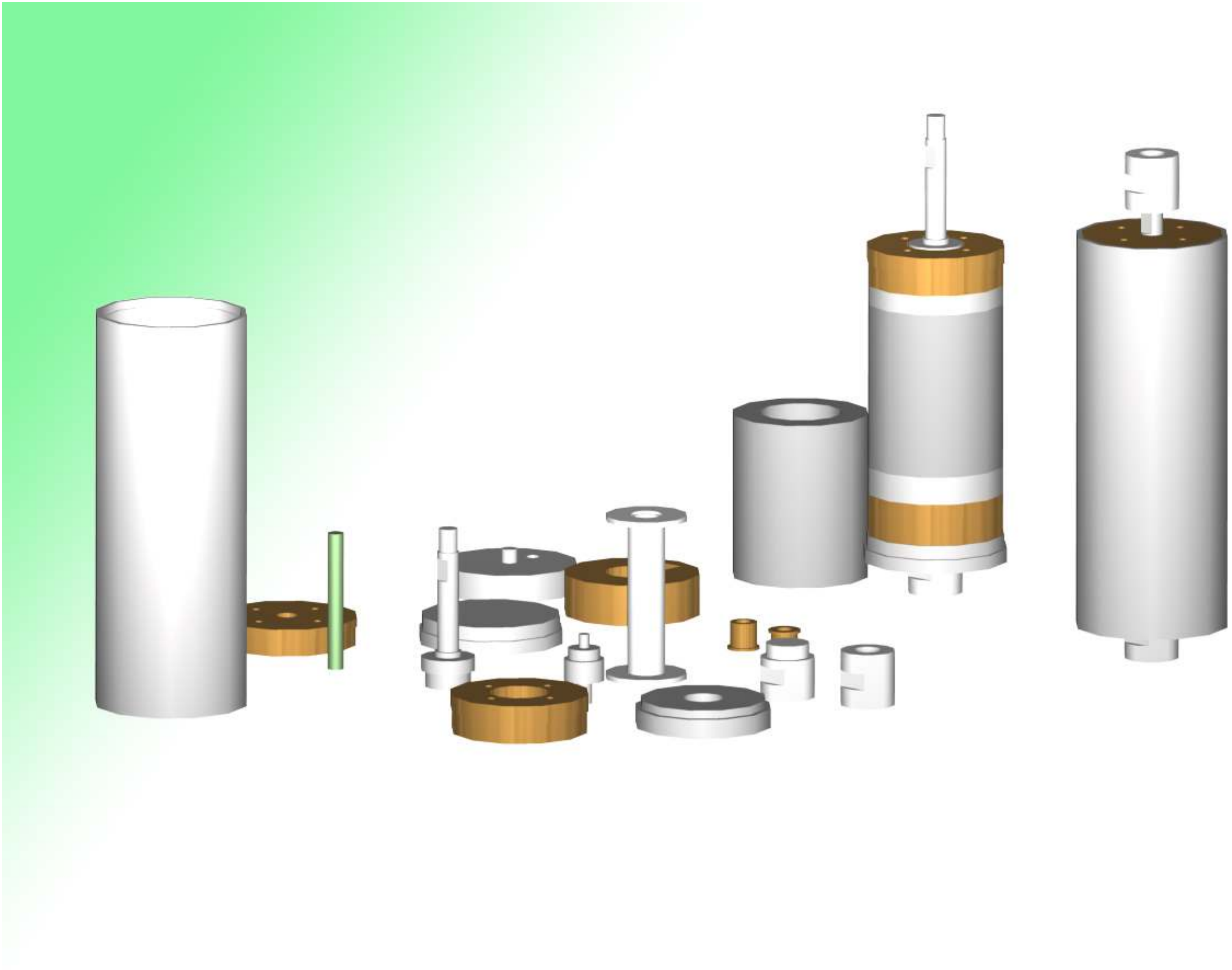

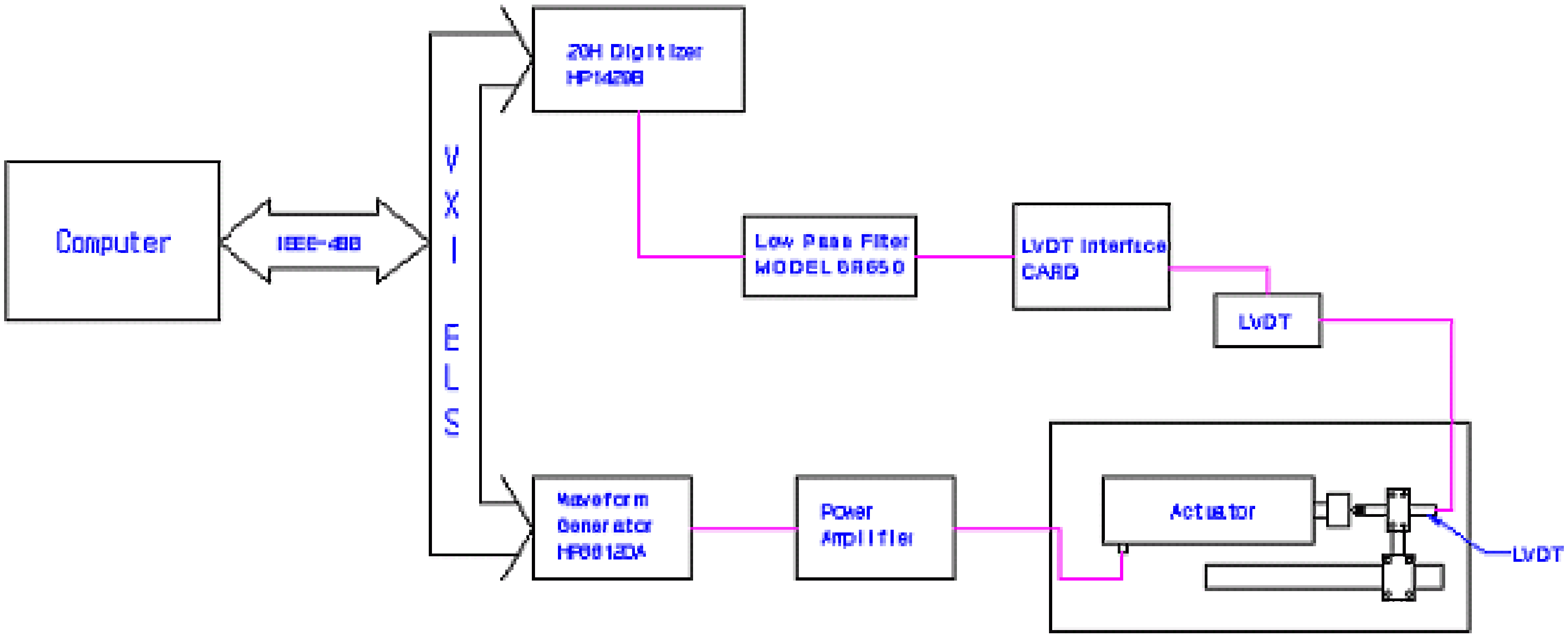

Computer
VXI
ELS
Low Pass Filter
LVDT Interface
CARD
LVDT
Waveform
Generator
Power
Amplifier
Actuator
LVDT

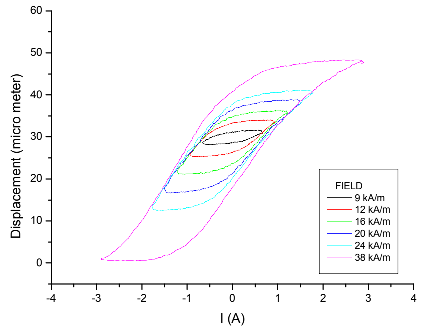
Displacement (micro meter)
I (A)
FIELD
9 kA/m
12 kA/m
16 kA/m
20 kA/m
24 kA/m
38 kA/m

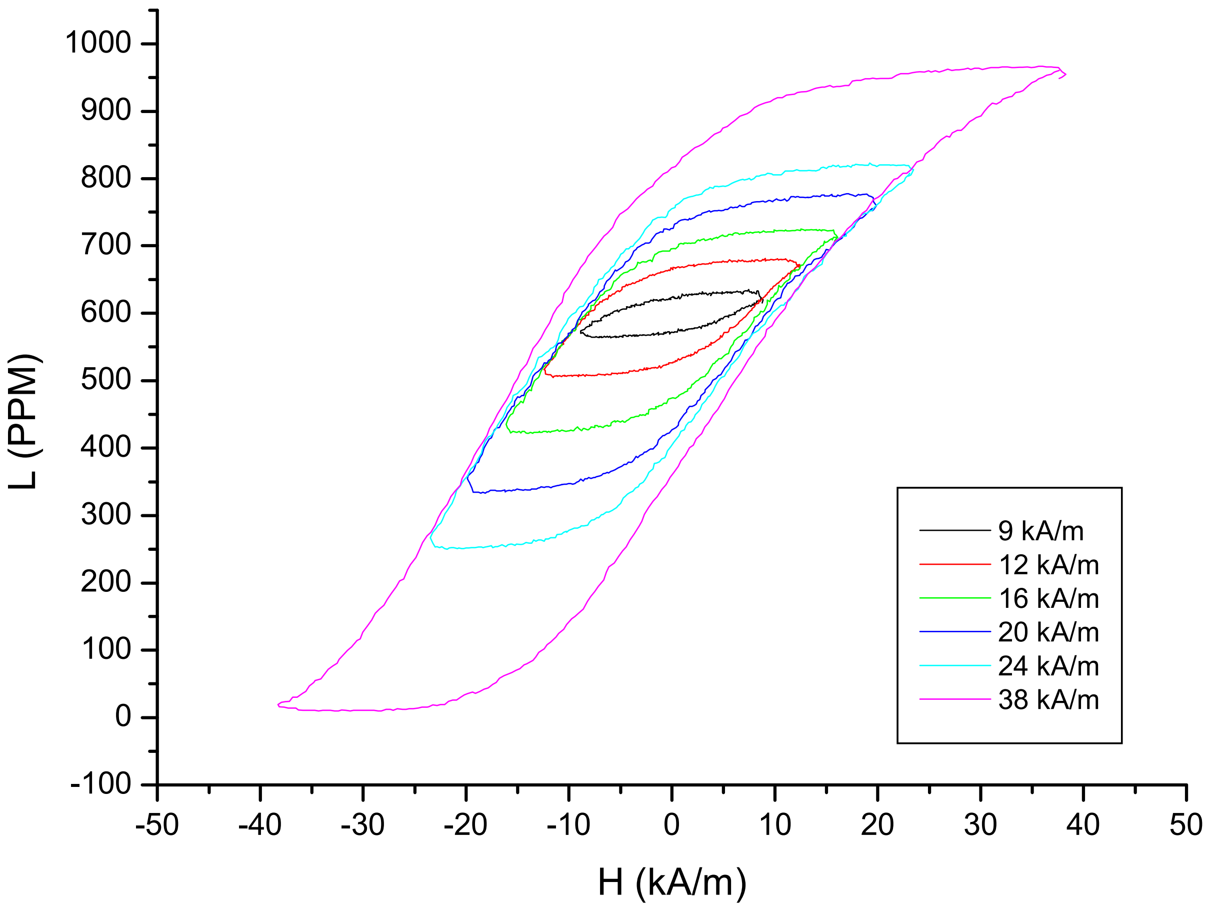
L (PPM)
H (kA/m)
9 kA/m
12 kA/m
16 kA/m
20 kA/m
24 kA/m
38 kA/m

Magnetostrictive displacement sensor

Villari Effect (Inverse of Joule Effect)

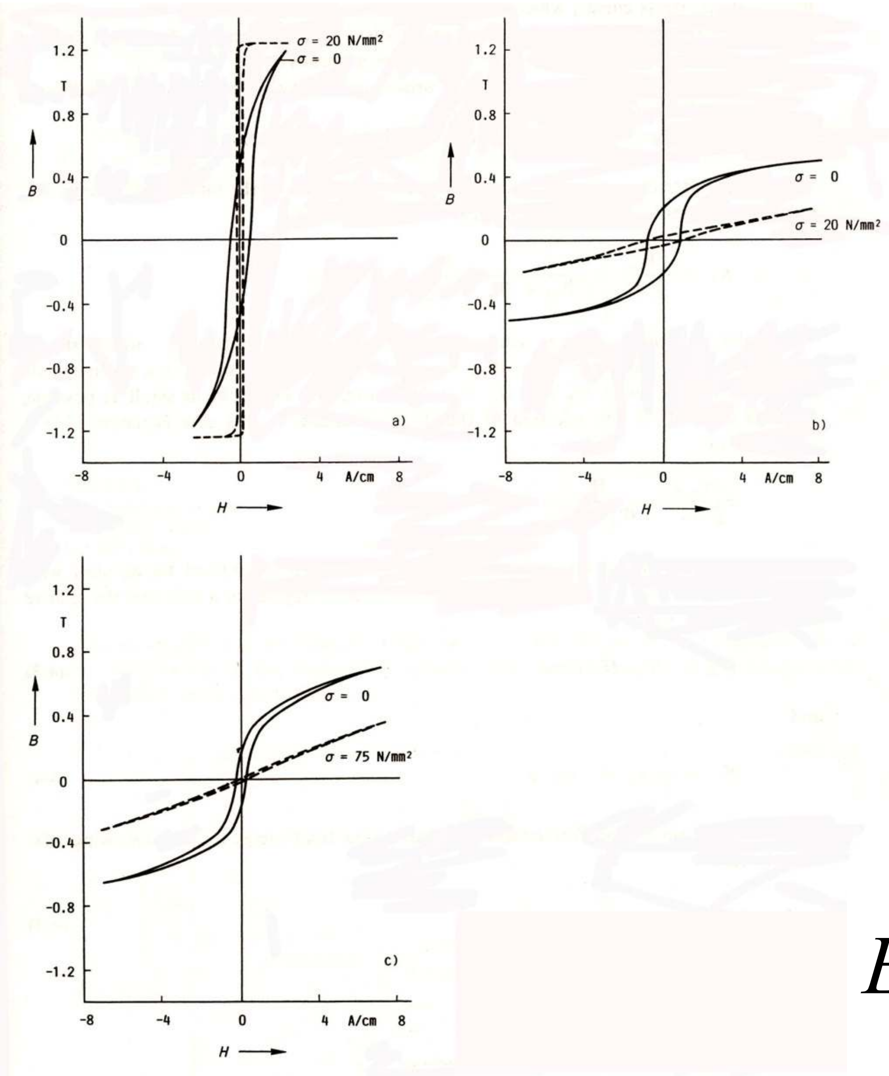

Hysteresis loops under tensile stress σ.

(a) Crystalline 68% NiFe λs = +25 · 10-6;

(b) crystalline pure Ni, λs = -35 · 10-6;

(c) amorphous Co-based alloy,

λs = -3,5 · 10-6.

$$E_{me} = \frac{3}{2}\lambda_s \cdot \sigma \cdot \sin^2 \varphi$$

Permeability depending on the stress

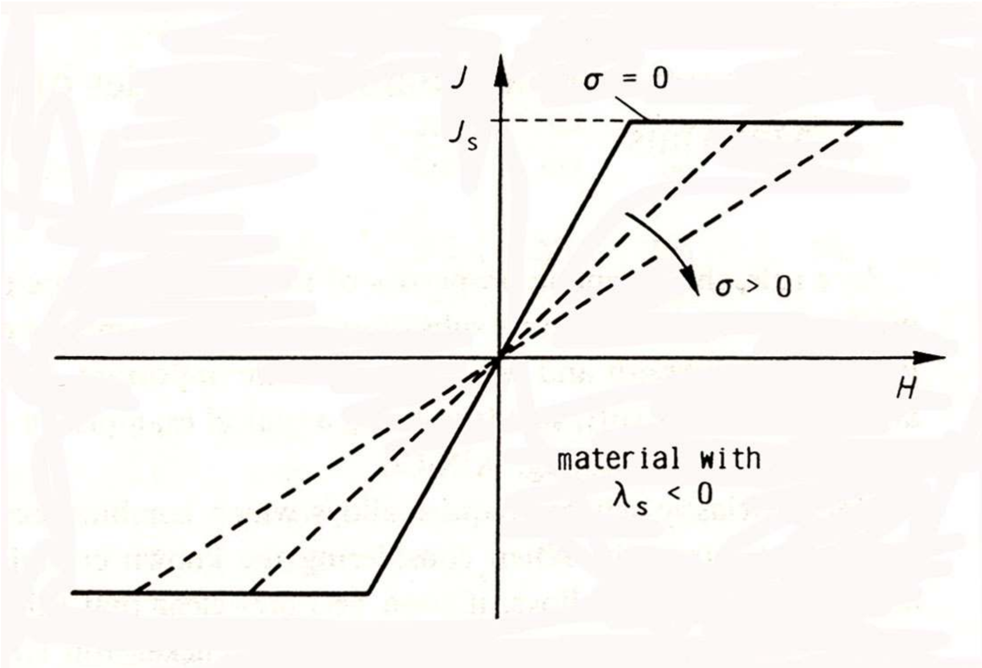

$$\mu_r = \frac{J_s^2}{3\mu_o \lambda_s Y} \frac{1}{\sigma}$$

Calculated magnetization curves under stress.

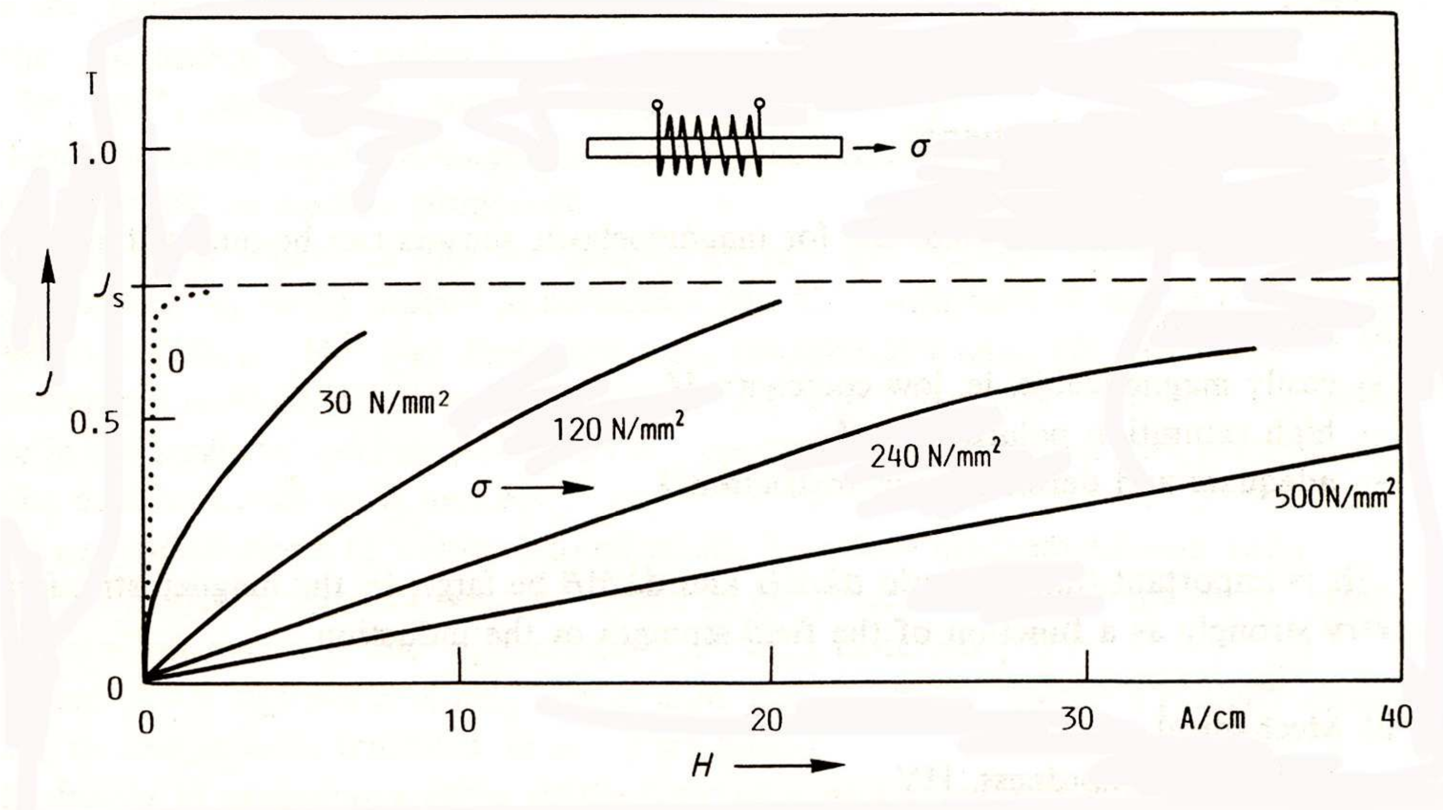

Variation of magnetization curve by an applied tensile force (Co-based amorphous alloy).

Alloy Requirement

Type	Alloy	$\lambda_s \cdot 10^{-6}$	H_c A/cm	J_s T	HV	R_p N/mm^2	E kN/mm^2
Crystalline	50 Co, 50 Fe	+70	1.4	2.35	200	400	230
	50 Ni, 50Fe	+25	0.05	1.55	110	140	140
	97 Fe, 3 Si	+9	0.1	2.0	180	350	150
	77 Ni, 15 Fe, Mo + Cu	±1	0.01	0.8	100	150	200
	77 Ni, 15 Fe, Mo + Cu +Ti + Nb	~0.5	0.025	0.5	220	500	200
	Spring steel 1.8159	−1	15	2.1	550	1500	
	Shaft steel CK 45		10	~2.1		450	
	Ni	−35	1.5	0.6	75	120	210
Amorphous[1)]	Fe_{80} B_{14} Si_6	+30	0.04	1.5	950		
	Fe_{40} Ni_{38} $(Mo, Si, B)_{22}$	+8	0.03	0.8	800		
	$(Co, Fe, Mo)_{73}$ $(B, Si)_{27}$	~0.2	0.003	0.55	1000	1500…	ca.
	Co_{75} Si_{15} B_{10}	−3.5	0.025	0.7	1000	2000	150
	Co_{68} Ni_{10} B_{14} Si_8	−8		0.85			
Crystalline	(Tb Dy) Fe_2[2)]	+2000	50	1.0	460	700[3)]	30

Materials for magnetoelastic sensors.

Why amorphous magnetic materials are important

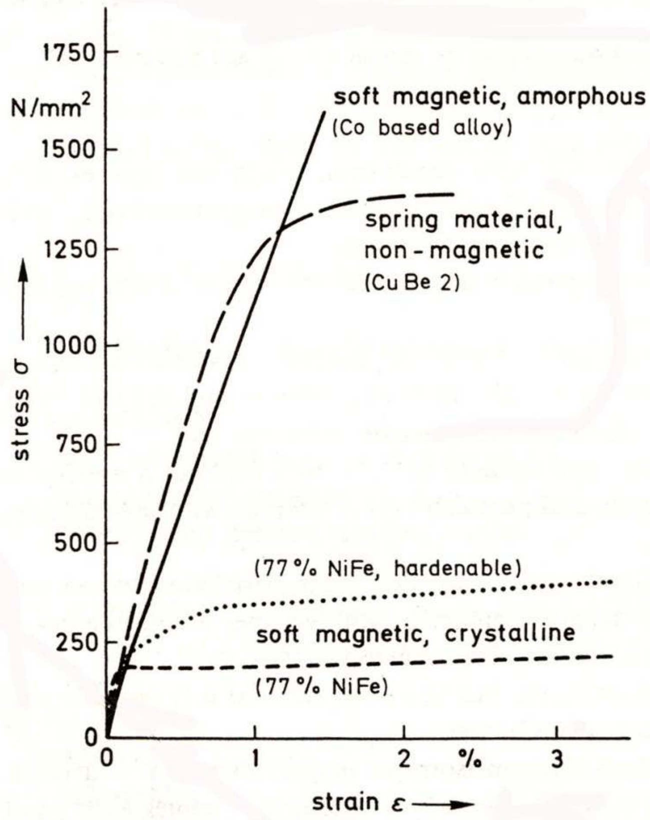

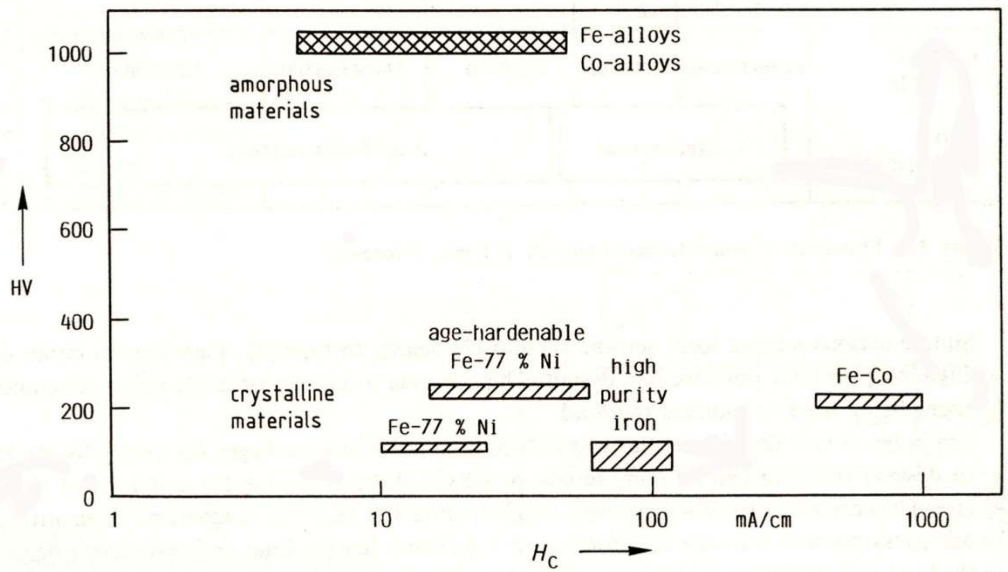

Coercivity and hardness of several materials.

Stress-strain curves of several materials.

Principles of magnetoelastic sensors

sensor type	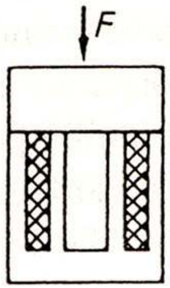 1	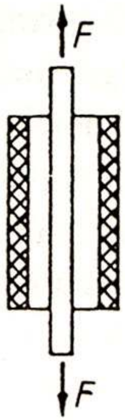 2	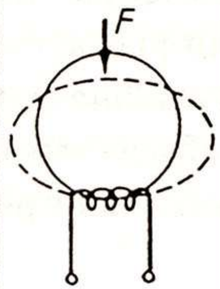 3	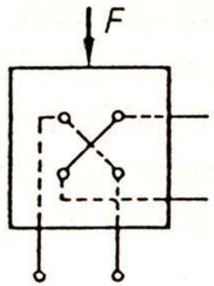 4	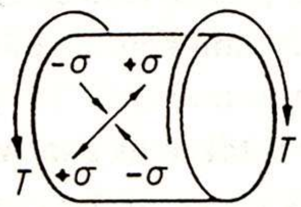 5
process variable	compression	tension	bending	compression	torsion
flux configuration	1-dimensional		2- or 3-dimensional		

Non-contact torque sensor

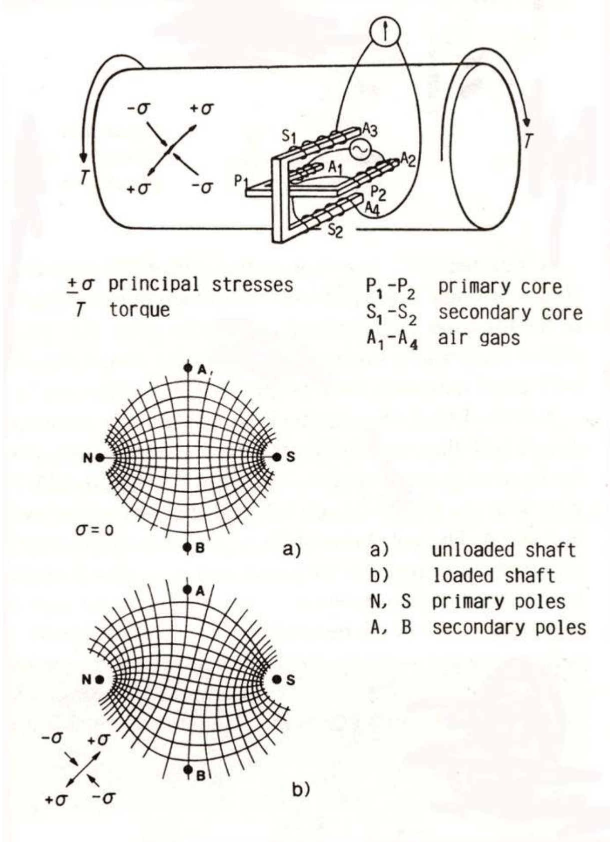

Principle of cross torductor torque sensor and flux pattern of sensor poles on the surface of a shaft
a) without and b)with torsional load

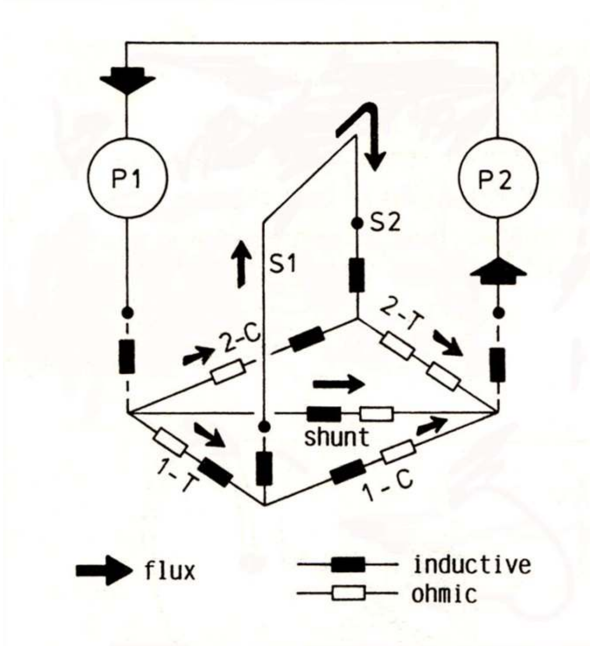

Equivalent magnetic circuit of cross type torque sensor

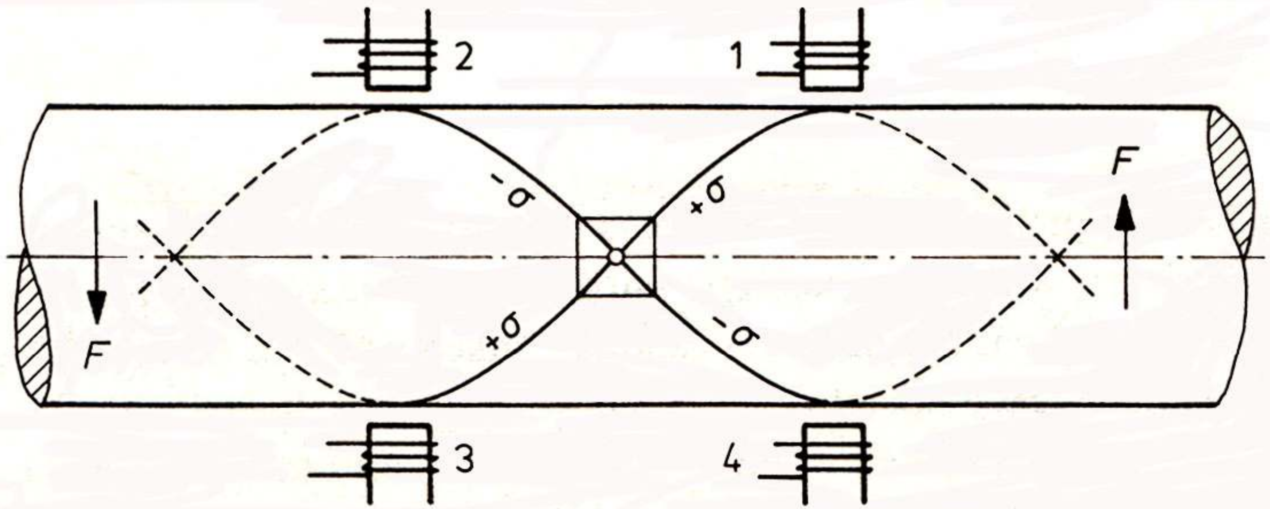

Helices of principal tensile and compressive stress on the surface of a shaft subjected to torsion [32]. Correlated changes of permeability are detected by four-branch yoke system with sensing coils 1,2,3 and 4 and a common excitation pole

Examples of torque sensors

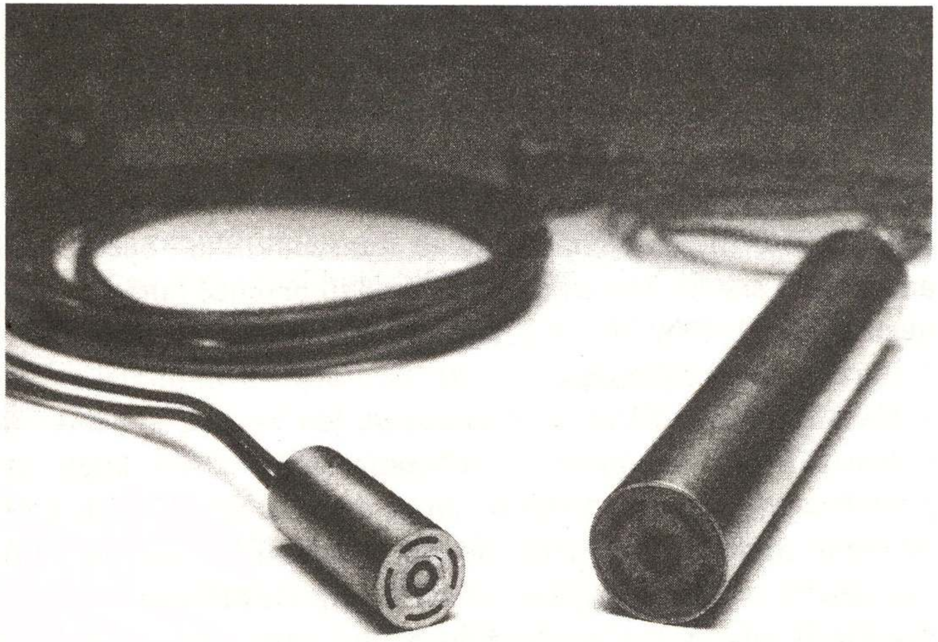

Four-branch type torque sensor heads. Pole structures realized by commercial multi-pole ferrites 14 and 18 min in diameter, (diameter of sensor head 17 and 24 mm, respectively)

Steel	Shaft material	Sensitivity in mV/Nm
C15	Cementation steel	1.00
C45	Heat-treatable steel	1.35
C60	Heat-treatable steel	4.43
42CrMo4	Heat-treatable steel	0.60
21CrMoV511	High-temperature construction steel	2.40

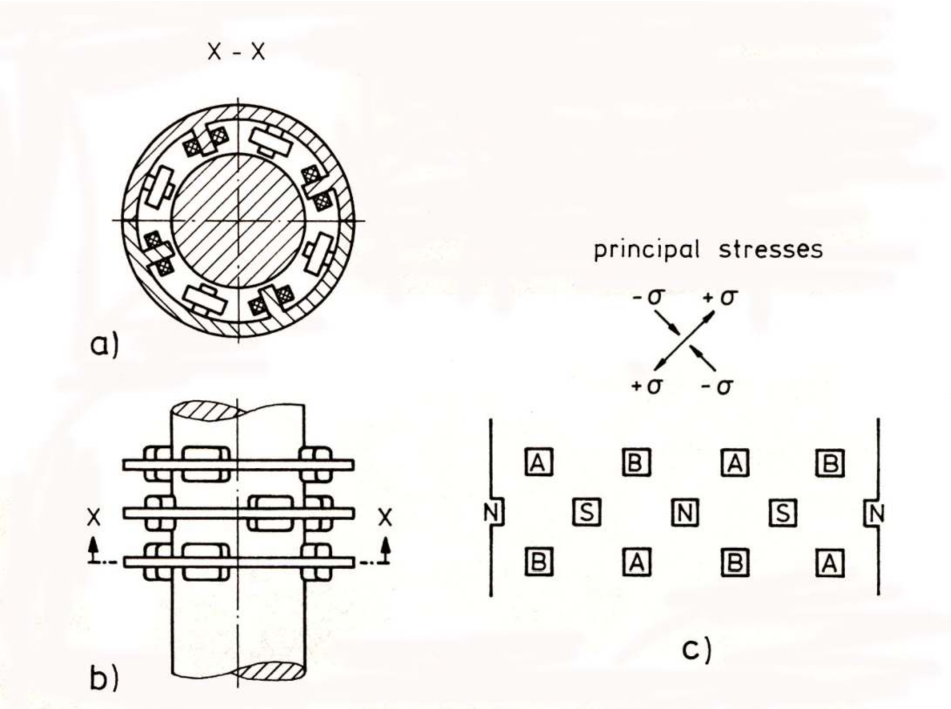

Principle of Ring Torductor torque transducer. (a, b) Physical structure, (c) evolution of the shaft surface under the transducer poles A and B

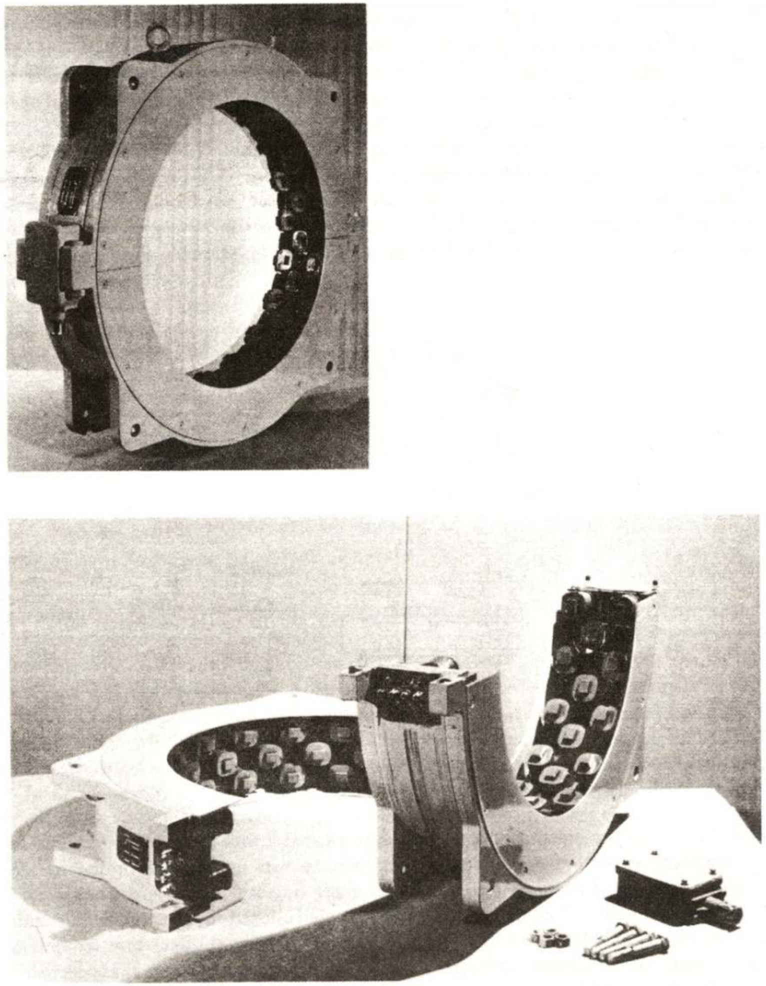

Ring torductor for measuring torque on ship propeller shafts (shaft diameter ca. 500 mm) (Courtesy ASEA Brown Boveri AG).

Principal designs of coaxial torque sensors

System variant	Coil design	"Magnetic" surface of shaft	Remarks of measurement effects
A		Homogeneous	Useful signal superposed with operating current induced voltage. Limited range of linearity. No detection of direction.
B	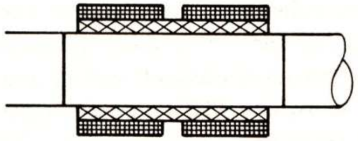	Homogeneous	No useful effect.
C	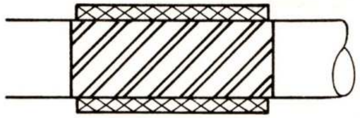	Grooved structure under 45° – one sided	Limited range of linearity. Principal asymmetry with respect to direction. Useful signal superimposed with operating current induced voltage.
D	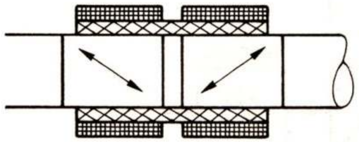	45° structure through "zero point" anisotropy	In principle good symmetry, linearity and zero point suppresion.
E	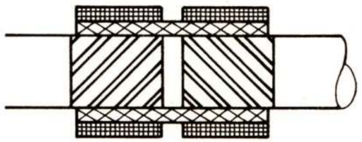	Symmetrical grooved structure under ±45°	As for D.

primary winding secondary winding

Schematic diagram of data processing electronics of a torque sensor

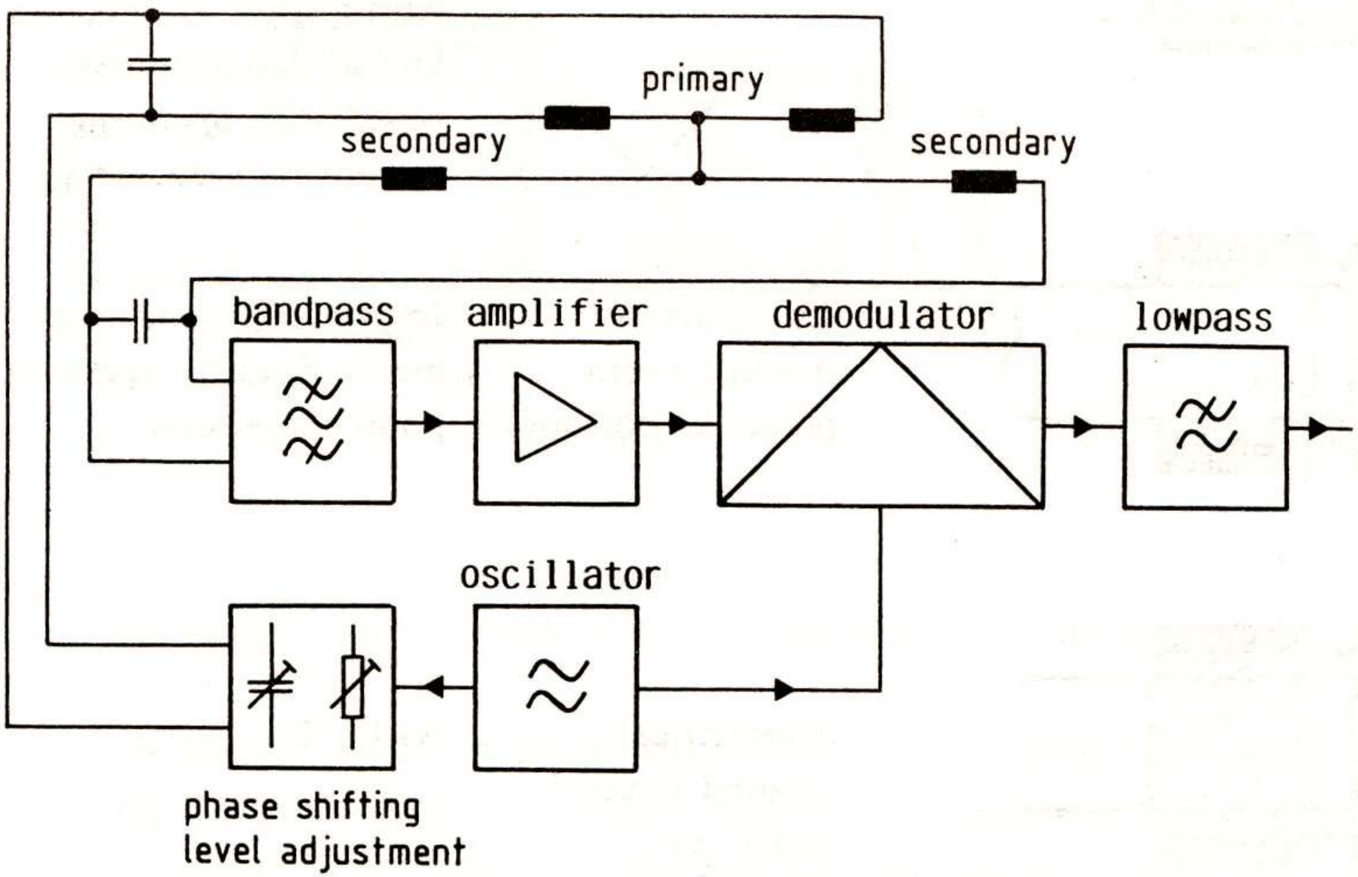

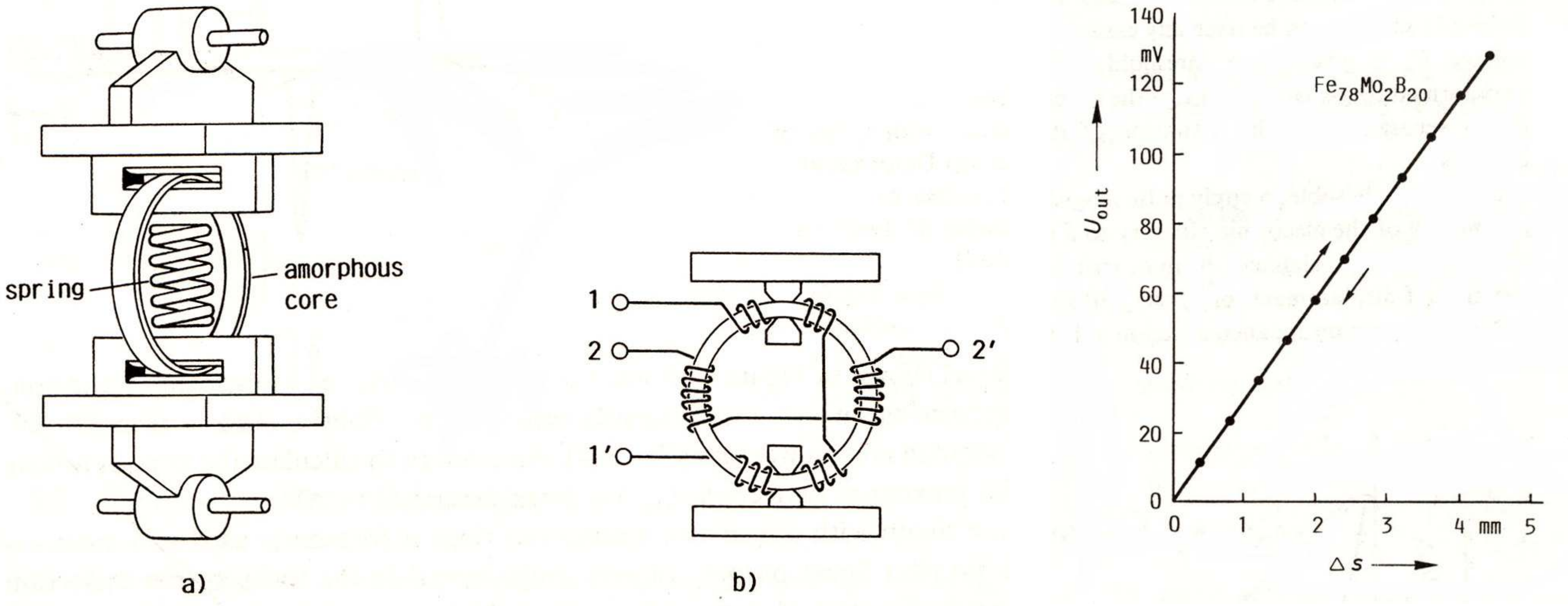

Extensometer. (a) Construction of strain sensing element using amorphous ribbon wound core; (b) configuration of lumped windings.

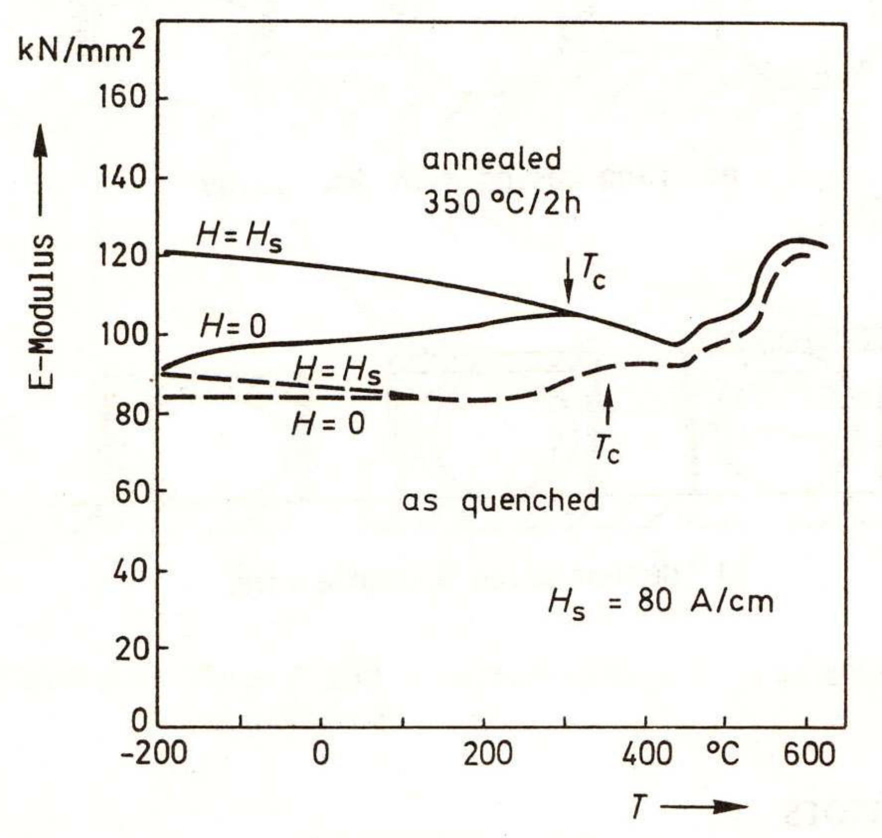

ΔE effect of an amorphous FeNi-based alloy (Fe40 Ni38 Mo4 B18). Hs: saturation field.

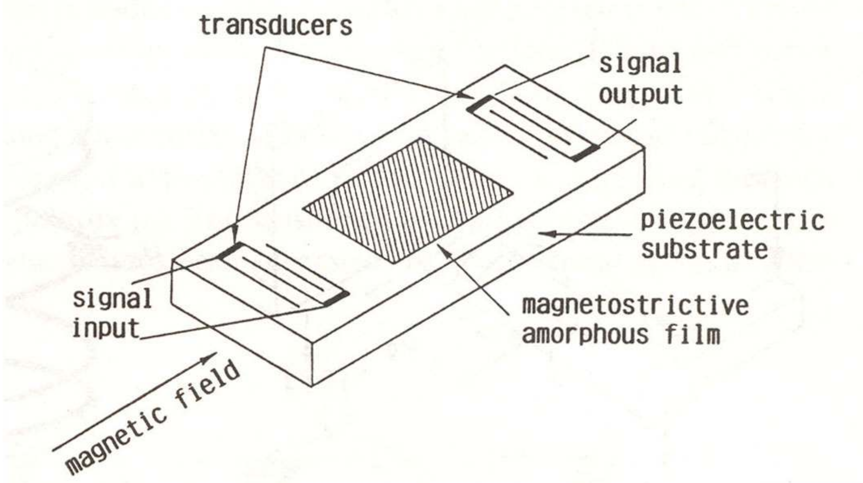

Magnetically tunable delay line.

Torque Sensors using Amorphous wire

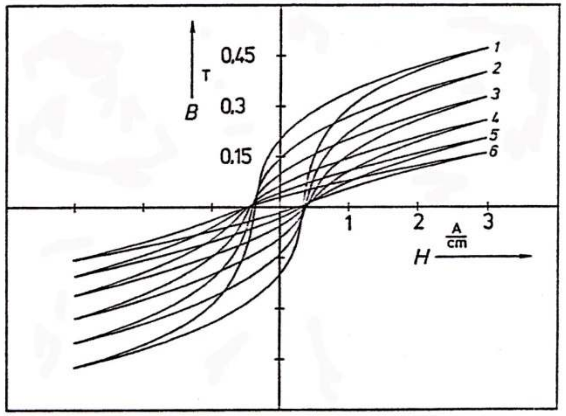

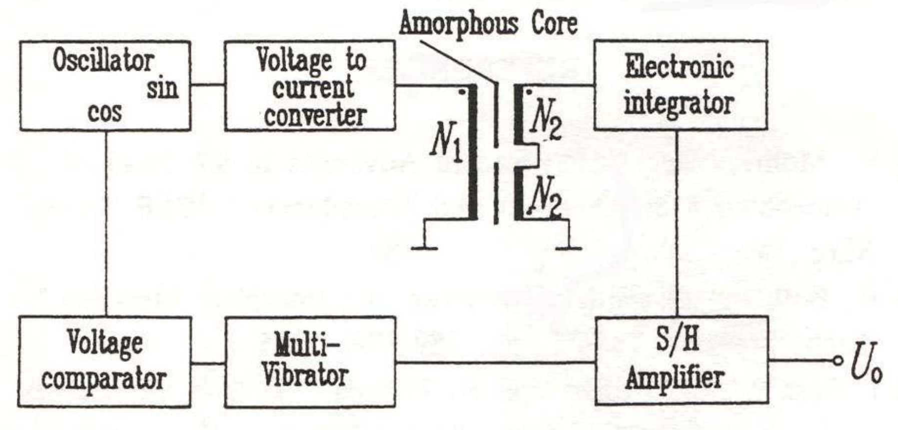

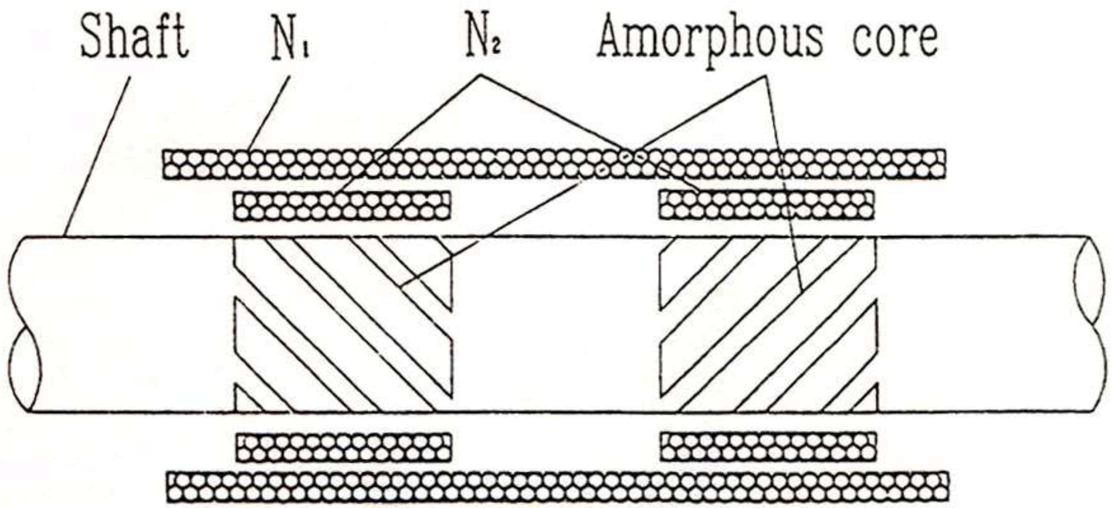

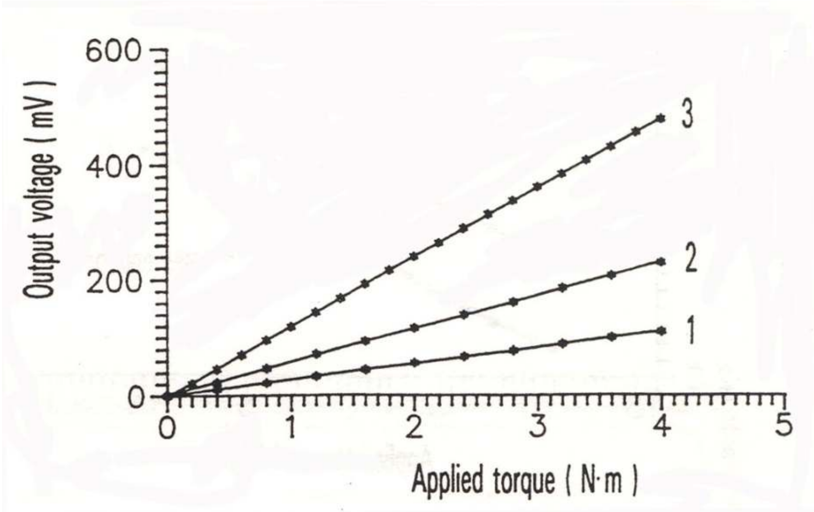
600
400
200
0
0
1
2
3
4
5
Output voltage (mV)
Applied torque (N·m)
3
2
1

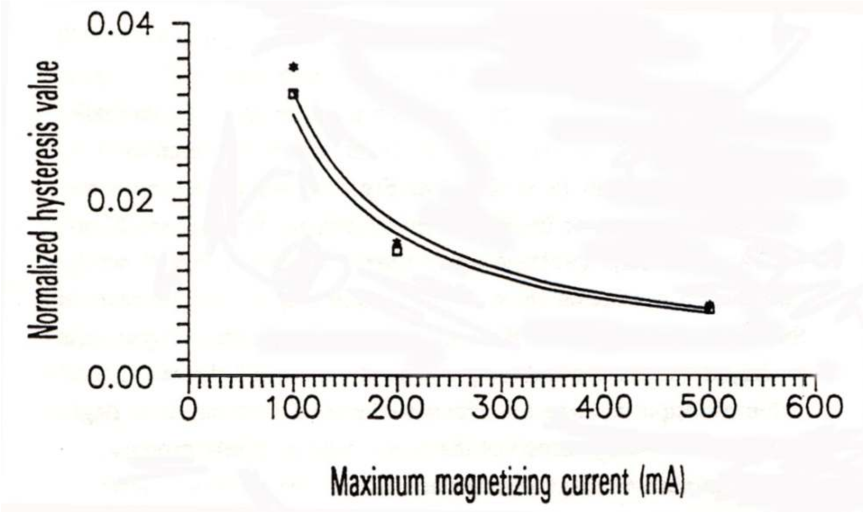
0.04
0.02
0.00
0
100
200
300
400
500
600
Normalized hysteresis value
Maximum magnetizing current (mA)

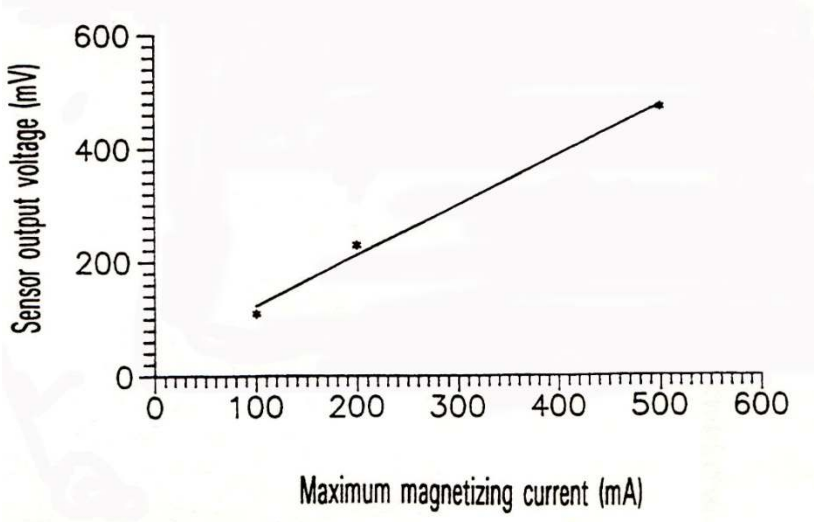
600
400
200
0
0
100
200
300
400
500
600
Sensor output voltage (mV)
Maximum magnetizing current (mA)

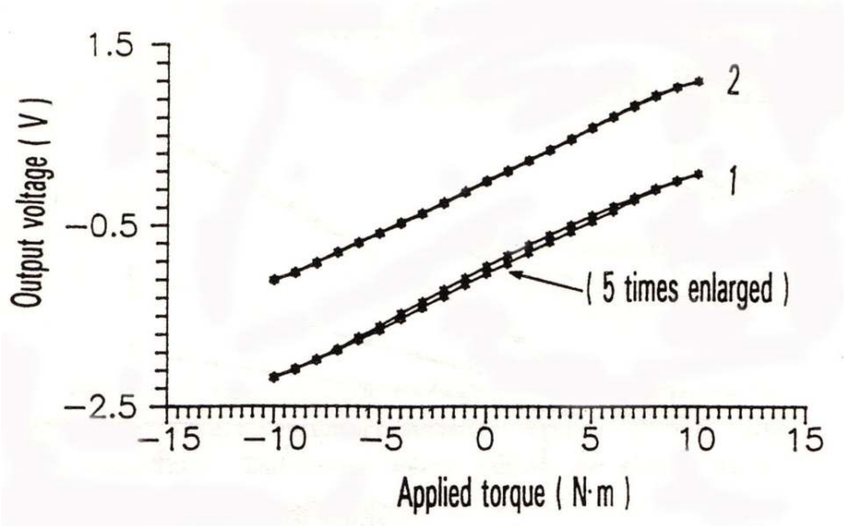
1.5
−0.5
−2.5
−15
−10
−5
0
5
10
15
Output voltage (V)
Applied torque (N·m)
2
1
(5 times enlarged)

Sixtus tonk효과(large Barkhausen효과)

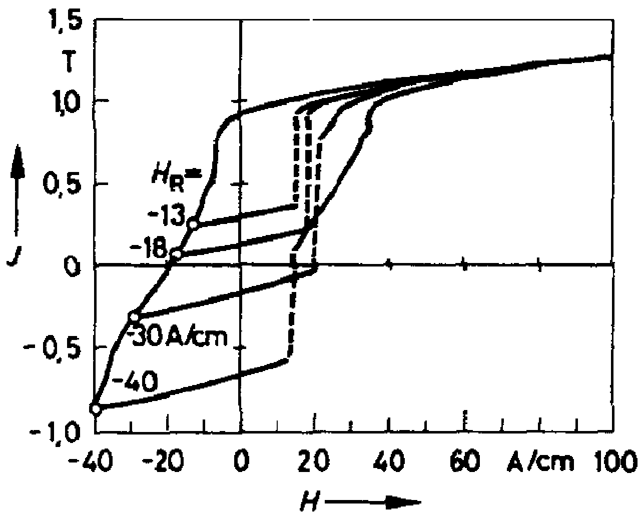

Hysteresis loops of a Wiegand wire for different reset fields.

Curie 온도 및 Hopkinson효과

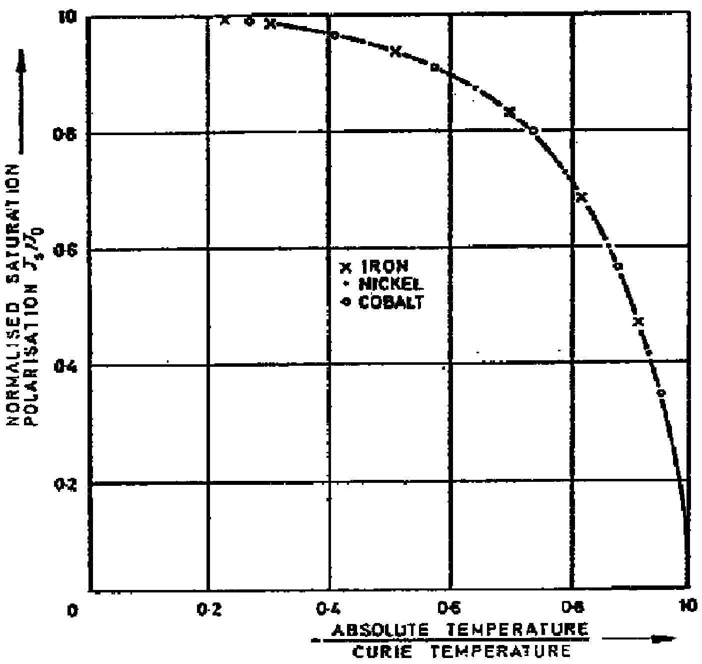

Relation between normalised saturation polarisation and normalised Curie temperature.

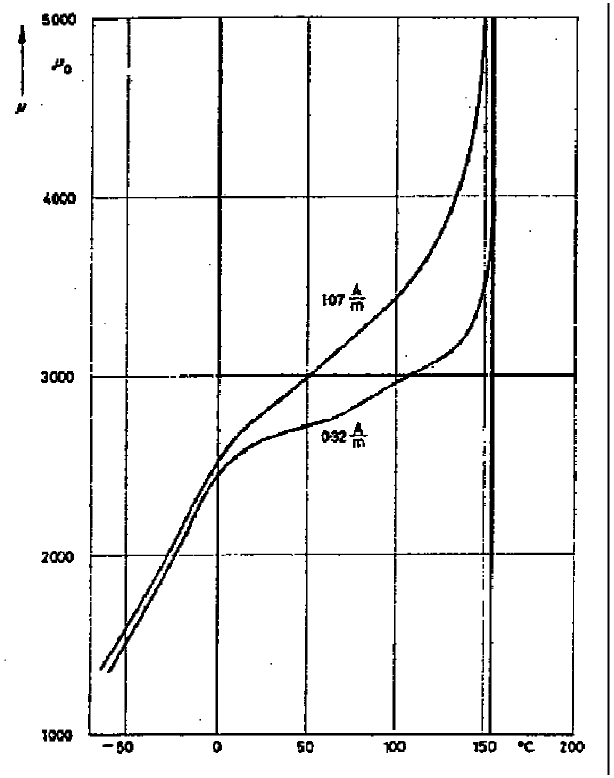

Permeability of a Mn-Zn ferrite as a function of temperature and field strength

Conclusions

1) Magnetic sensor 는 자동차, 공장자동화, 항공우주 및 군사용으로 많이 사용되고 있다.

2) 새로운 소재개발은 자기센서의 성능개발에 직접적인 영향을 준다.

3) 센서의 개발을 위해서는 다양한 전공지식이 요구된다.

(물리학, 재료공학, 기계공학, 전자공학)

4) 센서분야가 고부가가치를 창출하는 부품사업이다.

5) 핵심부품을 생산하는 중소기업의 item으로도 적절하다.